Evaluation of the Protective Capacity of Ice Hockey Goaltender Masks for Three Accident Events using Dynamic Response and Brain Stress and Strain

James Michio Clark

A thesis submitted to

The Faculty of Graduate and Postdoctoral Studies of the University of Ottawa

In partial fulfillment of the requirements for the degree for

Master of Science in Human Kinetics

Advisor

Thomas B. Hoshizaki, PhD

Committee Members

Patrick Bishop, PhD

Jing Xian Li, PhD

Faculty of Health Sciences

School of Human Kinetics

University of Ottawa

Acknowledgements

I would like to thank all of the individuals who have helped me in the completion of this thesis. First, I would like to thank my supervisor, Dr. Blaine Hoshizaki, for his guidance and advice. It has been an honour to have worked with and learned from a world-class researcher in the field of head impact biomechanics. A special thank you to Reebok-CCM for providing me with ice hockey goaltender masks. I would also like to thank my thesis committee members, Dr. Patrick Bishop and Dr. Jing Xian Li, for offering their expertise. Thank you for your feedback and insightful questions which have influenced the completeness of this thesis.

I would like to thank all my colleagues at the Neurotrauma Impact Science Laboratory with whom I have had the pleasure of working with over the course of my masters: Andrew, Dave, Anna, Marshall, Clara, Janie, Karen, Phil, Evan, Christian, Katrina, Lauren, Santiago, Gabrielle, Jessica and Wes. Thank you for the advice, support, and encouragement along the way.

Thank you to my family, and in particular my father, Jim Clark, for the support with my writing and proof reading my work. Finally, I would like to thank girlfriend Jazmin Habgood. Thank you for all of the support, encouragement and countless hours proof reading. Without her help I would not have been able to accomplish everything.

Abstract

Since the introduction of helmets the incidence of traumatic brain injuries (TBI) in ice hockey has greatly decreased, but the incidence of concussions has essentially remained unchanged. Despite goaltenders in ice hockey being the only players on the ice for the entire game, few have assessed the performance of ice hockey goaltender masks. In ice hockey, goaltenders are exposed to impacts from collisions, falls and projectiles. The objective of this study was to assess the protective capacity of ice hockey goaltender masks for three accident events associated with concussion. A helmeted and unhelmeted medium NOCSAE headform were tested under conditions representing three common accident events in ice hockey. Falls were reconstructed using a monorail drop. A pneumatic linear impactor was used to reconstruct collisions and projectile impacts were reconstructed using a pneumatic puck launcher. Three impact locations and three velocities were selected for each accident event based on video analysis of real world concussive events. Peak resultant linear acceleration, peak resultant rotational acceleration and rotational velocity of the headform were measured. The University College Dublin Brain Trauma Model (UCDBTM) was used to calculate maximum principal strain (MPS) and von Mises stress in the cerebrum. The results demonstrated the importance of assessing the protective capacity of ice hockey goaltenders masks for each accident, as each event created a unique response. A comparison of unhelmeted and helmeted impacts revealed ice hockey goaltender masks are effective at reducing the risk of both concussion and TBI for falls and projectiles, but less so for collisions. Further, the risk of more serious injuries was found to increase for falls and collisions as impact velocity increased. The results highlight the importance of impacting multiple locations when assessing the protective capacity of ice hockey goaltenders masks, as different impact locations result in unique responses. Overall this study demonstrated ice hockey goaltenders masks capacity to reduce the risk of concussion across three accident events.

Table of Contents

List of Figures

List of Tables

List of Equations

Equation 1: Maximum principle strain

$$\varepsilon 1,2 = \frac{\varepsilon_x + \varepsilon_y + \varepsilon_z}{3} \pm \sqrt{\left(\varepsilon_x - \varepsilon_y\right)^2 + \left(\varepsilon_y - \varepsilon_z\right)^2 + \left(\varepsilon_y - \varepsilon_z\right)^2}$$

Equation 2: Von Mises stress

$$\sigma = \sqrt{0.6\left[\left(\sigma_x - \sigma_y\right)^2 + \left(\sigma_y - \sigma_z\right)^2 + (\sigma_z - \sigma_x)^2\right]} + \sqrt{+3\left(\tau_{xy}^2 + \tau_{yz}^2 + \tau_{zx}^2\right)}$$

Equation 3: Headform rotational acceleration component (x)

$$\overrightarrow{\alpha_x} = \frac{\overrightarrow{a_{zS}} - \overrightarrow{a_{zC}}}{2S} - \frac{\overrightarrow{\alpha_{yT}} - \overrightarrow{a_{yC}}}{2T}$$

Equation 4: Headform rotational acceleration component (y)

$$\overrightarrow{\alpha_y} = \frac{\overrightarrow{a_{xT}} - \overrightarrow{a_{xC}}}{2T} - \frac{\overrightarrow{\alpha_{zF}} - \overrightarrow{a_{zC}}}{2F}$$

Equation 5: Headform rotational acceleration component (z)

$$\overrightarrow{\alpha_z} = \frac{\overrightarrow{a_{yF}} - \overrightarrow{a_{yC}}}{2F} - \frac{\overrightarrow{\alpha_{xS}} - \overrightarrow{a_{xC}}}{2S}$$

Equation 6: Headform rotational velocity

$$\overrightarrow{\omega_i} = \int_0^T \overrightarrow{\alpha_i}\, dt + c_1$$

Equation 7: Shear characteristics of the viscoelastic behaviour of the brain

$$G(t) = G_\infty + (G_0 - G_\infty)e^{\beta t}$$

Equation 8: Hyperelastic Law

$$C_{10}(t) = 0.9C_{01}(t) = 620.5 + 1930e^{-\frac{t}{0.008}} + 1103e^{-\frac{t}{0.15}}(Pa)$$

Equation 9: Video analysis impact velocity

$$v = \frac{d}{\left(\frac{F}{f}\right)}$$

Equation 10: Elemental rotation matrix

$$R_y(\theta) = \begin{bmatrix} \cos(\theta) & 0 & \sin(\theta) \\ 0 & 1 & 0 \\ -\sin(\theta) & 0 & \cos(\theta) \end{bmatrix}$$

Chapter 1. Introduction

1.1 Problem Statement

It is estimated that the annual direct and indirect cost of traumatic brain injury (TBI) in Canada is $3 Billion dollars with over 11,000 associated fatalities annually (Kendall et al., 2012a). Protective headgear and helmets have decreased the risk for TBI from collisions in sport. As such, skull fractures and other TBIs have largely disappeared from sports, however the incidence of mild traumatic brain injury (mTBI) or concussion remains common (Wennberg and Tator, 2003). It is estimated that 1.6 million to 3.8 million concussions occur as a direct result of participation in athletics (Faul et al., 2010; Finkelstein et al., 2006). Research into concussive injuries has shown that there may be links between mild traumatic brain injury (mTBI) and long-term health problems such as dementia and emotional distress, leading to suicide (Gasquoine, 1997; Guskiewicz et al., 2005). This creates concern for the safety and long-term health for those who participate in sports.

In ice hockey, concussions are one of the most common injuries sustained by athletes across all levels of play and age groups (Kelly et al., 1991; Cantu, 1996; Pashby et al., 2001; Powell et al., 2001; Marchie and Cusimano, 2003; Goodma et al., 2004; Flik et al., 2005; Agel et al., 2007). Injuries to the head in hockey typically occur as a result of body checking, collisions with the boards or the net, contact with the ice or contact with the puck (Gerberich et al., 1987; Emery and Meeuwisse, 2006). Considerable research has been conducted in an effort to decrease the incidence of concussion, however, this research has been focused on skaters with little research done on goaltenders. Studies report forwards and defenseman sustain more concussions than goaltenders (Benson et al., 2011; Emery et al., 2011; Donaldson et al., 2013; Hutchison et al.,

2013a) however a study in the Finish National Hockey League reported that concussions were most prevalent in goaltenders (Molsa et al., 1997). Concussions, along with head and knee injuries in goaltenders, are caused by player collisions, impacts to the ice and puck impacts to the head (LaPrade et al., 2009). Player collisions are reported as the most common accident event (LaPrade et al., 2009). Current standards for ice hockey goaltender masks involve drop tests to establish impact absorption properties of the mask and puck impacts to test for breakage of the cage at cold temperatures (International Organization for Standardization, 2003; Canadian Standards Association 2009; American Society for Testing and Materials, 2014). Research has shown collisions, falls and projectiles create unique impact conditions that influence the direction and magnitude of the dynamic response and subsequent brain tissue deformation stresses and strains (Post et al., 2013; Karton et al., 2013). These dynamic characteristics and have been shown to be associated with different levels of risk for concussion (Zhang et al., 2004; Kleiven, 2007; Kendall et al., 2012a; Zanetti et al., 2013). As current standards do not consider the three common accident events associated with concussion for ice hockey goaltenders masks it is unknown how protective goaltender masks are in providing adequate protection for this position. This study will provide ice hockey equipment manufacturers with information to develop more effective equipment to protect ice hockey goaltenders from the risk of concussion.

1.2 Research Question

How effective are ice hockey goaltenders masks at reducing the peak dynamic response and brain deformation following three distinct accident events of varying locations and inbound velocities?

1.3 Objectives

1. To describe the capacity of ice hockey goaltender masks to reduce the dynamic response of the National Operating Committee on Standards for Athletic Equipment (NOCSAE) headform as measured by peak resultant linear and rotational acceleration and rotational velocity for three accident events (fall, collision, projectile) of varying locations and velocities.
2. To describe the capacity of ice hockey goaltender masks to reduce the brain tissue deformation as measured by peak von Mises and peak maximum principal strain for three distinct accident events (fall, collision, projectile) of varying locations and velocities.

1.4 Variables

1.4.1 Independent variables

1. Accident event
    1. Fall
    2. Collision
    3. Projectile
2. Helmet
    1. No Helmet
    2. Ice Hockey Goaltender Mask (CSA certified)
3. Impact Parameters
    1. Velocity
        i. Lower Range
        ii. Mean
        iii. Upper Range
    2. Location

i. Low Incidence

ii. Medium Incidence

iii. High Incidence

1.4.2 Dependent variables

1. Dynamic Response
    1. Peak Resultant Linear Acceleration
    2. Peak Resultant Rotational Acceleration
    3. Peak Resultant Rotational Velocity
2. Brain Tissue Deformation
    1. Peak von Mises Stress
    2. Peak Maximum Principal Strain

1.5 Hypotheses

1.5.1 Experimental Hypothesis

1. It is hypothesized that ice hockey goaltender masks will reduce the dynamic response of the NOCSAE headform (peak resultant linear and rotational acceleration and peak rotational velocity) and brain tissue deformation characteristics (peak von Mises and peak maximum principal strain) when subject to the low velocity and three locations for all three accident events (fall, collision, projectile).
2. It is hypothesized that the three distinct accident events (fall, collision, projectile) will result in different dynamic response of the NOCSAE headform (peak resultant linear and rotational acceleration and rotational velocity) and brain tissue deformation characteristics (peak von Mises and peak maximum principal strain).

3. It is hypothesized that an increase in velocity will result in an increase in the dynamic response of the NOCSAE headform (peak resultant linear and rotational acceleration and rotational velocity) and brain tissue deformation characteristics (peak von Mises and peak maximum principal strain) for all three accident events (fall, collision, projectile).
4. It is hypothesized that impact location will result in different dynamic response of the NOCSAE headform (peak resultant linear and rotational acceleration and rotational velocity) and brain tissue deformation characteristics (peak von Mises and peak maximum principal strain) for all three accident events (fall, collision, projectile).

1.5.2 Null Hypothesis

1. An **ice hockey goaltender mask** will have no effect on **peak linear acceleration** when compared to a **bare headform** for low velocities of each accident event.
2. An **ice hockey goaltender mask** will have no effect on **peak rotational acceleration** when compared to a **bare headform** for low velocities of each accident event.
3. An **ice hockey goaltender mask** will have no effect on **peak rotational velocity** when compared to a **bare headform** for low velocities of each accident event.
4. An **ice hockey goaltender mask** will have no effect on **peak von Mises** when compared to a **bare headform** for low velocities of each accident event.
5. An **ice hockey goaltender mask** will have no effect on **peak maximum principal strain** when compared to a **bare headform** for low velocities of each accident event.
6. Changes in **accident event** will have no effect on **peak linear acceleration**.
7. Changes in **accident event** will have no effect on **peak rotational acceleration**.
8. Changes in **accident event** will have no effect on **peak rotational velocity**.
9. Changes in **accident event** will have no effect on **peak von Mises stress**.

10. Changes in **accident event** will have no effect on **peak maximum principal strain**.
11. Change in **inbound velocity** will have no effect on **peak linear acceleration**.
12. Change in **inbound velocity** will have no effect on **peak rotational acceleration**.
13. Change in **inbound velocity** will have no effect on **peak rotational velocity**.
14. Change in **inbound velocity** will have no effect on **peak von Mises stress**.
15. Change in **inbound velocity** will have no effect on **peak maximum principal strain**.
16. Change in **location** will have no effect on **peak linear acceleration**.
17. Change in **location** will have no effect on **peak rotational acceleration**.
18. Change in **location** will have no effect on **peak rotational velocity**.
19. Change in **location** will have no effect on **peak von Mises stress**.
20. Change in **location** will have no effect on **peak maximum principal strain**.

1.6 Significance

Hockey is a popular sport worldwide with a participation rate of over 1 million players in the USA and Canada alone (Stuart et al., 2002). Despite the fact that hockey is popular worldwide, (Russia, Slovakia, Slovenia, Finland, Norway, Austria, Czech Republic, Sweden, Switzerland, Latvia, and Japan) there has been very little research in the biomechanics of head injuries for ice hockey goaltenders. Previous research involving goaltenders has focused on descriptive epidemiology studies of hockey as a whole providing little insight into concussions in goaltenders. LaPrade et al. (2009) reviewed the NCAA Injury Surveillance System database for the 2000-2001 thorough to the 2006-2007 seasons to determine the incidence and accident events of NCAA intercollegiate ice-hockey injuries for goaltenders. It was found that the most common injuries to ice hockey goaltenders were knee ligament injuries and concussions (LaPrade et al., 2009). Nur et al. (submitted) compared the performance of four ice hockey goaltenders masks to protect the

athlete from puck impact as measured by head acceleration and peak force when impacted by pucks. When the four ice hockey goaltender masks were impacted at three locations at 25 m/s, the force values did not exceed the thresholds for injury. However, the masks did vary in the level of protection offered (Nur et al., submitted).

Collisions, falls and projectiles experienced by goaltenders in ice hockey are characterized by different impact parameters such as impact site, mass, velocity, angle of impact, and compliance of impactor, resulting in unique dynamic response curves and different head and brain injuries (Gennarelli et al., 1982; 1987; Zhang et al., 2001a; Kleiven, 2003, Pellman et al., 2003; Post et al., 2012a). The unique dynamic response curves have been associated with different levels of injury risk (Zhang et al., 2004; Kleiven, 2007; Kendall et al., 2012a; Zanetti et al., 2013). Rousseau (2014) reconstructed elbow-to-head and shoulder-to-head collisions in elite ice hockey players and found mean peak linear and rotational resultant acceleration for concussion cases to be 25 ± 11g and 3.0 ± 1.1krad/s^2, respectively. These values are both lower than 25% risk of concussion proposed by Zhang et al. (2004). However, Rousseau (2014) found maximum principal strain von Mises stress values to be similar to concussions resulting from head-to-head collisions in the National Football League and head impacts in rugby or Australian Rules Football (Kleiven, 2007; Patton et al., 2013; Zhang et al., 2004). Whereas, Kendall et al. (2012) found a head impacting the ice to produce peak linear and rotational accelerations of 264.4 ± 33.8g and 11204 ± 1867rad/s^2, respectively. This exceeds 80% risk of sustaining a concussion (Zhang et al., 2004). Furthermore, Rousseau et al. (2014) found puck impacts to also produce different dynamic response results, in which a 41m/s puck impact resulted in peak linear and rotational accelerations of 238 ± 48g and 21900 ± 1300rad/s^2, respectively. Surpassing 80% risk

of injury proposed by Zhang et al., 2004. Each of these accident events has been shown to produce unique dynamic responses in ice hockey skaters.

Reconstructing concussive accident events experienced by ice hockey goaltenders will provide a better understanding of the relationship between the event resulting in concussion and the dynamic response of the head and brain tissue deformation associated with the event. Helmets have been reported as an effective way of reducing head and brain injury in sports (Hoshizaki & Brien, 2004; McIntosh & McCrory, 2005) and will benefit from a better understanding of mechanisms of injury (Cantu & Mueller, 2003; McIntosh & McCrory, 2005). It is important that helmets be designed to protect players from injuries based on the unique risk of their sport. For example motor sport, cycling and alpine skiing use crash helmets and are primarily designed to manage a single high energy impacts. However, hockey helmets are designed to manage multiple impacts resulting from collisions and falls (Hoshizaki and Brien, 2004). The designs of these helmets differ in order to manage the unique risk of each particular activity. In ice hockey, skater's helmets consist of a plastic shell of polyethylene and either vinyl nitrile (VN) or expanded polypropylene (EPP) foam liners. Whereas ice hockey goaltenders masks are often made with a stiffer shell material such as carbon and Kevlar composite, fibreglass or polycarbonate and have a VN foam liner. This thesis was designed to provide determine the capacity of goaltender protective masks to protect athletes from impacts associated with concussive injuries in ice hockey.

1.7 Limitations

1. A medium NOCSAE headform was used in this thesis. The NOCSAE headform is not biofidelic and will not imitate the dynamic properties of a human head. Despite such limitations, the NOCSAE headform is widely accepted and used as a human head surrogate to certify football and lacrosse helmets (NOCSAE Standard). The NOCSAE

headform has been shown to produce slightly higher but correlated peak linear acceleration data when compared to cadaveric head impacts performed by Hodgson and Thomas (1971) (Kendall et al., 2012b). While cadaveric head drops have shown a high degree variability, (Ono et al., 1980; Nusholtz et al., 1984), the NOCSAE headform produces highly linear and repeatable data (Kendall et al., 2012b). The NOCSAE headform is also thought to have a more human-like response than the Hybrid III headform based on its more human-like anthropometry, a gel filled cavity to function as a brain and a more human-like material for the skull (nylon based) (Hodgson & Thomas, 1971). Resulting in the NOCSAE headform a reliable human head surrogate for this study.

2. The headform is attached to a neck form that is attached to a low resistant sliding table to allow for movement of the headform post impact. The effect of such a table on the impact mechanics has not yet been well defined.
3. Peak resultant kinematic measures alone may not fully measure the protective capacity of ice hockey goaltender masks. Peak magnitude of resultant accelerations does not take into account direction, which is reflected in the entire dynamic response. However, peak accelerations provide a reflection of changes in force, pressure and shear which cause damage to the brain (Holbourn, 1943) and has been found to be a prognostic indicator of head injury (Ommaya et al., 1967; Gurdjian & Gurdjian, 1975).
4. The maximal principle strain represents the highest strain value among the three axes. As a result, this is not a global representation of the strain experienced by the brain. Further, it is unknown in which axis, *x*, *y* or *z*, the highest strain will be experienced. Despite such limitations, maximal principle strain is commonly used to represent brain deformation

and has been identified as a possible indicator of concussion (Zhang et al., 2004; Kleiven, 2002; Willinger & Baumgarthner, 2003; Zhou et al., 1995), therefore providing valuable information in assessing the protective capabilities of ice hockey goaltender masks.

5. The University College Dublin Brain Trauma Model (UCDBTM) was the finite element brain model used in this study. The development of this model was based on adult male CT scans of cadavers and may not be representative of a 50^{th} percentile adult male. The differences could produce characteristic dynamic responses to impact but the relationship between the impact parameters and the headform response is assumed to be similar, providing a valid estimate of human brain tissue deformations from a head impact.
6. The validation of the element rotation used in this thesis was performed on a Hybrid III headform. The Hybrid III and NOCSAE headforms have been found to produce different dynamic responses, however the responses of the two headforms are highly correlated (Kendall et al., 2012b). As such in applying the element rotation used in thesis, it is assumed to produce a similar response, providing a valid method to rotate the coordinate system of the NOCSAE headform in order to conduct finite element analysis.

1.8 Delimitations

1. The UCDBTM is a partially validated model in which the brain stem has not yet been validated for finite element modeling. The brain stem was not be evaluated in this study. However, the baseline of the UCDBTM has been validated against cadaveric research (Nahum et al., 1977; Hardy et al., 2001) and reconstructions of real world traumatic brain injury incidents (Doorly and Gilchrist, 2006; 2007) with agreeable results. By not evaluating the brainstem the UCDBTM can provide valid estimates of human brain deformation.

2. The response of the brain model is dependent on the material properties that each respective part of the head/brain complex has been assigned. However, variations in the literature suggest that definitive material properties have not yet been established. Despite a lack of material characteristics, the UCDBTM's material properties are taken from Ruan (1994), Willinger et al. (1995), Zhou et al. (1995), and Kleiven and von Holst (2002) which allows the response of the model to be within the realm of possibility.
3. Impact parameters used for each accident event were based on concussions which occurred solely in elite ice hockey goaltenders and as such may not represent the protective capacity of ice hockey goaltender masks for other age levels. For ice hockey goaltenders of other age levels there may not be accessibility to injury reports and high quality video of the incident, potentially increasing error in the data analysis. By selecting solely elite ice hockey goaltenders it allows for access to injury reports and high quality game film for video analysis.
4. A single model of an ice hockey goaltender mask was tested. Different helmet models have been found to vary in their performance to an impact due to differences in shell and liner design (Rousseau, et al., 2009a; 2009b; Ouckama & Pearsall, 2014; Post et al., 2014; Nur, et al., submitted). However, the performance differences are small in magnitude (Rousseau, et al., 2009a; 2009b; Ouckama & Pearsall, 2014; Post et al., 2014; Nur, et al., submitted) and as such a single ice hockey goaltender mask model allows for a description of the protective capacity of ice hockey goaltenders masks.

Chapter 2. Literature Review

2.1 Classification of Head Trauma

Neurotrauma has been defined as the physical damage that results when the human skull and brain are suddenly or briefly subjected to intolerable levels of energy that is usually transmitted mechanically (Kleiven, 2002). There are two main types of classification for human head trauma which can be divided into focal injury, which affect the localized regions, and diffuse injury which occur in a more widespread area (Kleiven, 2002; Bailes & Cantu 2001).

Focal head injuries are caused by the force of contact and the head acceleration of a direct blunt trauma (Biasca et al., 2002). Typically these injuries are caused by severe translations which cause the brain to lag behind the skull and create stress on the structures that connect the brain to the skull or cause the brain to bump against the bony protuberances within the skull (Viano et al., 1989). These injuries have visible local damage such as hematomas, cortical or subcortical brain contusions (Bailes & Cantu 2001; McIntosh et al., 1996). In hockey, these injuries have been caused by blunt trauma such as being struck with a hockey stick, puck or falling on the ice and striking the head (Biasca et al., 2002). Wearing an approved standardized helmet can reduce the risk of these injuries (Bishop & Arnold, 1993; Bishop, 1997; Bishop, 2000). Current helmet testing certifications use a peak value of 275g as a pass/fail variable and are concerned with the prevention of TBI. As a result, TBI has largely disappeared from the sport of ice hockey (Hoshizaki & Brien, 2004).

Diffuse head injuries are caused by inertial effect of the mechanical blow to the head (Biasca et al., 2002). These injuries are named “diffuse” due to the large volumes of distribution of the stresses and strains which cause brain damage and subsequent clinical injury. They cannot be seen by the naked eye as they affect neural tissues deep to the skull and include diffuse axonal

injuries (DAI) and concussions (Kleiven, 2002, Bailes and Cantu 2001). The severity of these injuries can vary from mild to more severe cases of both concussions and DAI. DAI is thought to be caused primarily by rotations that cause and contribute to shearing of the white matter fibre tracts (Strich, 1961; Adams et al., 1982; Gennarelli et al., 1982). These injuries only account for 25% of head injury deaths but they are considered more serious because of the permanent neurology disability in survivors (Biasca et al., 2002).

Concussions are common in ice hockey and would be considered the mildest form of diffuse injury. This type of injury is thought to occur primarily due to rotations. When the head is rotated the skull interacts with the brain due to inward projections and rotates the brain. These rotations in combination with linear motion cause diffuse stresses and strains to brain tissue resulting in transient local deformations (Holbourn, 1943) which cause stretches and tears to nerve fibres (Strich, 1961). Stretching of neural tissue causes a change in structure and forces the opening of voltage-dependent K^+ channels, which leads to a marked increase in extracellular K^+ (Julian & Goldman, 1962; Takahashi et al., 1981; Hubschmann & Kornhauser, 1983; Katayama et al., 1990). An increase in extracellular K^+ leads to an excessive release of excitatory amino acids such as glutamate (Katayama et al., 1990). Normally, excessive extracellular K^+ is reabsorbed by surrounding glial cells (Kuffler, 1967; Ballanyi et al., 1987; Paulson & Newman, 1987), however injuries such as brain trauma or ischemia overcome this compensation (Hansen, 1977; Hansen, 1978; Astrup et al., 1980; D'Ambrosio et al., 1999). The high amounts of excitatory amino acids activate the opening of ligand-gated ion channels which increase the outflow K^+ and influx of calcium (Ca^{2+}). This creates a large excitatory process followed by a wave of relative neural suppression called spreading depression (Prince et al., 1973; Sugaya et al., 1975; Van Harreveld, 1978; Nicholson et al., 1981; Somjen & Giacchino, 1985). In an attempt to restore

ionic homeostasis, energy-requiring membrane pumps are activated (Bull & Cummins, 1973; Mayevsky & Chance, 1974; Rosenthal et al., 1979) and trigger an increase in glucose use (Shah & West, 1983; Sunami et al., 1989; Yoshino et al., 1991). The increase in energy demands cannot be met due to cerebral blood flow being decreased by the intra-cranial pressure, and the excessive accumulation of intracellular Ca2+ impaired mitochondrial function (Hovda et al., 1999; Giza and Hovda, 2001). Electrolyte homeostasis is usually restored within minutes but the brain can remain in a depressed state for several days (Katayama, 1990). In addition, the neural damage which occurs, often appears to be temporary in nature but can result in long term debilitating symptoms (McKee et al., 2010). Further, they are characterized by a cumulative effect, which may end an athlete's career (Biasca, 2000; Tegner, 2001; Tegner & Lorentzon, 1996; Kelly, 2001; Biasca et al., 1999; Echemendia et al., 2001; Rabadi & Jordan, 2001).

In spite of the success of managing focal type injuries, concussions are currently a great concern in recreational and professional sports (Delaney et al., 2002; Flik et al., 2005; Casson et al., 2010). Also, there is a lack of a collective agreement on the definition of concussion and severity of grading concussion injuries due to the diverse affects that injured individuals experience (Leclerc, et al., 2001). In severe cases, post-concussion syndrome is experienced and is defined by having at least three typical concussion symptoms present up to at least three months post injury (ICD-10, WHO 1989). Concussion symptoms are presented in a wide range and include physical signs such as loss of consciousness and amnesia, behavioural changes such as irritability, cognitive impairment such as slowed reaction times, sleep disturbances such as drowsiness, somatic symptoms such as headaches, cognitive symptoms such as feeling "in a fog" and/or emotional symptoms such as emotional liability (McCrory et al. 2009). In most cases, these symptoms resolve within a week to six months (Iverson et al., 2010). However, for those

individuals with post-concussion syndrome, symptoms can last several months (Roe et al., 2009; Sigurdardottir et al., 2009) causing potential gross effects on daily living which is known as post-concussive disorder (Ryan & Warden, 2003; Wood, 2004).

2.2 Dynamic Response Measures

Injury results when a tissue exceeds its level of tolerance to a specific load which can be in the form of acceleration, force energy or power (Horgan, 2005). During direct head impact, forces and pressures vary in degree and intensity in the brain (Holbourn, 1943). Despite research showing the brain stress and strain are the principal cause of injury, these measures are not feasible in vivo. Although linear and rotational accelerations do not directly cause damage to the brain, they are a reflection of changes in force, pressure and shear, (Holbourn, 1943) and can also be used to determine the change in velocity. Thus, acceleration of the head upon impact can be used to determine the injury mechanism (King et al., 2003). Linear acceleration is used in the assessment of helmet performance because it allows for an easy measurement and provides a comparison of helmet energy attenuating materials (Hoshizaki & Brien, 2004). However, linear and rotational accelerations do not exist on their own without the other in nature (Holbourn, 1943; Padgaonkar et al., 1975) and both are prognostic indicators of head injury (Ommaya et al., 1967; Gurdjian & Gurdjian, 1975). High peak linear acceleration has been shown to predict the risk of TBI including subdural haematomas and skull fractures (Holbourn, 1943; Ommaya & Hirsch, 1971; King et al., 2003), whereas rotational kinematics (acceleration, velocity) have been associated with mBTI or concussion type injuries (Holbourn, 1943; Gennarelli et al., 1982). Linear and rotational acceleration and rotational velocity are used as head injury parameters in this thesis to describe the dynamic impact response of a NOCSAE headform.

2.2.1 Linear Acceleration

When the head is impacted, it experiences accelerations which are a result of the forces generated by a collision (Newman, 1993). There have been some differences among the literature when relating linear acceleration as a mechanism of head injury. Linear acceleration is believed to be primarily related to focal type injuries, or traumatic events resulting from pressure gradients throughout the brain and/or skull deformation (Holbourn, 1943; Gennarelli, et al., 1972; King et al., 2003). Previous studies have shown intracranial pressure changes at the time of impact, although the degree to which it relates to brain injury varies among those experiments (Gurdjian, 1975). Despite differences, there is a similarity in the study which shows blunt impacts to the head resulting in intracranial pressure changes, as well as deformation of the skull. Pressure changes were found to be primarily related to acceleration and deceleration caused by an impact (Gurdjian, 1975). As a result, linear acceleration was determined as a measure of injury which can represent the internal pressure changes from impacts. Additionally, this measurement was used because at this time, linear acceleration was a variable that was measurable, despite the hypothesized influence of rotational acceleration (Holbourn, 1943).

Gurdjian et al. (1963) used mongrel dogs and found rotational acceleration alone could not cause enough damage to the brain to result in injury, and concluded that linear acceleration was important to consider for injury mechanisms. Ommaya and his associates (1966; 1971) supported Gurdjian's theory, that hypothesized rotational acceleration alone could not be the cause of mTBI. Ommaya and his associates (1966; 1971) compared direct impact and impulse loading (whiplash) in monkeys. They concluded that although rotational acceleration caused by whiplash can result in concussions, it requires higher levels of acceleration than direct impacts, making it a smaller contributor to the mechanism of injury. Ono et al. (1980) used monkeys to test traumatic

events in hopes of determining which form of acceleration was more detrimental to one's life. Ono et al. (1980) isolated each form of acceleration by using four devices capable of producing pure linear or rotational acceleration through direct impacts and impulse loading. They found that there was no direct correlation between rotational acceleration and concussion but a good correlation between liner acceleration and concussions. This observation led them to hypothesize that concussions were mostly caused by linear acceleration from direct impacts.

Current helmet safety standards use peak linear acceleration as validation criteria (Canadian Standards Association, 2009, Snell Memorial Foundation, 2010; American Society for Testing and Materials, 2014). As such, peak linear acceleration is still commonly used to describe injury and injury thresholds and should be considered.

2.2.2 Rotational Acceleration

The influence of rotational acceleration on the creation of head injuries is due to the principle that the three dimensional kinematics of the head after an impact influences the deformation characteristics of brain tissue and injury (Post and Hoshizaki 2012). Holbourn (1943) was the first to suggest that mTBIs are proportional to the amount of rotational acceleration experienced by the brain. Holbourn (1943) proposed that shear and tensile strains experienced from rotational acceleration are the main cause of injury. He demonstrated this theory by using a sudden rotation of a flask full of water to represent the skull brain interaction. The water will tend to stay in place as the glass flask rotates around it. However, the water attached to the inner surface of the flask will rotate with the flask. This caused the water on the inner surface of the flask to separate from the other water particles, in which shear and tensile strain tracts were observed. The observation of stretching and shearing tracts was thought to be similar to axonal damage under similar

loading. This led to the conclusion that rotational acceleration, and not linear acceleration, was responsible for concussions, haemorrhages and contra-coup injury (Holbourn, 1943).

A number of other studies have also reported the relationship between rotational acceleration and both focal and diffuse brain injury, and concluded that linear acceleration has little effect on injury mechanisms (Unterharnscheidt and Higgins, 1969; Gennarelli et al., 1971; Gennarelli, et al., 1972; Gennarelli, et al., 1979; Adams et al., 1981). Unterharnscheidt and Higgins (1969) applied a controlled rotational acceleration to squirrel monkeys and reported brain injuries including subdural haematoma, tearing of bridging veins, and lesions. Gennarelli et al. (1971) also found that rotational acceleration contributed more to concussive injuries, diffuse axonal injuries and subdural hematomas than linear acceleration alone. In a study by Gennarelli et al. (1972) using squirrel monkeys, it was revealed that an increased frequency and severity of cerebral concussion was found in monkeys who experienced rotation of the head over those who experienced pure translation. It was seen that although pure translation created higher magnitudes of peak linear acceleration (665-1230g) compared to monkeys which experienced rotation (348-1025g), all monkeys in the rotation group were concussed, in contrast to the pure translation group (Gennarelli et al., 1972). Sagittal plane rotational acceleration has also been seen to result in subdural haematoma, contusions, and discrete intra-cerebral haematoma in adult subhuman primates (Gennarelli et al., 1979; Adams et al., 1981).

Helmets are designed to decrease the risk of injury by decreasing the acceleration experienced by the head through energy attenuation. However, typically this decreases the risk of TBI by attenuating linear acceleration and is not designed to attenuate rotational acceleration. Contrary to the assumption that linear and rotational acceleration are highly correlated, previous studies have shown that helmets which have the ability to decrease linear acceleration may not manage

rotational acceleration as effectively (Hoshizaki & Brien, 2004; King et al., 2003; Rousseau et al., 2009a). Walsh et al. (2011) studied acceleration when impacting helmets and demonstrated that a change in one form of acceleration may not change the same in the other. Despite such research showing that rotational acceleration is related to injury, current helmet standards do not take into consideration rotational acceleration as a testing safety standard. However, a University of Ottawa Testing Protocol (uOTP) has been developed as the first protocol to consider both centric and non-centric impacts. Walsh et al. (2011) identified nine impact conditions (locations and angles) as producing either a peak linear or peak rotational acceleration with a value above 80% probability of sustaining mTBI as proposed by Zhang et al. (2004) as an estimate of brain injury thresholds. Five of the nine conditions identified were selected as the testing protocol. The purpose of this protocol is to consider both linear and rotational accelerations when testing helmet performance in order to decrease the risk of head injuries. As rotational acceleration has been shown to be important and a predictor of brain injury (Zhang, et al., 2001a), it should be considered in assessing the protective capacity of ice hockey goaltender masks.

2.2.3 Rotational Velocity

Despite rotational acceleration being the most common rotational kinematics measure to describe brain injury (Gennarelli et al. 1972; Zhang, et al., 2001a; Post et al., 2013b), rotational velocity has also been proposed as a mechanism of injury (Holbourn , 1943; Takhounts et al., 2008; 2013). In addition to proposing rotational acceleration as a mechanism of brain injury, Holbourn (1943) was also the first to propose rotational velocity as a mechanism of injury. Holbourn (1943) suggested that long duration is independent of the time for which the force acts. Hence, injury is proportional to the rotational acceleration of the head. However, for very short durations Holbourn (1943) suggested that the injury is proportional to the force multiplied by the time for

which it acts. Therefore, the injury is proportional to the change of rotational velocity of the head and rotational acceleration. The change-over from one law of injury to the next was said to be accompanied by a change in the distribution of the shear-strains and occur between 1/5 and 1/500 sec (Houlbourn, 1943). As such, rotational velocity may be an important measure to describe brain injury for impacts of short duration.

In addition to Holbourn (1943) a number of other studies have also reported rotational velocity as an important measure of brain injury (Hardy et al., 2001; 2007; Takhounts et al., 2008; 2013). Hardy et al. (2001; 2007) described the motion of the brain with respect to the motion of the skull and found rotational velocity to be the most convenient measure for comparison of brain and skull motion. It was seen that as the head began to rotate, the local brain tissue will remain in its potion and shape with respect to inertial frame, which causes relative motion between the brain and skull. Then, as the brain slows down, reaches steady state, or changes in direction, the brain motion will surpass that of the skull (Hardy et al., 2001; 2007). This demonstrated changes in rotational velocity reflected the motion between the brain and the skull.

In an investigation of TBIs using the next generation of Simulated Injury Monitor (SIMon) Finite Element Head, Takhounts et al. (2008) supported the theory, Holbourn (1943) , that the only way to deform or strain the brain which is contained within an almost un-deformable skull, is to rotate the skull. As such Takhounts et al. (2008) found none of the biomechanical injury metrics [cumulative strain damage measure (CSDM), dilatational damage measure (DDM), relative motion damage measure (RMDM), maximum principal stresses and strains] correlated with linear acceleration. While, three biomechanical injury metrics (CSDM, RMDM, and maximum principal strain) correlated well with angular acceleration and angular velocity in which rotational velocity correlated a little better with the three biomechanical injury metrics compared

to rotational acceleration (Takhounts et al., 2008). More recently, rotational velocity has also been found to correlate best with maximum principle strain and CSDM (Takhounts et al., 2013; Ouckama & Pearsall, 2014). As such, rotational velocity maybe important in describing brain injury and should be considered when assessing the protective capacity of ice hockey goaltender masks.

2.3 Influence of Impact Conditions on Dynamic Response

In order to be able to reconstruct an impact, the impact parameters of a collision must be taken into consideration. As the impact parameters such as impact site, mass, velocity, angle of impact, and compliance of impactor change, the resulting dynamic response curves vary creating unique and different head and brain injuries (Gennarelli et al., 1982; 1987; Zhang et al., 2001a; Kleiven, 2003, Pellman et al., 2003; Post et al., 2012a). The accident events which ice hockey goaltenders can sustain concussion differ in their impact parameters. It is important to understand the influence to which these varying impact parameters have on the dynamic response of the head.

2.3.1. Location

The location on the head where the impact occurs has been shown to have an influence on the resulting brain response and resulting head injury (Gurdjian et al., 1953; Gennarelli et al., 1982; 1987; Hodgson et al., 1983; Zhang et al., 2001a). Frontal impacts have been proven not to be a valid representation of head impacts of varying directions (Gennarelli, 1979; Zhang et al., 2001; Kleiven, 2003). Many studies have found that impacts to the side of the head are more prone to cause injuries than impacts to the forehead (Kleiven, 2003; Zhang et al., 2001a; Zhang et al. 2004; Delaney et al., 2006).

A number of studies have used primates and monkeys to study the effects of impact location. Gurdjian et al. (1982; 1987), used primates to demonstrate that lateral direction rotational

accelerations compared to anterior or posterior rotational acceleration was a more important contributor to concussions. They found that non-centroidal coronal rotation resulted in longer lasting comas compared to acceleration in the sagittal and horizontal directions (Gennarelli, et al., 1982). When subject to lateral impacts the primates displayed DAI in the corpus callosum and brain stem to a comparable degree as observed in severe human brain injury (Gennarelli, et al., 1982; 1987). Hodgson et al. (1983) studied front, side, rear and top impacts in anesthetised monkeys wearing a protective cap to determine the effects of impact site on the tolerance to concussions. Side impacts were found to produce the highest magnitude of linear and rotational acceleration accompanied with the longest period of unconsciousness, reflecting a decreased tolerance to concussion (Hodgson et al., 1983).

Lateral impacts have also been shown to pose a greater risk for injury in studies using finite element analyses and impacts to Hybrid III headforms. Zhang et al. (2001a; 2004) used finite element analyses to identify differences in skull deformations and relative brain dynamic responses between frontal and lateral impacts. Lateral impacts were found to produce higher levels of positive pressure and shear at the core of the brain. This led to the conclusion that lateral impacts have a decreased tolerance to risk of injury due to higher levels of shear and therefore increasing the sensitivity to rotational acceleration. Rousseau and Hoshizaki (2009) impacting a Hybrid III headform found that although rotational accelerations along the x axis did increase for eccentric impacts, they remained well below injury risk proposed by Zhang et al. (2004). However, in comparison rotational accelerations along the y-axis (side of the head) were higher, reaching over 50 percent brain injury risk when impacted through the centre of the head (Rousseau & Hoshizaki, 2009). From previous research it highlights the importance of lateral

frontal impacts compared to frontal impacts. Accident events which are more likely to impact the side of the head will likely pose a greater risk of concussion in ice hockey goaltenders.

2.3.2 Angle of Impact

It is important to consider the angle of impact as it changes the vector of an applied force. This applied force vector will have an effect on the dynamic impact response outcome (Barth et al., 2001) because a force is applied to a rigid body in one axis, creates rotation about the other two axes proportional to the perpendicular distance away from those axes.

Walsh and Hoshizaki (2010) compared resulting peak linear and rotational accelerations of impacts of varying angles to three different impact sites. A 50^{th} percentile head-and neck form was impacted at seven impact angles, which included impacts through the center of gravity, and at 5, 10 and 15 degree increments in both positive and negative directions. The vector components of the linear acceleration were found to vary significantly with impact angle, although the resultant acceleration remained uniform for two of the three impact sites (Walsh & Hoshizaki, 2010). The *x* and *y* vector components of peak linear accelerations showed a trade-off effect, in which if one increased the other decreased. However the *z* axis component remained inconsequential in peak linear acceleration magnitude with changing impact angle. Peak rotational acceleration component vectors were also shown to vary with impact angles; however they did not show an obvious pattern as with linear acceleration (Walsh & Hoshizaki, 2010). In varying the impact angle for side impacts, it produced a dramatic curve in rotation about the *z* axis as a result changes in the *x* and *y* components of linear acceleration. Overall, Walsh and Hoshizaki (2010) were able to reveal that inbound vector angle variation may result in a different dynamic response of the headform as seen through peak linear and peak rotational acceleration, particularly in the individual component vectors.

Research conducted by Walsh et al. (2011) continued to study the influence of impact angle on the response of a Hybrid III head and neckform by assessing multiple impact locations. In varying the impact angle on a location, it has been shown to produce different magnitudes of peak resultant linear and rotational acceleration, in which one was not indicative of the other (Walsh et al., 2011). This led the authors to identify specific impact conditions that are composed of a combination of location and angle that created high linear acceleration and low rotational acceleration when the impact was primarily directed through the center of gravity of the headform (near centric), and those that created low linear acceleration and high when the impact was directed off center (non-centric) creating more of a rotation. Thus when impact angle was varied, it created a non-centric condition which resulted in larger changes in magnitudes of acceleration (Walsh et al., 2011).

Further to support the influence of impact angle, Post et al. (2012a) showed that at a variety of impact vector conditions centred around the same impact site can produce different linear and rotational accelerations. Increasing the angle of impact, results in a decrease in the peak resultant linear acceleration, although peak resultant rotational acceleration showed no significant difference (Post et al., 2012a). It can be seen that a phenomenon occurs when the impact vector moves further from the centre of gravity of the target and produces lower linear acceleration increasing the rotational acceleration (Post et al., 2012a). It is important to determine the angle at which impacts occur in order to properly reconstruct concussive events in ice hockey goaltenders.

2.3.3 Inbound Velocity

Inbound velocity has been shown to influence the dynamic response for falls, projectiles and collisions (Rousseau et al., 2009a; Rousseau et al., 2009b; Post et al., 2013a Post et al., 2012

a; Kendall et al., 2012b; Rousseau et al., 2014). As such it is important to understand how inbound velocity influences the dynamic response for each accident event which ice hockey goaltenders experience.

Post et al. (2012a) reconstructed a fall which resulted in a subdural hematoma (SDH) without the presence of skull fracture for an 85 year old. The reconstruction allowed for a corridor of response in which the impact conditions were a velocity of 4.5 ± 0.5 m/s and angles of 0°, 12° and 24°. As expected, an increase in velocity led to an increased magnitude of the dynamic response, producing a range of dynamic responses across the three velocities of 285-601 g and 28.2-43.2 krad/s^2. A similar response was reported by Kendall et al. (2012b) when dropping Hybrid III and Hodgson-WSU headforms from different drop heights. Both headforms were found to have a linear relationship between linear and rotational accelerations with increasing drop heights (Kendall et al., 2012b), demonstrating both linear and rotational acceleration increase with increasing velocity in falls.

Rousseau et al. (2014) impacted ice hockey helmets and a bare headform with pucks at 17, 23, 29, 35 and 41 m/s. With increasing velocities the peak linear and rotational acceleration were shown to increase for both helmeted and unhelmeted conditions (Rousseau et al., 2014). Just as in falls, linear and rotational acceleration increase with increased velocity for puck impacts.

The influence of increasing velocity has also been documented to increase the magnitude of the dynamic response resulting from an impact in collisions (Rousseau et al., 2009a; Rousseau et al., 2009b; Post et al., 2013a). Rousseau et al. (2009a; 2009b) impacted ice hockey helmets at various velocities using a pneumatic linear impactor to represent player-to-player collisions in ice hockey. Peak linear and rotational accelerations were found to increase with increasing

velocity (Rousseau et al., 2009a; 2009b). Similar results were also found when impacting a bare headform (Rousseau et al., 2009a). Post et al. (2013a) examined the influence of velocity on the performance range of American football helmets. The results showed peak linear acceleration increased with velocity as expected with an increase in the energy of the impact. However, the peak rotational accelerations were similar at 5.5 m/s and 7.5 m/s but increased by approximately 40% for impacts at 9.5 m/s (Post et al., 2013a). The authors suggested this phenomenon is likely due to the linear impactor arm coupling with the helmet shell more effectively at this velocity as well as the helmet materials reaching the end of their functional ranges which forces a larger increase in magnitude for rotation (Post et al., 2013a).

In ice hockey, players can travel up to 30 mph (13.4 m/s) and pucks can exceed 100 mph (44.7 m/s) (Stuart & Smith, 1995). It is important to understand the influence of inbound velocity which has been shown to increase the magnitude of the dynamic response incurred from an impact (Rousseau et al., 2009a; Rousseau et al., 2009b; Kendall et al., 2012b; Post et al., 2012a; Post et al., 2013a; Rousseau et al., 2014).

2.3.4 Impact Mass

When players are anticipating contact, the effect of the impact mass may be lessened as players have the opportunity to prepare themselves, which typically results in a more linear acceleration (Barth et al., 2001). However, in cases where the impact is not expected, the impacting force creates torque, seen as head rotation, which has more severe outcomes (Barth et al., 2001). This effect of impacting mass was demonstrated by Pellman et al. (2003) through NFL impact reconstructions based from video analysis. In a typical player-to-player impact, the struck player was not aware of the striking player. This yielded a higher effective mass for the striking player because initially only the struck player's head is involved in the impact. As a result rapid

changes of head velocity were found (Pellman et al., 2003). Such an effect would be expected in ice hockey goaltenders as the primary focus is on the puck's location and trajectory while guarding the net and the goaltender does not anticipate collisions with players.

Striking techniques have been reported to increase effective impact mass in boxing and football (Viano et al., 2005; Viano et al., 2007; Walilko et al., 2005). Walilko et al., (2005) examined the punch force generated by Olympic boxers from five different weight classes. Higher weight class boxers were found to generate high punch force, in which punch force was the strongest predictor of severity outcomes (HIC, rotational acceleration etc.). The boxer's punch velocity had no significant correlation with weight class, peak punch force, or the severity of the punch. It was concluded that the effective mass of the punch was more important in determining the severity of the impact (Walilko et al., 2005). Effective striking mass of different injury accident events in ice hockey could also influence the severity of an impact. Kendall et al. (2012a) examined three distinct accident events in ice hockey. The peak linear acceleration values for a punch condition were lower than the shoulder and fall to the ice conditions. It can be seen that as mass increases from a 2 kg punch, the peak linear acceleration values increase (Kendall et al., 2012a).

Other studies have used variable mass to demonstrate the influence of striking mass on the response of the head (Hodgson, 1967; Shewchenko et al., 2005; Karton et al., 2013). Hodgson (1967) used variable mass and velocity to study the tolerance of facial bones to fracture. Solid metal cylinders were used for impacts with mass ranging from 0.9 kg to 7.9 kg in order to vary the force of the blow. The primary conclusion drawn from this research was that as the force of the impact increases, the time of fracture decreased (Hodgson, 1967). Research on the effects of ball headings in soccer examined the influence of ball mass, and found a lighter ball mass

provides a benefit for all of the response measures that were examined (Shewchenko et al., 2005). A decreased ball mass of 21-35% resulted in a reduction of up to 23% in peak linear and rotational accelerations measured in the head/neck response (Shewchenko et al., 2005). Karton et al. (2013) also showed an influence of striking mass on dynamic response when impacting centric and non-centric impact locations. Variations of 2 kg in striking mass were shown to influence the head response when the effective striking mass was below 10 kg (Karton et al., 2013). It has been shown that varying mass will vary the response of the head. Selecting the appropriate mass for collisions is essential to ensure the validity of the reconstruction. Rousseau and Hoshizaki (in press) found the effective mass of a shoulder check in ice hockey to be 12.9 ± 3.3 kg and the same mass will be used in this thesis.

2.4 Brain Tissue Deformation

Advanced finite element modeling (FEM) technology have allowed researchers to view injury risk from a brain tissue standpoint (Zhang, et al., 2003; 2004; Horgan & Gilchrist, 2003; 2004; Willinger & Baumgarthner, 2003; Kleiven, 2007). Historically experiments have used human head cadavers to study brain tissue deformation. However, research involving human head cadavers is limited to gross material properties and/or the kinematic response of the head. It is unable to offer information regarding muscle activation, functional changes and cellular/vascular response. Additionally, human head cadavers are often of older age adults and may not represent the population as a whole (Viano et al., 1989). The use of these mathematical models offers some advantages to these limitations as they attempt to represent the actual human system. FEM has the capability to represent the material properties of the brain tissue and demonstrate their respective sensitivity to varying mechanical inputs (Horgan, 2005).

Through the use of finite element modeling, the researcher has additional information to examine the effect of an impact on the deformation of brain tissue and potential injury (Forero Rudea et al., 2010). In real-life situations, an impact to the head rarely produces purely linear or purely rotational acceleration. It is more common that a combination of both linear and rotational acceleration occurs as a result of a head impact. In the past, researchers have made links between head acceleration and brain injury. However, it is suggested that the resulting curve created from an impact is more representative of actual brain injury, rather than the experienced peak resultant accelerations (Post et al., 2012b). Finite element modeling allows for the interpretation of linear and rotational loading curves and how they influence the response of neural tissue. This has led researchers to investigate the relationship between brain tissue stress and strain with injury (Zhang, et al., 2001a).

2.4.1 Human Head Anatomy

The brain is an extremely delicate organ that must be protected from injury but remain in contact with the rest of the body. In order to protect and support the brain it involves (1) the bones of the skull, (2) the cranial meninges, (3) the cerebrospinal fluid (Martini et al., 2009). The skull protects this brain from mechanical protection and the cranial meninges that surround the brain protect the brain from the skull acting as shock absorbers that prevent contact with the surrounding bones (Martini et al., 2009). The cranial meninges consists of three layers: dura mater (outermost), arachnoid mater (middle) and pia mater (innermost). The cranial meninges are connective tissue membranes that lie just external to the brain and serve four primary functions (1) to cover and protect the brain, (2) protect blood vessels and enclose the venous sinuses, (3)) contain cerebrospinal fluid and (4) form partitions within the skull (Marieb, 1998). The cerebrospinal fluid is located in the brain and spinal cord and forms a protective cushion that

gives some buoyancy to the brain. The cerebrospinal fluid effectively reduces the weight of the brain by around 97% and also serves to prevent the brain from crushing under its own weight (Marieb, 1998).

The adult brain has six major divisions: (1) the cerebrum, (2) the diencephalon, (3) the mesencephalon, (4) the pons, (5) the cerebellum and (6) the medulla oblongata (Martini et al., 2009). The cerebrum is the largest part of the brain. It is divided into two large cerebral hemispheres separated by the longitudinal fissure (Martini et al., 2009). The deep portion of the brain attached to the cerebrum is called the diencephalon and contains subdivisions of the epithalamus, thalamus, hypothalamus and pituitary gland (Martini et al., 2009). The mesencephalon, pons and medulla oblongata makes up the brainstem which connects the brain to the spinal cord.

2.4.2 Finite Element Modelling

Three-dimension finite analysis is used to describe the response of the brain tissue during and following an impact. Using finite element models allow for the estimation of cerebral tissue deformation. To do so, finite element models decompose the brain into small elements, in which each element has the material properties of the tissue it represents. The internal stresses and subtle internal motions of the modelled structures can be analyzed to predict injury (Ward & Nagendra, 1985).

One of the earliest three-dimensional head models was developed by Ward and Thompson (1975). This model was validated against experiments by Nahum et al. (1977) on cadavers, for frontal impacts. The model described human head anatomy as linear elastic and included the brain, dura folds, ventricles and brain stem. The skull and cerebrospinal fluid (CSF) were assumed to be rigid and did not include the falx and tentorium (Ward & Thompson, 1975)

The model used in this thesis is the University College Dublin Brain Trauma Model (UCDBTM). The baseline of UCDBTM was validated against cadaveric pressure responses conducted by Nahum et al. (1977) and brain motion research conducted by Hardy et al. (2001). Further validations were conducted by Doorly and Gilchrist (2006; 2007) using reconstructions of real world traumatic brain injury incidents with agreeable results. The geometric parameters of the model were based on Computed Tomography (CT) scans of human male cadaver (Horgan & Gilchrist, 2003; Horgan & Gilchrist, 2004; Horgan, 2005). The head and brain finite element model is comprised of ten parts: the scalp, skull (cortical and trabecular bone), pia, falx, tentorium, cerebrospinal fluid (CSF), grey and white matter, cerebellum and brain stem. In total, the model consists of 26,000 elements in which the scalp, falx and tentorium were modeled using shell elements, cortical bone, trabecular bone, CSF, cerebrum, cerebellum and brain stem using brick elements and the dura with membrane elements.

Horgan and Gilchrist (2003) examined the effects of the bulk and shear modulus of the brain and CSF by way of a parametric study. They found that intracranial pressure and von Misses response was largely effected by the short-term shear modulus of the brain and the bulk modulus had the greatest effect of the *contre*-coup pressure when CSF was modeled using a coupled node definition. Due to such observations of intracranial pressure differences, Horgan and Gilchrist (2003) highlighted the need of carefully modeling for the depth and volume of CSF and the thickness of the skull in order to predict pressure disruption accurately. As such, the cortical and trabecular bone were modeled with brick elements of varying thickness and the depth of the CSF layer was 1.3 mm to simulate the norm for the average adult male. In addition, to simulate the brain skull interface the CSF was model with a high bulk modulus and low shear modulus so that

it would behave in a similar fashion to a fluid. The contact interception at the brain skull interface specified no separation and used a friction coefficient of 0.2 (Miller et al., 1998).

2.4.3 Neural Tissue Deformation Metrics

Research has indicated that brain deformation variables are associated with concussion type injuries. Brain deformation variables which have been associated with and deemed useful in predicting injury risks are strain (Bain & Meaney, 2000; Zhang et al., 2003; Kleiven, 2007), strain rate (Galbraith et al., 1993; Zhang et al., 2003) product of strain and strain rate (King et al., 2003; Zhang et al., 2003), maximum principal strain (Kleiven, 2007), Von Mises stress (Willinger et al., 2001; Anderson et al., 2003; Willinger & Baumgartner, 2003; Kleiven, 2007), and shear stress (Zhang et al.,, 2004). The two brain deformation metrics to be used in this thesis are maximum principal strain and von Mises stress as they have been used in previous research of head injury reconstruction to quantify the amount of brain tissue deformation from head impact (Willinger and Baumgartner, 2003; Zhang et al., 2004; Kleiven, 2007).

2.4.3.1 Maximum Principal Strain

Maximum principal strain is commonly used to represent brain deformation and has been identified as a possible indicator of concussion (Zhang et al., 2004; Kleiven, 2002; Willinger & Baumgarthner, 2003; Zhou et al., 1995). Maximum principal strain is described by tissue elongation relative to its original length. This elongation occurs in the tissue along one of the principle axes (Silva, 2006). That is, the greatest elongation in either the *x*, *y* or *z* axis will be recorded. Maximum principal strain is calculated using the following equation where ε is the strain in a given axis:

$$\varepsilon 1,2 = \frac{\varepsilon_x + \varepsilon_y + \varepsilon_z}{3} \pm \sqrt{\left(\varepsilon_x - \varepsilon_y\right)^2 + \left(\varepsilon_y - \varepsilon_z\right)^2 + \left(\varepsilon_y - \varepsilon_z\right)^2} \qquad [1]$$

2.4.3.2 Von Mises Stress

Von Mises stress is a measure commonly used in engineering that represents a threshold variable or yield criteria for ductile materials. There are three types of stress which can act on the brain tissue. Tensile stress pulls apart the brain tissue, compressive stress pushes the tissue towards itself and shear stress skews it. Von Mises stress takes the sum of all the tensors involved in the stress of a structure and gives a result in uniaxial stress as one value measured in units of pressure. In doing so it accounts for different directions of strain upon an element and is commonly used among researchers (Silva, 2006). Von Mises stress is calculated using the following equation:

$$\sigma = \sqrt{0.6\left[\left(\sigma_x - \sigma_y\right)^2 + \left(\sigma_y - \sigma_z\right)^2 + (\sigma_z - \sigma_x)^2\right]} + \sqrt{+3\left(\tau_{xy}^2 + \tau_{yz}^2 + \tau_{zx}^2\right)} \qquad [2]$$

Where σ is the normal stress in a given axis and τ is the shear stress in a given axis and is measured in Pascals (Pa).

2.5 Proposed Injury Thresholds

The aim of research investigating injury thresholds is to link the mechanism of injury to an engineering variable that could predict the injury. A tolerance level is defined as the magnitude of loading which results in a specific injury at a specified injury severity level (Zhang, 2001b). Research has been conducted in attempts to establish brain injury thresholds for dynamic response and brain tissue deformation (Willinger & Baumgarthner, 2003; Zhang et al., 2004; Kleiven, 2007).

2.5.1 Dynamic Reponses Thresholds

A variety of methodologies have been used to estimate thresholds for sustaining a concussion based on the dynamic responses of the head. Both Kleiven (2007) and Zhang et al. (2004) reconstructed and filmed NFL football impacts using physical models inside a laboratory. Zhang

et al. (2004) proposed threshold values on the basis of 25%, 50% and 80% probability of sustaining a concussion for peak linear and rotational accelerations. These estimated values for linear acceleration were 66, 82, and 106 g and rotational acceleration values of 4600, 5900, 7900 rad/s^2. However, there is some disagreement among these values. Willinger and Baumgarthner (2003) found that concussions were probable when rotational accelerations were approximately 3000-4000 rad/s^2. Rowson et al. (2012) found a 50% probability of concussion for rotational acceleration and velocity to be 6383 rad/s^2 associated with 28.3 rad/s, respectively when 335 collegiate football players' helmets were instrumented with the Head Impact Telemetry (HIT) System. Whereas, McIntosh et al. (2014) reconstructed Australian rules football impacts using Mathematical Dynamic Models (MADYMO) and proposed a 50% probability of concussion for linear acceleration, rotational acceleration and rotational velocity of 65.1 g, 3958 rad/s^2 and 22.2 rad/s respectively. Despite disagreement, Zhang et al. (2004) proposed brain injury thresholds are widely used in the literature and prove to be of use when assessing risk of injury.

Thresholds proposed by Zhang et al. (2004) maybe specific to helmet-to-helmet collisions in football and may not apply to other accident events associated with concussion. Different accident events have been shown to characterize different levels of risk using reconstructive research (Zhang et al., 2004; Kleiven, 2007; Kendall et al., 2012a; Zanetti et al., 2013). Rousseau (2014) reconstructed twenty-seven elite ice hockey collisions involving shoulder-to-head and elbow-to-head contact and found very different results compared to Zhang et al. (2004). For shoulder impacts peak rotational acceleration was found to reliably predict concussion and a 50% probability of sustain a concussion was established at 9.2, 6.9, 4.6, and 2.2 krad/s^2 for impulse durations of 15, 20, 25, and 30 ms, respectively. Whereas, peak linear acceleration was found to reliably predict concussion for extended elbow strikes to the head, in which 23, 15, and

7 g for impulse durations of 15, 20, and 25 ms, respectively (Rousseau, 2014). Demonstrating impacts in ice hockey are associated with a different threshold of injury than football impacts due to different accident events.

2.5.2 Brain Tissue Tolerance Thresholds

Finite element modeling has also been used to establish estimated mTBI thresholds using brain deformation variables. Willinger and Baumgarthner (2003) conducted real world head injury simulations to determine risk of injury. They found von Mises stress values of 18 kPa and 38 kPa to be associated with a 50% risk of moderate and severe neurological lesions respectively (Willinger & Baumgarthner, 2003). Zhang et al. (2004) reconstructed twenty-four head-to-head collisions that occurred in professional football games and proposed threshold values on the basis of 25%, 50% and 80% probability of sustaining an mTBI. Thresholds for shear stress in the midbrain were estimated as 6.0, 7.8, and 10.0 kPa respectively, while strain levels for the grey matter were about 0.14, 0.19 and 0.24, respectively (Zhang et al., 2004). Kleiven (2007) also reconstructed head to head collisions in professional football to determine risk of sustaining a concussion. Von Mises stress of 8.4 kPa and maximum principal strain of 0.21 in the corpus callosum or 0.26 in the grey matter of the brain represented a 50% probability of concussion (Kleiven, 2007). Rousseau (2014) reconstructed elite ice hockey collisions involving shoulder and elbow impacts. A 50% risk of sustaining a concussion for maximum principle strain were values of 0.30, 0.14, and 0.15 following a shoulder check, extended elbow strike, or tucked-in elbow strike to the head, respectively (Rousseau, 2014). It is important to consider the above tolerance thresholds with consideration, as different brain models can produce different responses to the same input (Deck & Willinger, 2009) and different events have been shown to produced different brain stresses and strains (Zhang et al., 2004; Kleiven, 2007; Kendall et al.,

2012a; Zanetti et al., 2013; Post et al., 2015b). As such, the proposed tolerance thresholds may be specific to the brain model used and the accident event analyzed.

2.6 Accident Events

Recent research has shown that the most common accident events leading to TBI and concussion in sports involves: falls, collisions, punches and projectiles (Kendall et al., 2012a). Each of these accident events creates a unique impact condition that influences the direction and magnitude of the dynamic response and subsequent brain tissue deformation stresses and strains (Post et al., 2013; Karton et al., 2013). The resulting brain injury caused by these accident events is influenced by the impact characteristics involved, such as impact location, mass, velocity, compliance of the surface (stiffness), and impact vector (Hoshizaki et al., 2013). In ice hockey there is a high risk for concussion due to high speeds, physical contact and rigid objects (Delaney, 2004). Players can reach skating speeds of up to 30 mph (48 km/h) and sliding speeds of up to 15 mph (24 km/h) (Sim & Chao, 1978; Bancroft, 1989; Goodman et al., 2001). This poses a particular risk to goaltenders from collisions with out of control players, as their primary objective is to secure the net and prevent the puck from going into their own goal (LaPrade et al., 2009). Furthermore, goaltenders are the last line of defence for pucks reaching velocities of up to 120 mph (193 km/h), which given its weight of 170 g, translates into approximately 567 lbs (258 kg) of force (Sim & Chao, 1978). As a result of this environment ice hockey goaltenders have suffered concussions from collisions, falls and puck impacts, where collisions with players were the most common accident event resulting in concussion. Other contacts such as impacts to the ice and puck impacts make up a smaller protection of reported concussions (LaPrade et al., 2009). Little research has reconstructed the accident events leading to injuries associated with concussion in ice hockey goaltenders and to date, research has focussed on the accident events

leading to concussion in hockey skaters and other sports. This research must be examined to gain perspective into the response of the head and brain tissue for goaltenders.

2.6.1 Falls

Falls are the most common accident event leading to brain injury in the population (Styrke et al., 2007). Typically impacts from falling result in high magnitude and short duration linear and rotational acceleration (Post et al., 2012a; Post, 2013; Post et al., 2014a). This high magnitude and short duration linear and rotational acceleration most frequently results in TBI (Hoshizaki et al., 2013). Such high magnitude events have been seen in the reconstruction of real world TBIs (Doorly and Gilchirst, 2006; Post et al., 2012a; Post et al., 2013b). Doorly and Gilchirst (2006) reconstructed falls of an 11 year old boy who sustained a right lateral frontal intra-cerebral haemorrhagic contusion and a traumatic subarachnoid haemorrhage and a 76 year old woman whom sustained a large parenchymal haemorrhage of the right temporal lobe, and a small focal bleed on the cortical surface of the left frontal lobe. Simulations using Mathematical Dynamic Models (MADYMO) revealed linear and rotational accelerations 366.36 g and 36.945 krad/s^2, respectively for the boy and 236.52 g and 33.887 krad/s^2 for the woman. The resulting stress and strain levels from these accelerations were in agreement with previous literature (Doorly and Gilchirst, 2006). Post et al. (2012) reconstructed a fall which resulted in a subdural hematoma (SDH) without the presence of a skull fracture for an 85 year old which resulted in a range of dynamic responses across three velocities of 285-601 g and 28.2-43.2 krad/s^2. In reconstructing falls to study the influence of dynamic response and brain deformation metrics on the occurrence of SDH in different regions of the brain, Post et al. (2013b) also observed high magnitude responses. When looking at the pure magnitude of the responses in peak linear and rotational accelerations causing SDHs in distinct regions, the parietal lobe was found to be the highest

(462.6 g and 53859 rad/s^2), followed by the frontal lobe (372.4 g and 30690 rad/s^2) and the occipital lobe has the lowest (311.8g and 22371 rad/s^2) which resulted in maximum principal strain, von Mises stress, shear strain, and product of strain and strain rate for focal SDH consistent with values reported in the literature (Post et al., 2013b).

A great deal of effort has been undertaken in order to reduce the risk of TBI by setting injury thresholds used in helmet standard development (Hoshizaki and Brien, 2004). As such skull fractures and other TBIs have largely disappeared from sports, the incidence of concussions remains common (Wennberg and Tator 2003). As a result, even when wearing a helmet, falling has been shown to be associated with a high risk of concussion in ice hockey. Kendall et al (2012a) compared three common accident events associated with concussion in ice hockey and it was found that a fall to the ice generated the linear acceleration and maximum principal strain. The resulting values revealed linear acceleration, rotational acceleration and maximum principal strain to be 264.4 g, 11204 rad/s^2 and 0.424, respectively Kendall et al (2012a). Thus the linear and rotational acceleration values obtained are above 80% risk (106 g and 7900 rad/s^2) for concussion (Zhang et al., 2004) and the peak maximum principal strain value obtained in the prefrontal cortex was greater than those associated with 50% risk (0.19 – 0.26) for concussion (Zhang et al., 2004; Kleiven, 2007). This shows a great risk of concussions due to falls when wearing a player's helmet and similar results would be expected if a goaltender mask was worn. Furthermore, it has also been seen by Pellman et al. (2003) in research of professional American football players and research by Lincoln et al. (2013) of boy's high school field lacrosse that a secondary impact of a player's head impacting the ground may contribute to a concussion. Out of control players colliding with goaltenders and knocking them over could pose a high risk of concussion. Thus the reconstruction of falls in ice hockey goaltenders is important to consider.

2.6.2 Collisions

Collisions between two players are the cause of the majority of concussions in ice hockey (Gerberich et al., 1987; Flik et al., 2005; Delaney et al., 2006; Hutchinson, 2011). While goaltenders are not thought of as being involved in collisions, LaPrade et al. (2009) found such collisions to be a common accident event resulting in concussion when studying injuries in NCAA intercollegiate ice hockey goaltenders. All seven head injuries in men's ice hockey goaltenders resulted in concussion and were caused by contact with a player in four cases, while five of the six head injuries to women's ice hockey goaltenders resulted in concussion with three being caused by player contact (LaPrade et al., 2009). These types of collisions with goaltenders can occur as a result of a player who loses control while on a breakaway, body checks where players may be pushed into the goal crease or from on-ice altercations where contact may be made with the goaltender (Liberman & Mulder, 2007). It is important to minimize the number of collisions to protect goaltenders and avoid the incidence of head trauma for this position. As no previous research has examined collisions to ice hockey goaltenders, collisions involving elbow shoulder and helmet impacts in ice hockey and football can be used to gain a perspective into the response of the head to collisions.

Research reconstructing flagrant fouls in ice hockey can give some insight into what might occur if a skater's elbow collides with a goaltender. Coulson et al. (2009) recruited eight male hockey players in order to reconstruct various flagrant fouls in ice hockey to determine the peak linear and rotational accelerations of a Hybrid III head form. Of particular interest to collisions is the reconstruction of elbow impacts. Coulson et al. (2009) had participants strike a headform moving at 0.56 ± 0.11 m/s with maximal force. Coulson et al. (2009) found mean peak linear and rotational accelerations for elbowing trials to be below 25% probability of sustaining a

concussion proposed by Zhang et al. (2004). Individual peak linear acceleration generated during elbowing trials was well above 50% probability thresholds and in individual peak rotational accelerations was above 80% probability threshold, highlighting how dangerous elbowing an opponent can be as it is highly probable that this striking technique will lead to a concussive injury. The severity of elbow impacts to goaltenders could be greater due to collisions with out of control players having greater inbound velocities than elbow impacts conducted in Coulson et al. (2009). Increases in velocity have been found to increase accelerations experienced by a headform (Post et al., 2013a). As elbowing is the most common illegal play in ice hockey, and the majority of concussions resulting from illegal play are the result of elbowing (Flik et al., 2005).

Shoulder impacts provide another accident event which has been shown to have a high risk of concussion. Kendall et al. (2012a) found shoulder impacts to the side (centre of gravity) of the headform to produce peak linear and rotational accelerations of 112.5 g and 9659 rad/s^2, which are above 50% risk for concussion (Zhang et al., 2004; Kleiven, 2007). Average maximum principle strain (MPS) values were found to be 0.035 which are associated with 50% risk for concussion. Further, the shoulder was found to produce the highest MPS values in the dorsal-lateral prefrontal cortex (0.370) and primary motor cortex (0.370) (Kendall et al., 2012a), demonstrating the high risk of concussion shoulder impacts pose to ice hockey skaters. Rousseau (2014) reconstructed real world shoulder checks and found impacts resulting in concussion had much lower average peak linear and rotational acceleration values of 28 ± 7 g and 3.6 ± 1.1 krad/s^2 but similar maximum principle strain values of 0.30 ± 0.08. The differences experienced by these two studies are likely due to difference in compliance of the impactor striker used. Kendall et al. (2012a) used an impacting striker fitted with a hemispherical nylon pad covering a

modular elastomer programmer (MEP) 60 Shore Type A (0.05m thick) disc covered with a Pro shoulder pad with a plastic cap. Whereas Rousseau (2014) using a more complaint striker which consisted of a nylon disc covered with a 142 mm thick layer of vinyl nitrile R338V foam and a Reebok 11k shoulder pad. The compliance of this impactor was selected as it was found to produce a linear acceleration peak and duration similar to shoulder checks to a Hybrid III headform performed by ice hockey players (Rousseau & Hoshizaki, 2015). However, goaltenders wear different helmets than skaters and the response of the headform may not accurately reflect that of goaltenders as differences in shell geometry, foam type, and foam may influence the response (Rousseau et al., 2009a). Shoulder impacts are an important accident event to examine in ice hockey goaltenders.

Helmet to helmet collisions can pose a risk of concussion to ice hockey goaltenders as they can collide with out of control players. Research in American Football and ice hockey has reconstructed helmet to helmet impacts and allow for an understanding of how the head responded to such impacts. Zantetti et al. (2013) compared helmet to helmet impacts of three different player positions in American Football. By reconstructing impacts to a linebacker, wide receiver and lineman it allowed for variations in velocity, mass and location. The results showed that all three positions produced significantly different dynamic responses and maximum principle strain. The three dependent variables were highest in the linebacker (158.7 g, 10 361.7 rad/s^2 and 0.616) followed by the wide receiver (54.9 g, 5570 rad/s^2 and 0.213) and the lineman produced the lowest (31.6 g, 1951rad/s^2 and 0.112) (Zanetti et al., 2013). The linebacker represents a high risk of concussion for both linear and rotational acceleration (Zhang et al., 2004), whereas maximum principle strain thresholds proposed by Kleiven (2007) associate both the linebacker and wide receiver were at a risk of concussion. The differences in these results

would account for the difference in impact parameters. Both the linebacker and wide receiver impacts occurred to the side of the head, whereas the lineman impact was to the front of the head. Impacts to the side of the head have been shown to result in higher dynamic response than impacts to other locations (Guskiewicz & Mihalik, 2006). In addition, the high mass that was present in the lineman reconstructions (28kg) was not present in the other reconstructions and may have had less of an influence on the injury severity than other impact characteristics such as location and velocity (Zanetti et al., 2013). An inbound mass greater than 10 kg has been found to have comparatively less of an influence on the dynamic response and brain tissue deformation (Karton et al., 2013). In the reconstruction of helmet-to-helmet collisions in goaltenders the impact characteristics will likely shape the dynamic response and brain tissue deformation experienced.

2.6.3 Projectiles

Injuries caused by projectiles typically involve impacts where the head is hit with a low mass, high velocity projectile such as a baseball or hockey puck. These impacts produce very short duration of linear and rotational acceleration pulses through the brain tissue as a result of the very high velocity of the projectile object (approx. 35 – 40 m/s) (Rousseau et al., 2014). As the goaltenders primary role is to prevent pucks from entering the goal, this subjects goaltenders to such impacts and risk of injury.

Limited research has assessed puck impacts to an ice hockey goaltender mask. Nur et al. (submitted) compared the performance of four ice hockey goaltenders masks to protect the athlete from puck impact as measured by head acceleration and peak force when impacted by pucks. The findings indicated that the masks had some performance differences. The differences in accelerations among the masks were likely due to the type of padding (foam), the density of

the padding, and the amount of padding of the mask (Rousseau et al., 2009a). Further Nur et al. (submitted) found that thicker masks produced lower peak force values than thinner masks. However despite performance differences no one mask proved superior to the others in terms of injury prevention. When goalie masks were impacted at 25 m/s it was found that nearly all of the impacts produced linear and rotational accelerations below the 25% probability of sustaining a concussion. Only chin impacts to mask 1 generated a rotational acceleration of 4796 rad/s^2 which is associated with 25% risk of concussion (Zhang et al., 2004). In assigning the peak forces Nur et al. (submitted) found all impacts except for chin and side impacts on mask 2 produced a peak force which exceed 132.4 N associated with a threshold for contusions (Bush et al., 2010). It was demonstrated at 25 m/s goaltenders can sustain contusions but there is a low risk for sustaining a concussion. However, pucks can travel much faster than 25 m/s as the official National Hockey league record for a slap shot was set at 48 m/s (174 km/h) and skilled amateur players can shoot the puck at velocities above 20 m/s (108 km/h) (Roy & Dore´, 1975; Pearsall et al., 1999; Gilenstam et al., 2009; Wu et al., 2003). Thus has research examining the protective capabilities of ice hockey goaltenders masks has been limited to 25 m/s, greater puck velocities must be examined to understand the effect of puck impacts in a game situation.

Rousseau et al. (2014) tested the capacity of ice hockey helmets to reduce head accelerations and brain deformation following a puck impact at 17, 23, 29, 35 and 41 m/s. It was found that peak linear acceleration, peak rotational acceleration and peak maximum principal strain (MPS) were significantly reduced for helmeted trials compared to bare headform at all five tested velocities (Rousseau et al., 2014). At 17 and 23 m/s, the helmeted data showed peak linear accelerations below 50% risk of concussion (Zhang et al., 2004). However, the helmet was only able to keep peak rotational accelerations below a 50% risk for 17 m/s (Zhang et al., 2004). The concussion

thresholds proposed by Zhang et al. (2004) were calculated using a logistic regression analysis of 21 reconstructed head impacts, which occurred in the National Football League. The proposed concussion risk may be specific to head-to-head collisions in football, although there is currently no data available for proposed concussion risk as a result of puck impacts. As such, the thresholds proposed by Zhang et al. (2004) give values which can be used for comparative proposes. Similar results to Rousseau et al. (2014) were found by Ouckama & Pearsall (2014) when subjecting five ice hockey helmet models to puck impacts. Ouckama & Pearsall (2014) found the majority of impacts at 24.2 m/s resulted in linear and rotational acceleration below 50% risk of concussion (Zhang et al., 2004). Whereas, impacts at 33 m/s resulted in linear and rotational acceleration exceeding 80% risk of injury (Zhang et al., 2004). Furthermore, Rousseau et al. (2014) found that impact at 23 m/s and above was found to produce MPS associated with concussion (Kleiven, 2007; Galbraith et al., 1993; Bain & Meaney, 2000; Yu et al., 2009; Cater et al., 2006; Elkin & Morrison, 2007). Thus, for puck impacts at high velocities there is a high risk of concussion (Ouckama & Pearsall, 2014; Rousseau et al., 2014).

It has also been shown that the performance of a helmet decreases after the first impact at 35 m/s and above (Rousseau et al., 2014). This indicates that a helmet should be changed after one impact of a puck. It is especially important to do so at the professional level as impacts at 41 m/s for the second and third impacts generated peak acceleration above 250 g, which is an average of the values found in the literature for frontal bone fractures (Yoganandan & Pintar, 2004). Goaltenders who act as the last line of defence face multiple impacts to the head in a single game and are at risk of serious injury. As such it is important to reconstruct puck impacts to the head of goaltenders to understand the level of protective ice hockey goaltenders mask provide.

2.7 Summary

Concussions remain a major health and safety concern in sports. In ice hockey current helmet testing certifications are primarily concerned with the prevention of TBI. As a result TBI has largely disappeared from the sport of ice hockey but concussions remain a concern. Previous research has made attempts to establish injury thresholds for dynamic response and brain tissue deformation. However, such thresholds may be accident events specific as different accident events have been shown to characterize different levels of risk. This is due to different accident events creating unique impact conditions that influence the direction and magnitude of the dynamic response and subsequent brain tissue deformation stresses and strains. The resulting brain injury caused by these accident events is influenced by the impact characteristics involved, such as impact location, mass, velocity, compliance of the surface (stiffness), and impact vector. As ice hockey goaltenders can sustain concussion for collisions, falls and projectiles, there lies importance in understanding how these accident events influence the dynamic response and brain tissue deformation in order to better protect ice hockey goaltenders.

Chapter 3. Methods

The main objective of this research was to assess the protective capacity of ice hockey goaltender masks for three accident events associated with concussion. Events resulting in concussion in ice hockey goaltenders were identified, captured on video and analyzed to determine impact parameters. The impact parameters were used to define the impact conditions for falls, collisions and projectiles. Three impact locations and three velocities were selected to represent each accident event. A helmeted and unhelmeted medium NOCSAE headform attached to an unbiased neckform (Walsh & Hoshizaki, 2012) was used to assess the protective capacity of ice hockey goaltenders masks. Peak linear accelerations were measured using a "3-2-2-2" array of accelerometers mounted in the NOCSAE headform and rotational accelerations were calculated to describe the dynamic impact response (Padgaonkar et al., 1975). Rotational velocity was also determined by integrating the resulting rotational acceleration. The dynamic response from the impacts served as input into the UCDBTM to determine the deformation response characteristics, von Mises stress and maximum principal strain, within the brain tissue.

3.1 Dynamic Impact Testing

3.1.1 Hockey Equipment

In the case of collisions a Reebok 11k shoulder pad was used as the impacting surface to simulate shoulder-to-head impacts. A commercially available puck (0.166lg) was used to simulate puck-to-head impacts. Nine commercially available CCM 9000 goaltenders mask were tested. The mask is made of a fiberglass shell, a carbon steel cage and VN foam liner. All ice hockey goaltenders masks used in this study were certified by Canadian Standards Association (CSA).

3.1.2 NOCSAE Headform and Unbiased Neckform

A medium NOCSAE headform and an unbiased neckform were used for all impact conditions. The NOCSAE headform with a mass of 4.85 ± 0.01 kg was attached to an unbiased neckform with a mass of 2.11 ± 0.01 kg (Walsh & Hoshizaki, 2012) (Fig. 1). The NOCSAE headform was based on cadaveric data and was designed to respond similarly to the human head to an impact (Hodgson & Thomas, 1971). The unbiased neckform was created to match the mass and dimensions of the Hybrid III neckform with four centred and unarticulated rubber butyl disks of radius 68.0 mm and height 21.5 mm recessed slightly and serially inside aluminium disks measuring 85.6 mm in radius and 12.8 mm in height (Walsh & Hoshizaki, 2012). The Hybrid III neckform was designed and validated for impacts in the anterior/posterior direction (y-axis) and it is unknown how the bias will influence the dynamic impact response of a headform. The unbiased neckform has been designed to respond the same to impacts in all directions and therefore eliminate any potential biased effects of the Hybrid III neckform (Walsh & Hoshizaki, 2012).

Figure 1: NOCSAE headform and unbiased neckform

Nine calibrated single-axis Endevco7264C-2KTZ-2-300 accelerometers (Endevco, San Juan Capistrano, CA) were fixed in an orthogonal position near the centre of gravity of the headform using the "3-2-2-2" array developed to measure and calculate three-dimensional motion during an impact (Padgaonkar et al., 1975). Three accelerometers were mounted at the centre of gravity of the headform, two at the front (F), two on the side (S) and two on the top (T) (Fig. 2). The following equations were used to calculate the rotational acceleration based on first principles of rigid body dynamics and linear accelerations:

$$\overrightarrow{\alpha_x} = \frac{\overrightarrow{a_{zS}} - \overrightarrow{a_{zC}}}{2S} - \frac{\overrightarrow{\alpha_{yT}} - \overrightarrow{a_{yC}}}{2T} \qquad [3]$$

$$\overrightarrow{\alpha_y} = \frac{\overrightarrow{a_{xT}} - \overrightarrow{a_{xC}}}{2T} - \frac{\overrightarrow{\alpha_{zF}} - \overrightarrow{a_{zC}}}{2F} \qquad [4]$$

$$\overrightarrow{\alpha_z} = \frac{\overrightarrow{a_{yF}} - \overrightarrow{a_{yC}}}{2F} - \frac{\overrightarrow{\alpha_{xS}} - \overrightarrow{a_{xC}}}{2S} \qquad [5]$$

Where α_i is the rotational acceleration for the component $i\ (x, y, z)$ and a_{ij} is for the linear acceleration for component $i\ (x, y, z)$ along the orthogonal arm $j\ (S, T, F)$ (Padgaonkar et al., 1975). The right-hand rule was used to define the coordinate system for the headform (Walsh et al., 2011) in which the positive axis is directed towards the right ear and caudally for the *x*, *y* and *z*, respectively (Walsh et al., 2011).

Figure 2: Orthogonally positioned 3-3-3-2 accelerometer array.

In order to determine the rotational velocity the resulting rotational accelerations must be integrated. The following equation was used to calculate the rotational velocity.

$$\overrightarrow{\omega_i} = \int_0^T \overrightarrow{\alpha_i}\, dt + c_1 \qquad [6]$$

Where ω_i is the rotational velocity for the component i (x, y, z), α_i for the rotational acceleration for component i (x, y, z), $c_1 = \omega_{i-1}$ and T is the time interval between samples.

3.1.3 Monorail Drop Rig

The monorail drop rig consists of a 4.7 m long rail and has a drop carriage in which the NOCSAE headform and an unbiased neckform was attached (Fig. 3). The 4.7 m track was bolted to the wall and the ceiling to minimize the movement of the system and background noise or vibration. The drop carriage runs along rails on ball bushings to reduce the effects of friction on the inbound velocity of the headform and was released by a pneumatic piston. A Modular Elastomer Programmer (MEP) anvil was used to simulate a goaltender's head hitting the playing surface. The base of the anvil was fixed to the floor by 6 concrete bolts. The monorail drop rig was connected to a computer equipped with Cadex Software (Cadex Inc., St-Jean-sur-Richelieu,

QC); a multi-functional program used to set up the impact parameters. The desired inbound velocity of the impact was entered into the software program. This triggered the carriage to rise to the corresponding drop height.

Figure 3: Monorail drop rig with unhelmeted NOCSAE headform attached.

3.1.4 Pneumatic Linear Impactor

The pneumatic linear impactor consists of three major components: the support/piston frame, the impacting arm and the table housing the NOCSAE headform. The frame supports the impacting arm, the compressed air canister and the piston (Fig. 4a). The pneumatic piston was fired via an electronically controlled solenoid with the air supplied from the compressed air canister which propels the impacting arm (mass = 13.1 ± 0.1kg) towards the headform. The mass of the impacting arm was similar to that calculated for shoulder-to-head impacts in ice hockey reconstructions (Rousseau & Hoshizaki, 2015). The end of the impacting arm in the case of shoulder impacts was fitted with a striking surface consisting of a nylon disc (diameter 13.2 mm) covered with a 142 mm thick layer of vinyl nitrile R338V foam and a Reebok 11k shoulder pad (Fig. 4b). This striker was found to produce a linear acceleration peak and duration similar to that

of ice hockey players for impacts to the temporal region of a Hybrid III headform at low and high velocities (Rousseau & Hoshizaki, 2015).

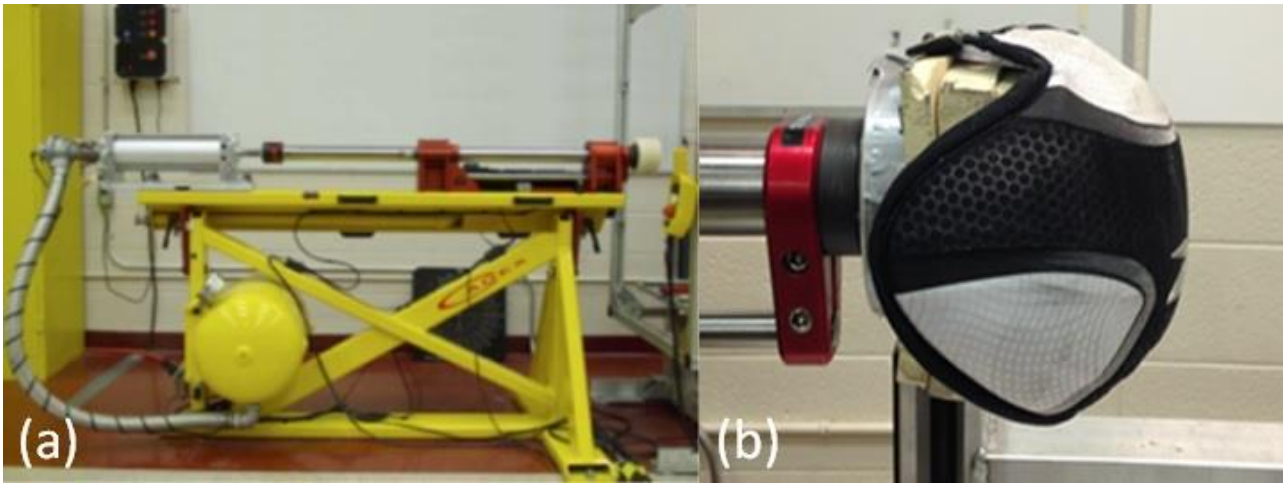

Figure 4: Pneumatic Linear Impactor: (a) frame supporting the impacting arm, (b) shoulder pad striker.

3.1.5 Pneumatic Puck Launcher

The pneumatic puck launcher (Fig. 5) consists of three major components: the support frame, air cannon and the table housing the NOCSAE headform. The frame supports an air cannon and the compressed air canister. The puck was fired by compressed air which is operated electronically by a control station. The puck travels 0.6200 ± 0.0005 m down the barrel of the puck launch before it was released.

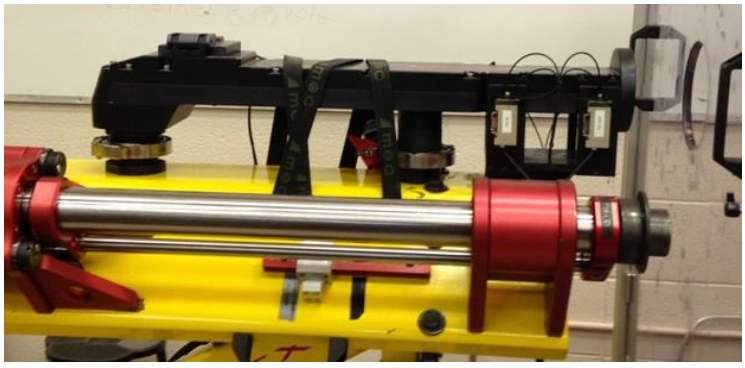

Figure 5: Pneumatic puck launcher.

3.1.6 Sliding Table

In impact conditions which used the pneumatic linear impactor or pneumatic puck launcher, the NOCSAE headform was supported by a low-friction sliding table (mass = 16.6 ± 0.1kg) (Fig . 6). The sliding table runs on a ball bearing installed on the bottom of the table that allow it to slide backwards with little resistance upon impact. The table was able to traverse backwards 0.54m after impact, allowing it to react in a realistic manner after impact. A foam braking system was used to stop the headform and sliding table after impact. A movable locking base on the table was used to attach the headform. This movable locking base allowed the headform to be oriented in five degrees of freedom: fore-aft (x), lateral (y) and up-down (z) translation, as well as fore-aft (y) and axial rotation (z) and remain fixed in position during testing.

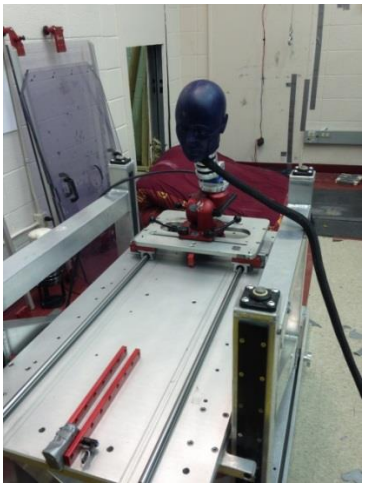

Figure 6: Sliding table with NOCSAE head and unbiased neckform attached.

3.2 University College Dublin Brain Trauma Model

A finite element model of the brain developed at the University College Dublin named the University College Dublin Brain Trauma Model (UCDBTM) (Horgan & Gilchrist, 2003; 2004) was used in this thesis. The head geometry of the UCDBTM was derived from computed tomography (CT) and magnetic resonance imaging scans (MRI) of a male human cadaver (Horgan and Gilchrist, 2004). The model of the head and brain consists of 26, 000 hexahedral

elements representing the scalp, skull, pia, falx, tentorium, CSF, grey and white matter, cerebellum and brain stem (Horgan & Gilchrist, 2003; 2004). The material characteristics of the model were taken from Ruan (1994), Willinger et al. (1995), Zhou et al. (1995), and Kleiven and von Holst (2002) (Tables 1 and 2).

Table 1: Material properties of UCDBTM

Material	Young's modulus (MPa)	Poisson's Ratio	Density (kg/m^3)
Scalp	16.7	0.42	1000
Cortical Bone	15000	0.22	2000
Trabecular Bone	1000	0.24	1300
Dura	31.5	0.45	1130
Pia	11.5	0.45	1130
Falx	31.5	0.045	1140
Tentorium	31.5	0.45	1140
CSF	Water	0.5	1000
Grey Matter	Hyperelastic	0.49	1060
White Matter	Hyperelastic	0.49	1060

Table 2: Material characteristics of the brain tissue for the UCDBTM

Material	G_0	G_∞	Decay Constant (Gpa)	Bulk Modulus (s^{-1})
Cerebellum	10	2	80	2.19
Brain Stem	22.5	4.5	80	2.19
White Matter	12.5	2.5	80	2.19
Grey Matter	10	2	80	2.19

The material behaviour of the brain tissue was modeled as viscoelastic in shear with a deviatoric stress rate dependent on the shear relaxation modulus (Horgan & Gilchrist, 2003). The compressive behaviour of the brain is considered elastic. The nature of the shear characteristics of the viscoelastic behaviour of the brain was defined using the following equation:

$$G(t) = G_\infty + (G_0 - G_\infty)e^{\beta t} \qquad [7]$$

Where G_∞, is the long term shear modulus, G_0, is the short term shear modulus and β is the decay factor (Horgan & Gilchrist, 2003). To simulate the skull brain interface, the cerebral spinal

fluid (CSF) was modeled using solid elements with low shear modulus and a high bulk which allows it to behave like water. The contact interaction at the skull brain interface was assigned no separation and used a friction coefficient of 0.2 (Miller et al., 1998). The brain shear is modeled as hyperelastic and is represented by the following equation:

$$C_{10}(t) = 0.9C_{01}(t) = 620.5 + 1930e^{-\frac{t}{0.008}} + 1103e^{-\frac{t}{0.15}}(Pa) \qquad [8]$$

where C_{10} is the mechanical energy absorbed by the material when the first strain invariant changes by a unit step input and C_{01} is the energy absorbed when the second strain invariant changes by a unit step (Mendis et al., 1995; Miller & Chinzei, 1997) and t is the time in seconds. The results of the model are displayed as a gradient of high to low deformation that is experienced throughout the brain tissue, resulting from impact (Fig. 7).

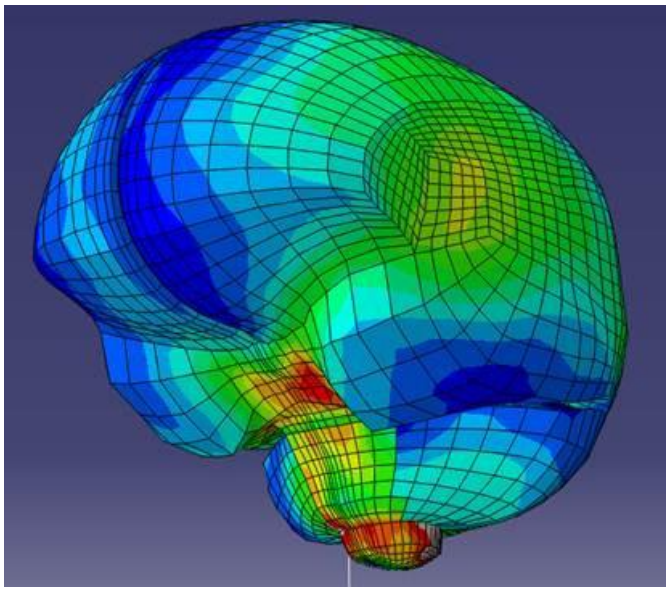

Figure 7: UCDBTM showing a gradient of high to low deformation throughout the brain

3.3 Research Design

To describe the capacity of ice hockey goaltender masks to reduce the dynamic response and tissue response characteristics within the brain, the research of this thesis consisted of bare helmeted impacts as seen in Tables 3-5 and bare headform impacts outlined in Table 6.

Table 3: Fully crossed 6 x 4 research design for falls to a helmeted headform

	A1	**A2**	**A3**
B1	A1B1	A2B1	A3B1
B2	A1B2	A2B2	A3B2
B3	A1B3	A2B3	A3B3

Legend:

Velocity:

A1: 3.5 m/s

A2: 4.2 m/s

A3: 5.0 m/s

Location:

B1: Rear-D

B2: L4-D

B3: R3-D

Table 4: Fully crossed 6 x 4 research design for collisions to a helmeted headform

	C1	**C2**	**C3**
D1	C1D1	C2D1	C3D1
D2	C1D2	C2D2	C3D2
D3	C1D3	C2D3	C3D3

Legend:

Velocity:

C1: 5.2 m/s

C2: 7.3 m/s

C3: 9.1 m/s

Location:

D1: R3-C

D2: R2-E

D3: R1-B

Table 5: Fully crossed 6 x 4 research design for projectile impact to a helmeted headform

	E1	**E2**	**E3**
F1	E1F1	E2F1	E3F1
F2	E1F2	E2F2	E3F2
F3	E1F2	E2F3	E3F3

Legend:

Velocity:

E1: 29.3 m/s

E2: 35.8 m/s

E3: 42.3 m/s

Location:

F1: Front-D

F2: R1-B

F3: R3-D

Table 6: Research design for bare headform impacts

	B1	B2	B3	D1	D2	D3	F1	F2	F3
G1	B1G1	B2G1	B3G1	-	-	-	-	-	-
G2	-	-	-	D1G2	D2G2	D3G2	-	-	-
G3	-	-	-	-	-	-	F1G3	F2G3	F3G3

Legend:

Velocity:

G1: Fall, 3.5 m/s G2: Collison, 5.2 m/s G3: Projectile 29.3 m/s

3.3.1 Procedures

3.3.1.1 Event Identification and Video Capture

A search was conducted through the National Hockey League's (NHL) injury reports for diagnosed concussions sustained by goaltenders occurring between the 2000-2001 and 2013-2014 seasons. All concussion recorded were diagnosed by a medical doctor. A combination of TSN.ca and rotoworld.com was used in order to search through goaltenders' injury history. Details of concussive events were recorded using information obtained from these two sources. The information obtained was then used to search through the internet for videos of injuries occurring before the 2007-2008 season. The information obtained for injuries occurring during the 2007-2008 to 20013-20014 was used to search through game film available on NHL GameCenter provided by nhl.com. When a concussive event was found, it was recorded using WM capture 7 (San Anselmo, CA) with a frame rate of 25 fps and a bit rate of 6000 Kbps. The capture video was then analyzed.

3.3.1.2 Video analysis

A primary video analysis was performed using the Heads Up Checklist (HIUC) (Hutchinson et al., 2013a; Hutchinson et al., 2013b; Hutchinson et al., 2014). The HIUC is a standardised framework for coding accident events leading to concussions in ice hockey using digital video images (Hutchinson et al., 2013b). As such it was used to code accident events and determine if

the event was a single impact to the head. Concussive events which are a result of multiple impacts to the head will be excluded from further analysis.

Further video analysis was completed using Kinovea 0.8.20 (open source, kinovea.org) in order to determine impact parameters. In order to determine the impact velocity and angle, a scaling reference must be established on the playing surface. Professional ice hockey games are played on an ice surface which adheres to the dimensions and specifications of their respective league. The ice rinks are 61.0 m in length and 25.9 m in width and covered in markings (lines and circles) which can be used to identify location and distances (Fig. 8). If a sufficient number of lines and circles are provided within the plane of view of a camera which, a scaling reference can be created, which can convert pixels to meters. By establishing a perceptive plane, it allowed for the measurement of distances and angles on the playing surface. The velocity of an impact was calculated by measuring the distance between the struck player and the impacting surface (Fig 9).

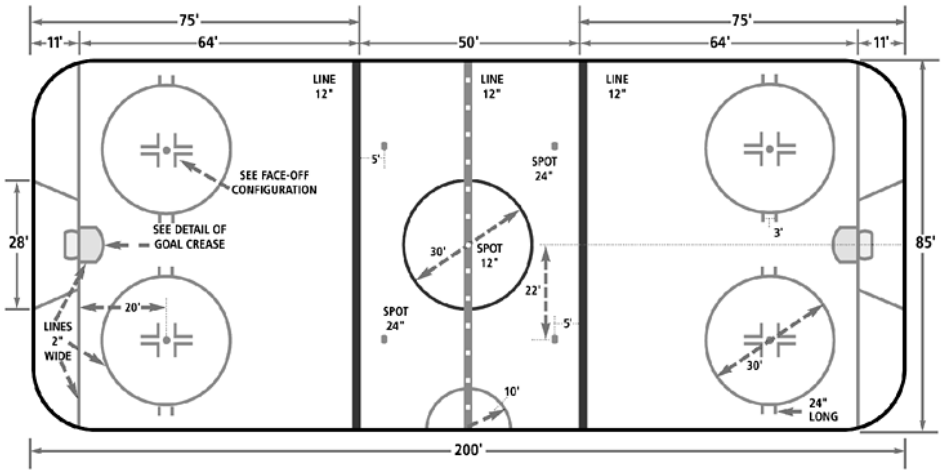

Figure 8. Standard ice rink in North America with dimensions, in feet (imperial unit).

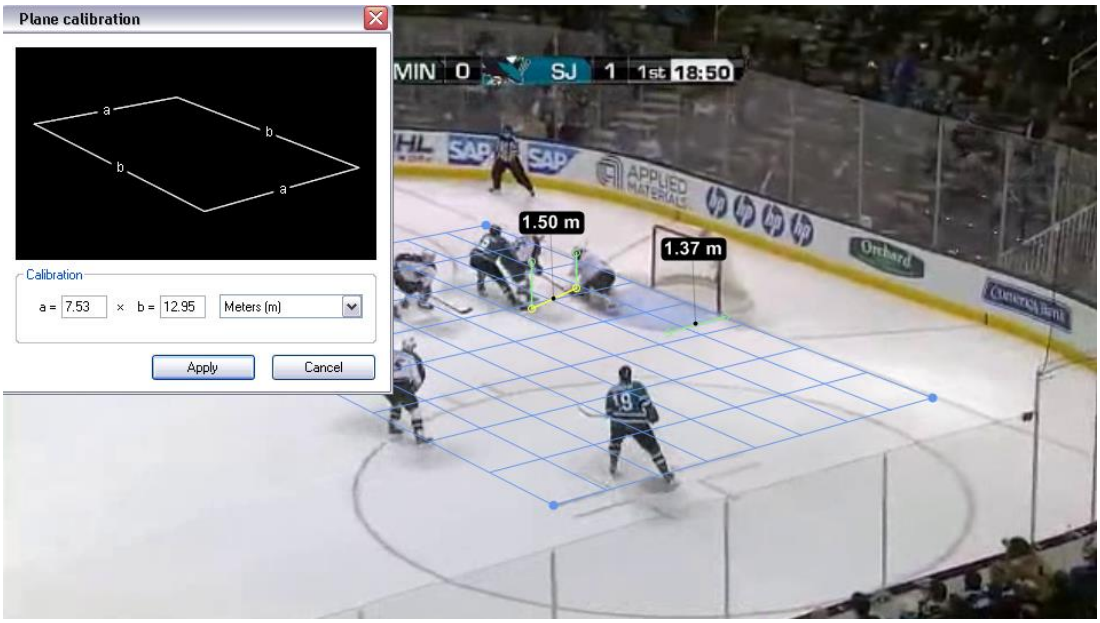

Figure 9: Example of a perspective grid calibration used to calculate velocity in ice hockey.

The following equation will be used to determine the impact velocity:

$$v = \frac{d}{\left(\frac{F}{f}\right)} \qquad [9]$$

Where v, is the impact velocity, d, is the distance, F, is the number of frames and f is the frame rate. Errors associated with the conversion of pixels to meters have been assessed by performing the scaling process for three different events and measuring a third known distance (Rousseau, 2014). The influence of the error was found to be ± 5 % and has been accounted for by adding a lower and upper bound velocity to the reconstructions (Rousseau, 2014). The impact angle was determined by measuring between the angle orientation of the head and the inbound impactor (Fig. 10). If no camera angle of the impact provides a sufficient number of lines and circles to create a scaling reference the case was excluded.

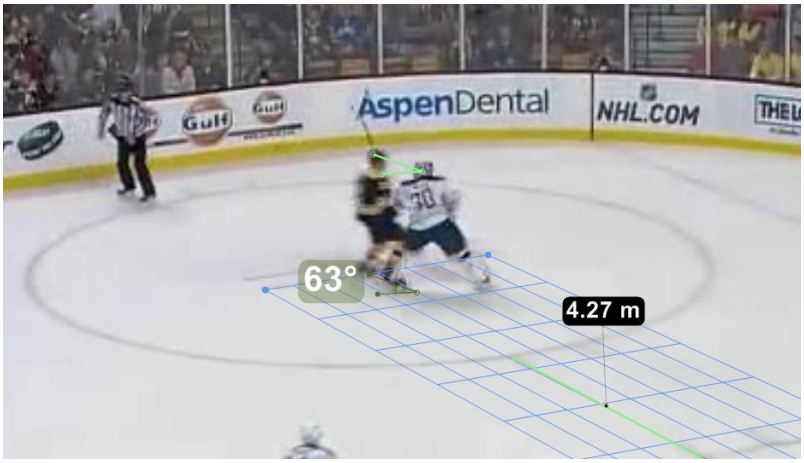

Figure 10: Example measurement of impact angle.

The location of impact location was labelled using a reference illustrated in Figure 11 (Rousseau, 2014). In one coordinate system the head was divided in 12 sectors of 30° in the transverse plan. In which eyes forward is 0°. In the second coordinate system the head was divided into 6 levels in the sagittal plane. This reference system created rectangular regions of at most 5cm in width, where the head circumference is the longest and 4.51 cm in height (Rousseau, 2014). Rousseau (2014) found the level of precession provided by this system to be comparable to other studies reporting impact location (Crisco et al., 2010; Fréchède and McIntosh, 2009; Hutchison, 2011; Mihalik et al., 2008; Pellman et al., 2003).

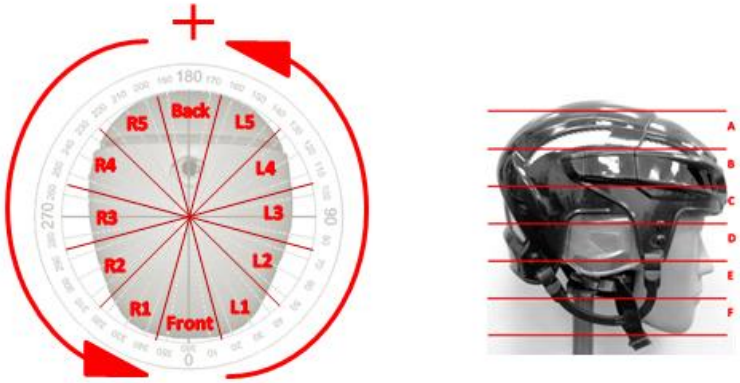

Figure 11: Top and side view of a head illustrating the 12 sectors and five levels used in the reconstruction protocol.

The impact elevation was also determined. To simplify the determination of impact elevation, and head elevations, impact elevation was determined separately. Head elevation was defined as the angle the neck is pitched relative to the vertical. Impact elevation was defined as the angle the impactor travels relative to horizontal. In the case where there was both a head elevation and impact elevation, the two angles were used to determine the overall elevation.

3.3.1.3 Test Protocol

The protective capacity of ice hockey goaltender masks was assessed. In order to assess the protective capacity of ice hockey goaltenders mask a helmeted NOCSAE headform was impacted by three accident event conditions at three locations and three velocities unique to each accident event. The bare headform was also impacted at the lowest velocity for each accident event condition to assess the baseline performance of the ice hockey goaltender mask. The three accident events assessed were falls, collisions and projectiles. The locations and velocities for each accident event condition were defined by real world concussions suffered by ice hockey goaltenders. The locations were selected based on frequency of occurrence. Low, medium and high incidence locations were selected. The velocities chosen were based on magnitude, in which the lower range, mean and upper range velocities for each accident event was selected. Each impact condition was performed three times for a total of 108 impacts. A total of nine ice hockey goaltender masks were tested. Three masks were used for each accident event and a new mask was tested at each velocity.

A variety of impact reconstruction equipment was used in order to simulate the three accident events seen to cause concussions in ice hockey goaltenders. Falls were reconstructed using a monorail drop rig with a MEP anvil to simulate the head impacting the ice. The headform was dropped at inbound velocities of 3.5, 4.2 and 5.0 m/s and impact the locations of Rear-D, R4-D

and R3-D. A pneumatic linear impactor fitted with a shoulder pad striker was used to reconstruct collisions, simulating shoulder-to-head impacts (Rousseau & Hoshizaki, 2015). The inbound velocities were 5.2, 7.3 and 9.1 m/s and impact at R3-D, R2-E and R1-B locations. To reconstruct the projectile condition a pneumatic puck launcher was used to launch a puck at the headform in order to simulate puck impacts. Pucks were launched at velocities of 29.3, 35.8 and 42.3 m/s to the locations of Front-D, R1-B and R3-D.

3.3.1.4 Finite Element

In order to input the resulting dynamic response for the reconstructions into the finite element model an elemental rotation was applied to the coordinate system. To align the coordinate system of the NOCSAE headform and the finite element model the coordinate system of the NOCSAE headform must be rotated 25° clockwise in the y-axis. The following elemental rotation was applied to rotate the coordinate system of the NOCSAE headform

$$R_y(\theta) = \begin{bmatrix} \cos(\theta) & 0 & \sin(\theta) \\ 0 & 1 & 0 \\ -\sin(\theta) & 0 & \cos(\theta) \end{bmatrix} \qquad [10]$$

Where, θ is the angle by between the coordinate system of the NOCSAE headform and the finite element model. The element rotation was validated for head impacts using a dynamic impact testing protocol. An adult 50th percentile Hybrid III headform (4.54 ± 0.01 kg) was attached to an unbiased neckform (2.11 ± 0.01 kg) (Walsh & Hoshizaki, 2012). The accelerometers were mounted on a block in a 3-2-2-2 accelerometer array (Padgaonkar et al., 1975). The accelerometers block was mounted at the centre of gravity of the headform in a flat orientation (0°) and an angled orientation in which the coordinate system was rotated 25° clockwise in the y-axis (Appendix A, Fig. 33). A pneumatic linear impactor fitted with a striker consisting of hemispherical nylon pad and 35.71 ± 0.01 mm thick vinyl nitrile 602 foam disk underneath was

used to impact the headform at 5 m/s for four impact sites. (Appendix A, Fig. 34). Three impacts were performed for each impact condition. The element rotation shown in Equation 10 was applied to the conditions in which the accelerometer block was mounted at an angled orientation. Mean linear and rotational acceleration-time histories were calculated for the resultant and each component (x, y, z) of each impact condition. A 95% confidence interval of the difference was applied to each mean linear and rotational acceleration-time history in order to compare the shape of the loading curves. The resulting linear and rotational acceleration-time histories are presented in Appendix A Figures 35-38. The results demonstrated that both accelerometer block orientations produced mean linear and rotational acceleration-time histories similar in shape, direction and magnitude for both the resultant and each component (x, y, z). As the rotated linear and rotational acceleration-time histories performance similar loading curves the resulting brain tissue deformation stresses and strains will produce similar results (Post et al., 2012b). Therefore, the element rotation described in Equation 10 was deemed valid for head impacts and can be applied to resulting dynamic response in order to use finite element analysis to describe brain injury risk.

The resulting dynamic response served as input to the finite element model, the UCDBTM. This model was used to approximate the magnitude and location of peak maximum principle strain (MPS) and von Mises stress (VMS) in the cerebrum which goaltenders experience during the three accident events. The cerebrum was divided into ten regions which represent functional areas associated with the symptoms of concussion (Fig 12) (Pellman et al., 2004). These ten regions have particular roles in motor and physiological human response and if any injury occurs it may be represented by losses of functioning as represented by these distinct regions (Table 7).

Segmenting the brain in such a method allows for the identification of changes in stress and strain levels in these regions according to the type of injury reconstructed.

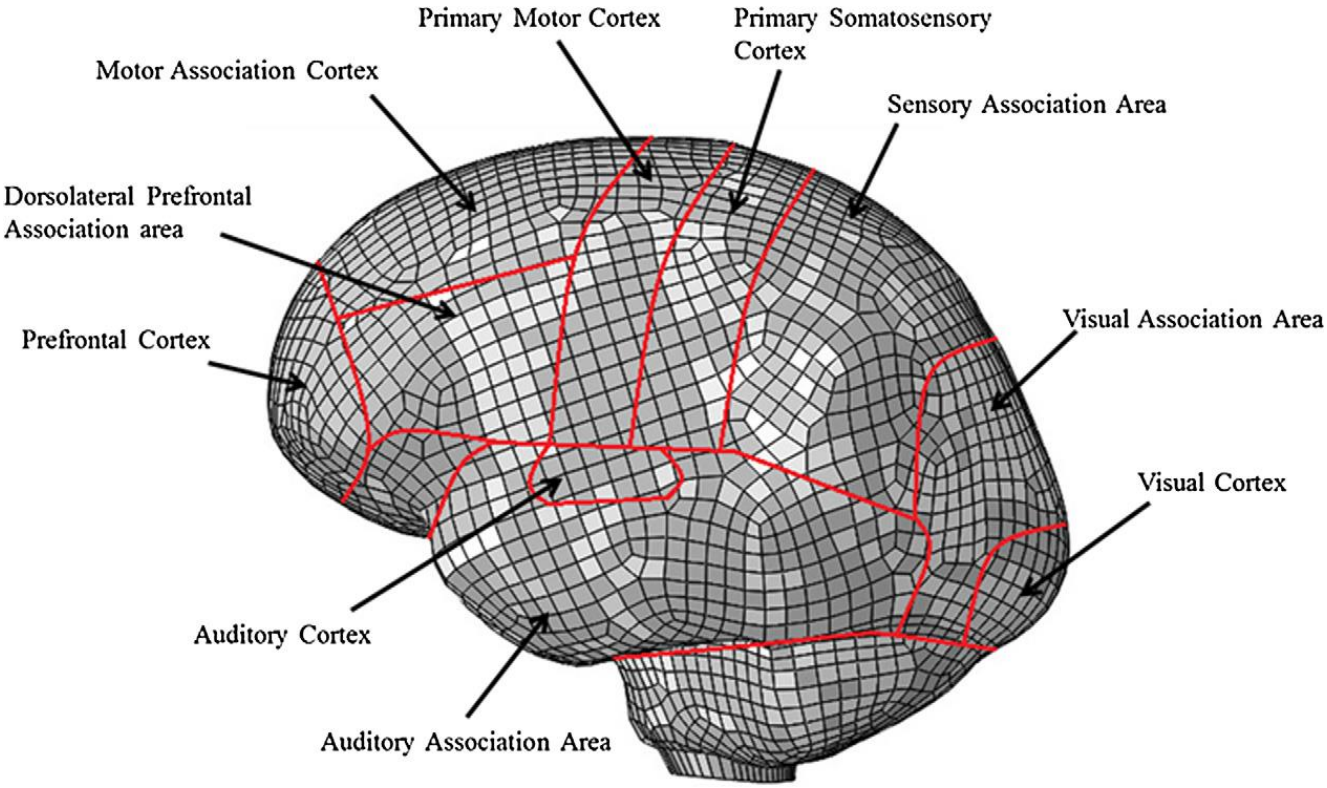

Figure 12: The ten regions of the brain analysed by the UCDBTM.

Table 7: Functionality of the ten brain regions used in this thesis

Region of the Brain	Functionality	Reference
Prefrontal Cortex	Decision-making and social behaviour	Yan et al. (2009)
Dorsolateral Prefrontal Association Area	Memory and organization	Yan et al. (2009)
Motor Association Cortex	Planning and execution of movement patterns	Luppino & Rizzolatti (2001)
Primary Motor Cortex	Planning and execution of movement patterns	Luppino & Rizzolatti (2001)
Primary Somatosensory Cortex	Sense of touch and proprioception	Price (2000)
Sensory Association Area	Sensory integration and perception of the environment	Price (2000)
Visual Association Area	Sensory integration and perception of the environment	Price (2000)
Visual Cortex	Visual information	Braddick et al. (2001)
Auditory Association Area	Sound recognition	Purves et al. (2001)
Auditory Cortex	Sound processing	Creutzfeldt et al. (1989a; 1989b)

3.3.2 Data collection and Processing

The inbound velocity of the impact was collected in various ways depending on the system used. The linear impactor and puck inbound velocities were collected by National Instruments VILogger and analyzed using Bioproc 2 (data analysis software developed by Dr. D.G.E. Robertson, University of Ottawa, 2008). The inbound velocity for the monorail drop rig was measured using a photoelectric time gate placed within 0.02 m of the impact site. Signals from the nine accelerometers were collected at 20 KHz by a TDAS Pro Lab system (DTS, Seal Beach CA) and filtered through a 1000 Hz low pass Butterworth filter using SAE J211 Class 1000 protocol (SAE, 2007). Data analysis and filtering was completed using BioProc3, software developed by Dr. D.G.E. Robertson, University of Ottawa (2008).

3.3.3 Statistical Analysis

All data were expressed as mean and standard deviations. The velocities and locations selected from video analysis of concussive events are described in Tables 3-5 (p.55). To assess the protective capacity of ice hockey goaltender masks the data was separated by accident event, location and velocity conditions. Independent sample t-tests were then used to compare each dependent variable (peak linear acceleration, peak rotational acceleration, peak rotational velocity, VMS and MPS) in the helmeted and unhelmeted condition. Unhelmeted data was removed from further statistical analysis. One-way ANOVAs with the independent variables accident event (falls, collisions and projectiles) were used to analyze the five dependent variables: peak linear and rotational acceleration and rotational velocity, MPS and VMS to compare the effect of accident events. One-way ANOVAs were conducted by collapsing all the velocities and locations selected from the video analysis for each accident event. To examine the influence of velocity and location, data was separated by accident events. Then Two-way ANOVAs with the independent variable of velocity and location were used to analyze the five dependent variables: peak linear and rotational acceleration and rotational velocity, MPS and VMS. The Two-way ANOVAs were performed by conducting one two-way ANOVA for each dependent variable in which all velocities and locations selected from the video analysis were analyzed together. When significant was found a post hoc Tukey test was performed. The probability of making a type 1 error for all comparisons was set at $\alpha=0.05$. All data analyses was performed using the statistical software package of SPSS 19.0 for Windows (SPSS Inc, Chicago, IL, USA).

Chapter 4. Results

The overall objective of this study was to assess the performance of an ice hockey goaltender mask for three accident events associated with concussion. To assess the protective capacity of ice hockey goaltender masks, independent sample t-tests were completed. To determine the effect of accident events, one-way ANOVAs were conducted. Two-way ANOVAs were completed to examine the influence of velocity and location of impact. The following section presents the results for both the dynamic response and brain deformation.

4.1 Dynamic Response Results

The mean and standard deviations for peak resultant linear and rotational acceleration and rotational velocity for falls are shown in Tables 8.

Table 8: Mean peak dynamic response (±1 standard deviation) for the NOCSAE headform from falls.

Location	Velocity (m/s)	No Helmet/Helmet	Linear Acceleration (g)	Rotational Acceleration (rad/s^2)	Rotational Velocity (rad/s)
Rear-D	3.5	No Helmet	180.4 (4.2)	9517 (124)	28.8 (2.0)
		Helmet	67.5 (2.9)	2019 (124)	9.5 (0.6)
	4.2	Helmet	98.5 (4.7)	4137 (146)	15.5 (1.1)
	5.0	Helmet	149.5 (4.9)	6236 (432)	24.3 (1.7)
L4-D	3.5	No Helmet	157.9 (0.5)	13253 (149)	31.5 (0.1)
		Helmet	36.1 (4.2)	2962 (99)	18.0 (0.7)
	4.2	Helmet	70.3 (4.8)	5710 (845)	23.7 (1.2)
	5.0	Helmet	164.2 (14.4)	10317 (707)	35.4 (1.6)
R3-D	3.5	No Helmet	208.4 (8.5)	14626 (823)	32.8 (1.5)
		Helmet	63.5 (3.8)	3334 (148)	16.9 (0.5)
	4.2	Helmet	101.3 (6.2)	4693 (542)	21.3 (0.1)
	5.0	Helmet	174.2 (6.0)	11274 (1903)	38.5 (3.8)

Table 9 presents the mean and standard deviations for peak resultant linear and rotational acceleration and rotational velocity for projectiles.

Table 9: Mean peak dynamic response (±1 standard deviation) for the NOCSAE headform from projectiles.

Location	Velocity (m/s)	No Helmet/Helmet	Linear Acceleration (g)	Rotational Acceleration (rad/s^2)	Rotational Velocity (rad/s)
Front-D	29.3	No Helmet	166.7 (4.7)	23281 (437)	14.6 (0.7)
		Helmet	28.9 (1.5)	3667 (116)	5.7 (0.2)
	35.8	Helmet	37.9 (1.7)	3470.4 (266)	6.8 (0.9)
	42.3	Helmet	45.7 (8.3)	5160 (2043)	8.6 (1.6)
R1-B	29.3	No Helmet	94.0 (1.3)	14655 (1060)	11.1 (0.6)
		Helmet	33.1 (0.4)	3540 (174)	5.6 (0.3)
	35.8	Helmet	43.0 (0.4)	4358 (570)	6.5 (0.2)
	42.3	Helmet	51.7 (1.4)	4663 (687)	6.7 (1.5)
R3-D	29.3	No Helmet	68.5 (1.5)	7640 (343)	4.8 (0.20)
		Helmet	31.6 (1.6)	2246 (800)	2.3 (1.0)
	35.8	Helmet	44.5 (0.4)	4882 (276)	4.0 (0.1)
	42.3	Helmet	56.4 (0.6)	5496 (217)	3.9 (0.5)

Mean and standard deviations for peak resultant linear and rotational acceleration and rotational velocity produced collisions are presented in Table 10.

Table 10: Mean peak dynamic response (±1 standard deviation) for the NOCSAE headform from collisions.

Location	Velocity (m/s)	No Helmet/Helmet	Linear Acceleration (g)	Rotational Acceleration (rad/s^2)	Rotational Velocity (rad/s)
R3-C	5.2	No Helmet	30.0 (0.7)	1703 (73)	26.5 (0.4)
		Helmet	26.2 (0.8)	1604 (61)	21.5 (0.5)
	7.3	Helmet	40.4 (0.6)	2310 (133)	24.3 (0.6)
	9.1	Helmet	48.1 (3.3)	2932 (209)	26.6 (1.5)
R2-E	5.2	No Helmet	18.6 (0.5)	3047 (161)	36.6 (1.0)
		Helmet	18.2 (0.7)	2216 (231)	27.1 (1.5)
	7.3	Helmet	25.9 (0.3)	3241 (117)	30.8 (1.5)
	9.1	Helmet	30.8 (0.8)	3809 (265)	32.4 (5.1)
R1-B	5.2	No Helmet	23.0 (0.7)	1814 (150)	24.0 (0.2)
		Helmet	19.4 (0.4)	1555 (53)	17.2 (1.7)
	7.3	Helmet	29.8 (0.4)	2441 (78)	20.8 (1.1)
	9.1	Helmet	32.8 (0.7)	2443 (233)	18.6 (4.1)

4.1.1 Independent Samples T-tests

Independent sample t-tests were conducted for each dynamic response variable to assess the protective capacity of ice hockey goaltender masks as measured by peak linear and rotational acceleration and rotational velocity. The velocities and locations used for analysis are presented in Tables 3-6 (p. 55 - 56).

4.1.1.1 Linear Acceleration

Helmeted conditions for falls produced significantly lower peak linear acceleration compared to unhelmeted falls for all conditions ($p < 0.01$). Helmeted projectile impacts produced significantly lower peak linear acceleration compared to unhelmeted projectile impacts for all conditions ($p < 0.01$). Collisions to a helmeted headform resulted in significantly lower peak linear acceleration compared to collisions to a bare headform for impacts to locations R3-C and R1-B ($p < 0.01$). However there was no significant difference between helmeted and unhelmeted collisions to R2-E ($p > 0.05$). Therefore, all null hypotheses regarding the effect of ice hockey goaltenders mask compared to a bare headform on peak linear acceleration were all rejected, except for collisions to the R2-E location. Figure 13 shows the mean peak linear accelerations obtained for all accident events to an unhelmeted and helmeted condition at low velocities.

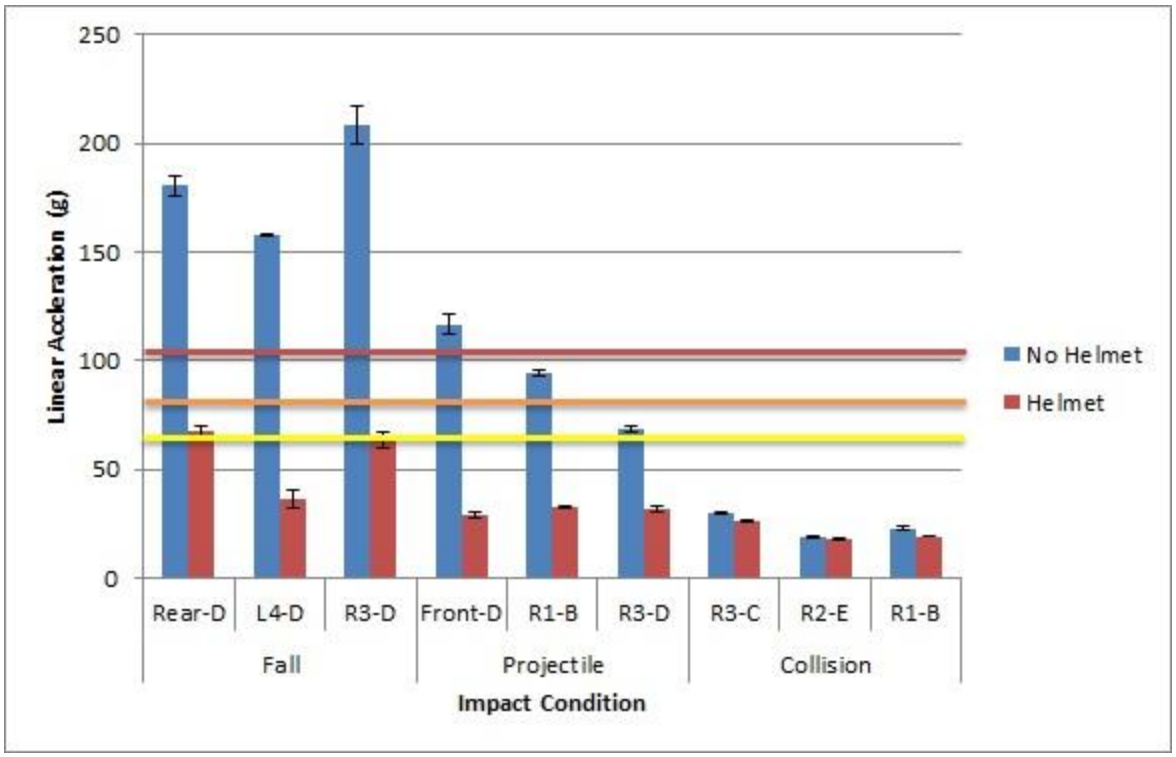

Figure 13: Mean peak linear accelerations for helmeted and unhelmeted impacts at low velocities of each accident event. The three lines represent a 25 (yellow), 50 (orange) and 80 % (red) probability of sustaining a concussion (Zhang et al., 2004).

4.1.1.2 Rotational Acceleration

Falls for a helmeted headform resulted in significantly lower peak rotational acceleration compared to falls for an unhelmeted headform for all fall conditions ($p < 0.01$). All projectile impacts to a helmeted headform produced significantly lower peak rotational acceleration compared to projectile impacts to an unhelmeted headform ($p < 0.01$). Helmeted collisions resulted in significantly lower peak linear acceleration compared to unhelmeted collisions for impact locations R2-E ($p < 0.01$) and R1-B ($p < 0.05$). There was no significant difference between helmeted and unhelmeted collisions to R3-C ($p > 0.05$). As a result, all null hypotheses regarding the effect of ice hockey goaltender's masks compared to a bare headform on peak rotational acceleration were all rejected, except for collisions to the R2-E location. Mean peak linear accelerations obtained for all accident events to an unhelmeted and helmeted conditions at low velocities are shown in Figure 14.

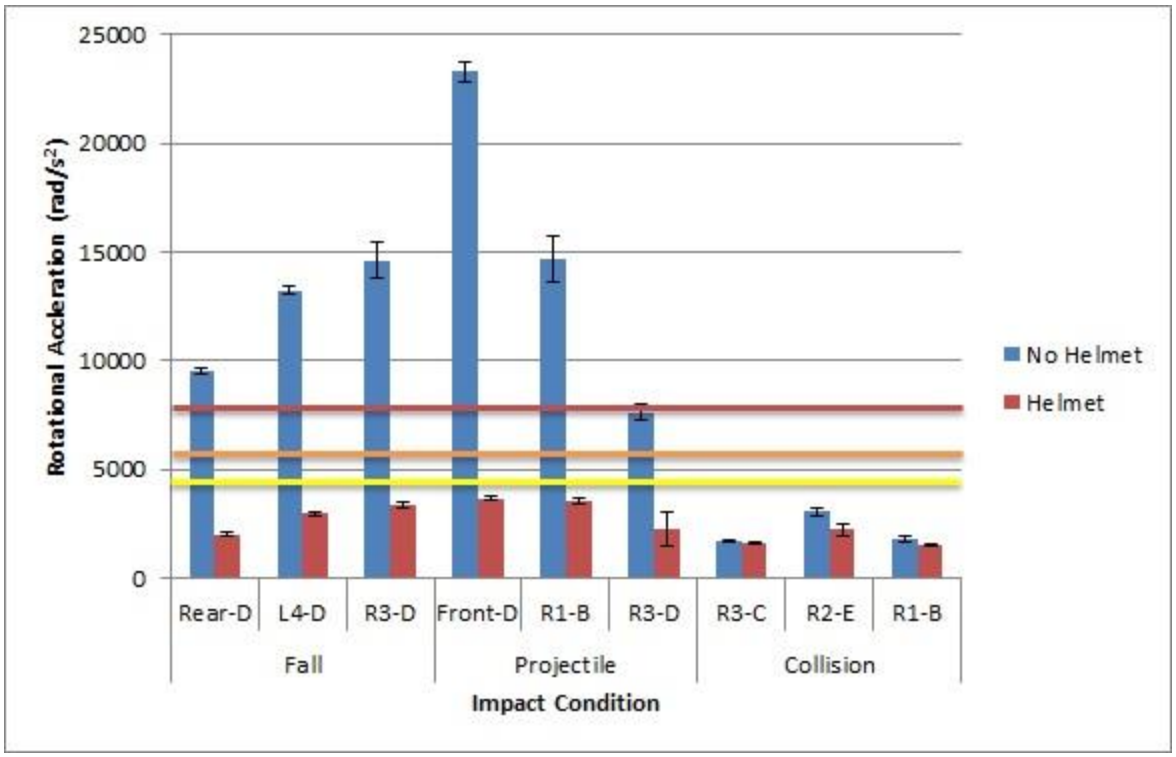

Figure 14: Mean peak rotational accelerations for helmeted and unhelmeted impacts at low velocities of each accident event. The three lines represent a 25 (yellow), 50 (orange) and 80 % (red) probability of sustaining a concussion (Zhang et al., 2004).

4.1.1.3 Rotational Velocity

Peak rotational velocity was found to be significantly lower in all helmeted fall conditions compared to unhelmeted fall conditions ($p < 0.01$). All helmeted projectile impacts produced significantly lower peak rotational velocities compared to unhelmeted projectile impacts ($p < 0.05$). Peak rotational velocity for all collisions to a helmeted headform was found to be significantly lower than collisions to an unhelmeted headform ($p < 0.01$). All null hypotheses regarding the effect of ice hockey goaltender's masks compared to a bare headform on peak rotational velocity were all rejected. Figure 15 presents mean peak rotational velocities obtained for all accident events to an unhelmeted and helmeted condition at low velocities.

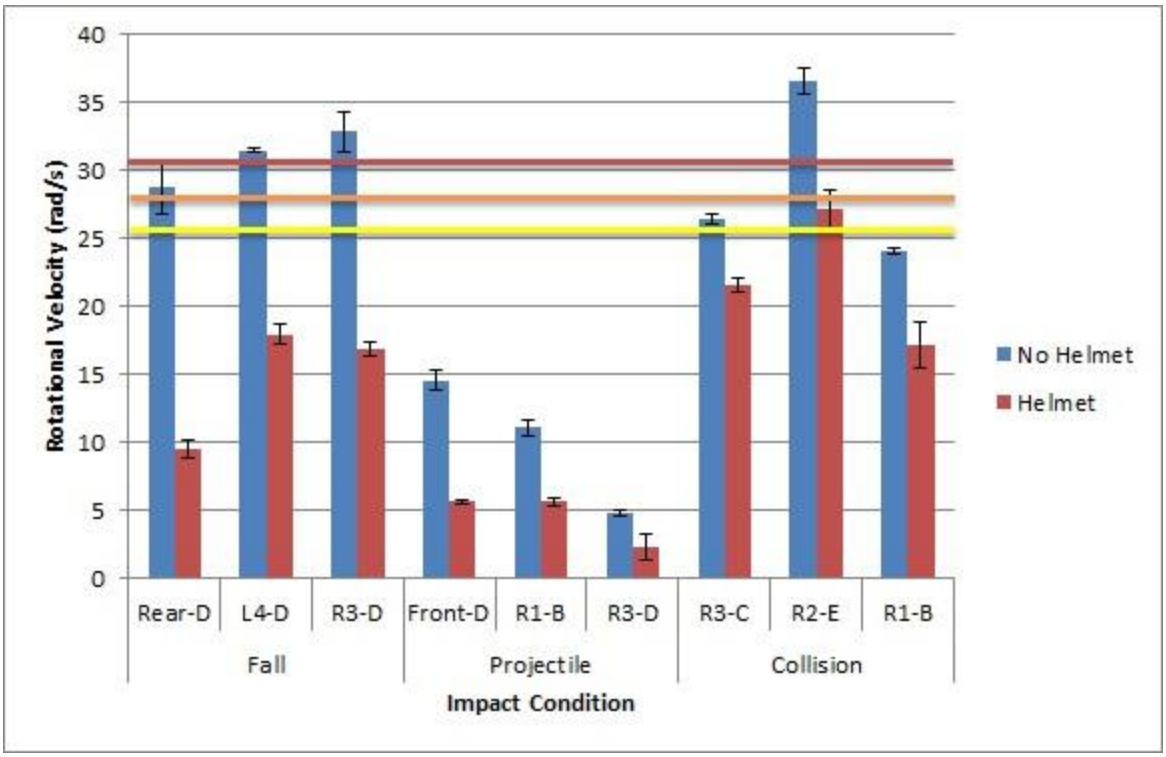

Figure 15: Mean peak rotational velocities for helmeted and unhelmeted impacts at low velocities of each accident event. The three lines represent a 25 (yellow), 50 (orange) and 80 % (red) probability of sustaining a concussion (Zhang et al., 2004).

4.1.2 One-Way Analysis of Variance (ANOVA)

One-way ANOVAs were conducted to determine the effect of accident events on peak linear and rotational acceleration and rotational velocity. Tables 3-5 (p. 55) present the velocities and locations analysed.

4.1.2.1 Linear Acceleration

For peak linear acceleration, there was a significant main effect for accident events ($p < 0.01$). The null hypothesis regarding the effects of accident event on peak linear acceleration was rejected. Tukey post hoc tests revealed peak linear acceleration was significantly different for fall/projectile and fall/collision ($p < 0.01$) but no significant difference was found between projectile and collisions ($p > 0.05$). Figure 16 presents the mean peak linear accelerations obtained of helmeted impacts for each of the three accident events.

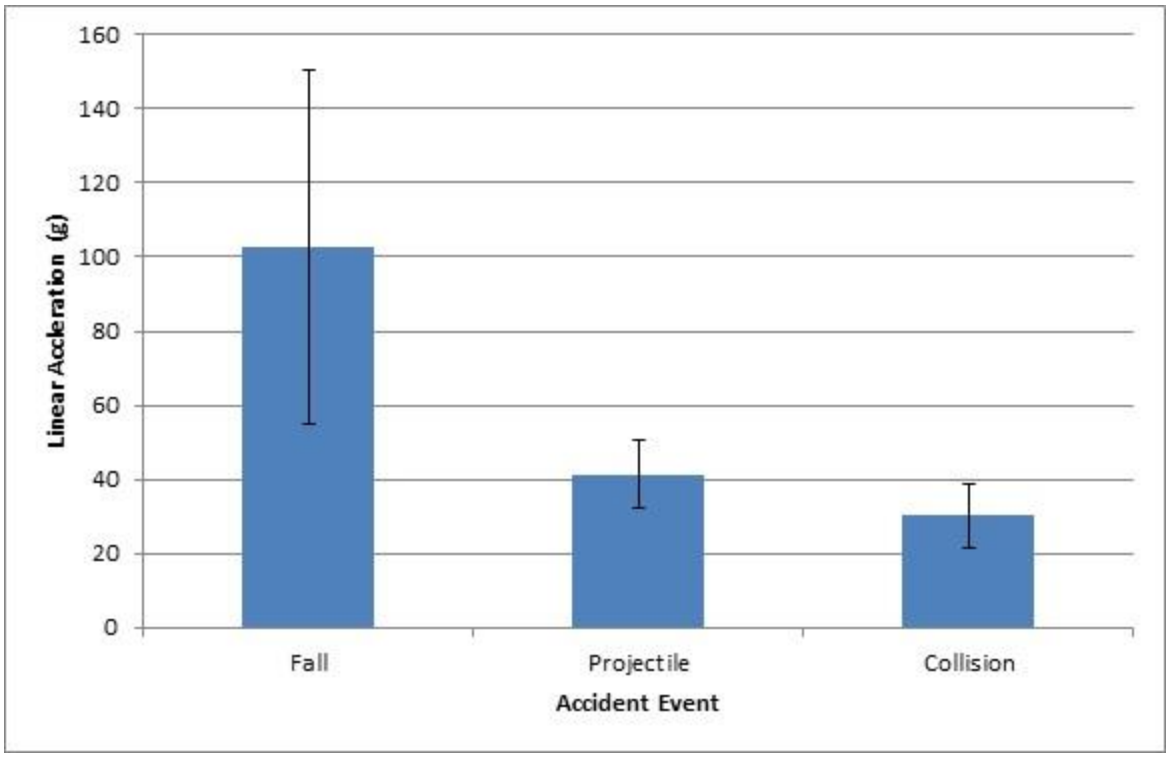

Figure 16: Mean peak linear acceleration for helmeted impacts of each accident event.

4.1.2.2 Rotational Acceleration

A significant main effect of accident events was found for peak rotational acceleration ($p < 0.01$). As a result the null hypothesis regarding the effects of accident event on peal rotational acceleration was rejected. All accident events were found to produce significantly different peak rotational accelerations ($p < 0.05$). Mean peak linear accelerations obtained of helmeted impacts for each of the three accident events are illustrated in Figure 17.

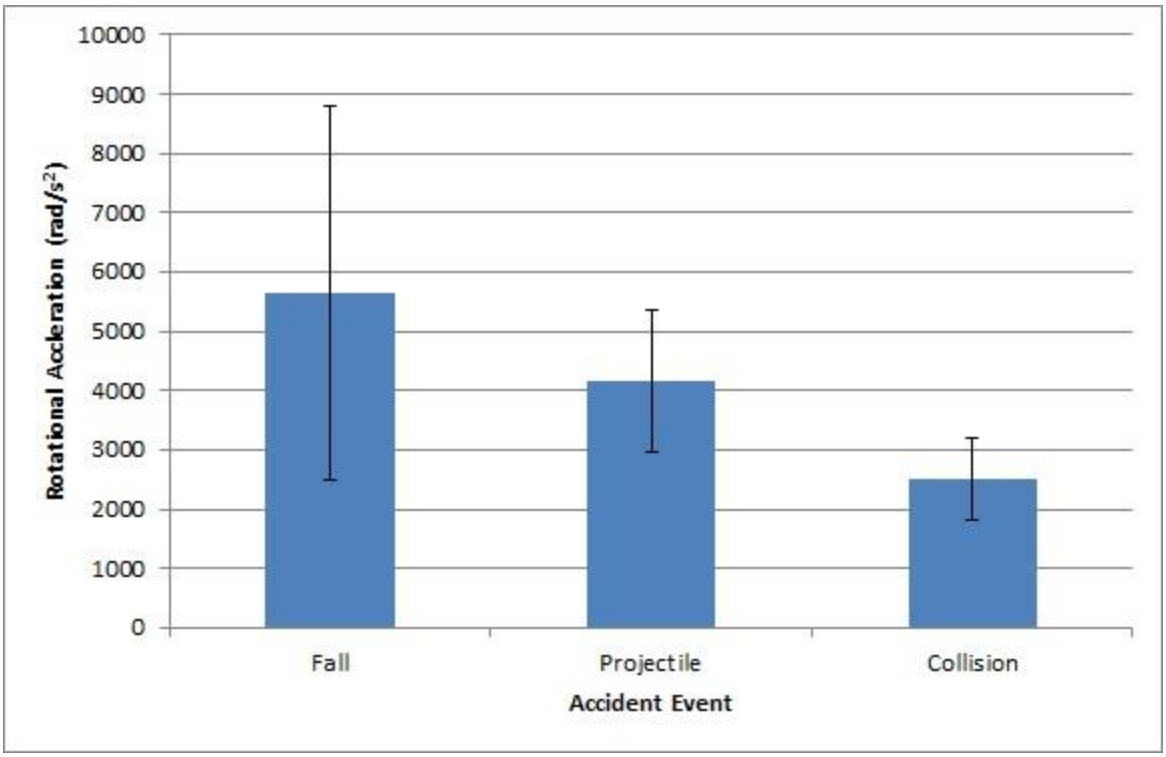

Figure 17: Mean peak rotational acceleration for helmeted impacts of each accident event.

4.1.2.3 Rotational Velocity

Accident events were found to have a significant main effect as measured by peak rotational velocity ($p < 0.01$). The null hypothesis regarding the effects of accident event on peal linear acceleration was rejected. Tukey post hoc tests showed peak rotational velocities were significantly different for fall/projectile and projectile/collision ($p < 0.01$) but no significance was found between fall and collision conditions. Figure 18 shows the mean peak rotational velocities obtained of helmeted impacts for each of the three accident events.

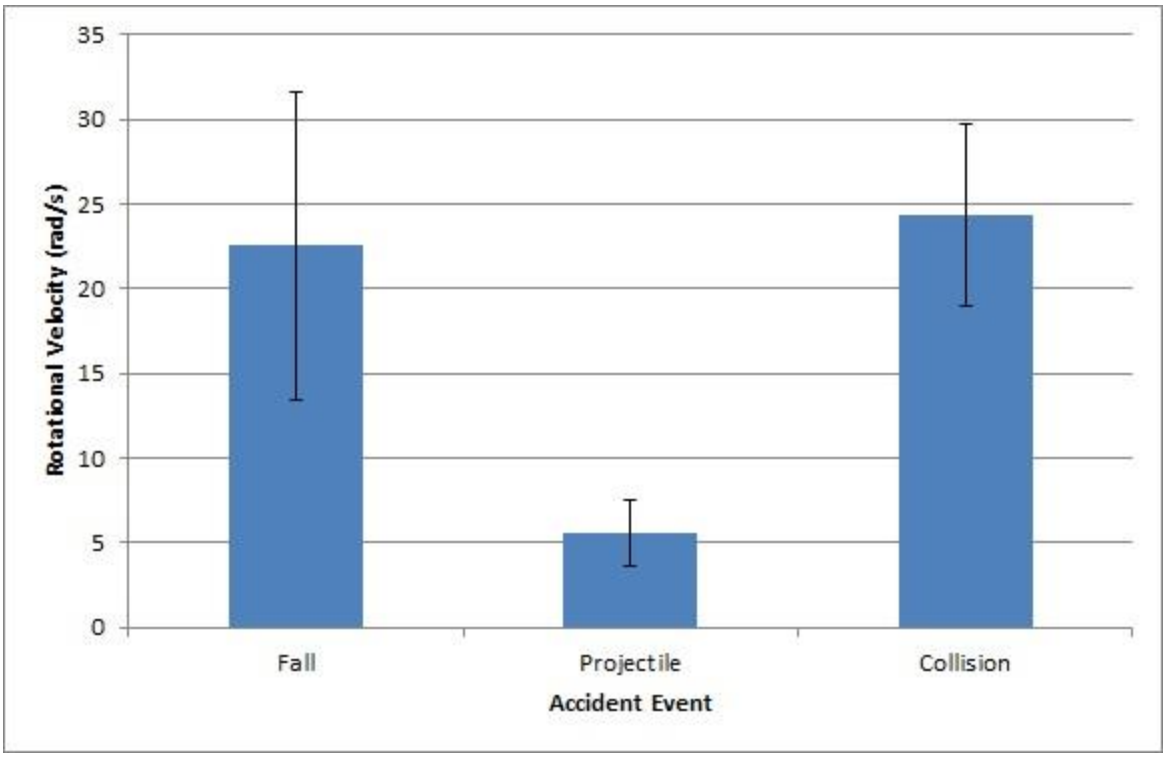

Figure 18: Mean peak rotational velocity for helmeted impacts of each accident event.

4.1.3 Two-Way Analysis of Variance (ANOVA)

To examine the influence of velocity and location of impact on peak linear and rotational acceleration and rotational velocity two-way ANOVAs were completed. Velocities and locations used in the two-way ANOVA are shown in Tables 3-6 (p. 55).

4.1.3.1 Linear Acceleration

Significant main effects for velocity and location were found for peak linear acceleration of fall conditions ($p < 0.01$). Peak linear accelerations of fall conditions were found to have a significant interaction effect for velocity and location ($p < 0.01$). Projectile impacts were found to have significant main effects of velocity and location for peak linear acceleration ($p < 0.01$). No significant interaction effect was found between velocity and location for peak linear accelerations produced by projectile conditions ($p > 0.05$). For peak linear acceleration produced by collisions significant main effects were found for velocity and location ($p < 0.01$). A significant interaction effect was found between velocity and location for peak linear

accelerations resulting from collisions. The null hypotheses regarding the effect of inbound velocity and impact location on peak linear acceleration were rejected for all accidents events. Tukey post hoc tests revealed significant differences between all three velocities for peak linear acceleration of fall conditions ($p < 0.01$). All three velocities were found to be significantly different for peak linear acceleration produced by projectile impacts ($p < 0.01$). Significant differences in peak linear accelerations were also found between all three velocities for collisions ($p < 0.01$). The effect of velocity on mean peak linear accelerations for all accident events is presented in Figure 19.

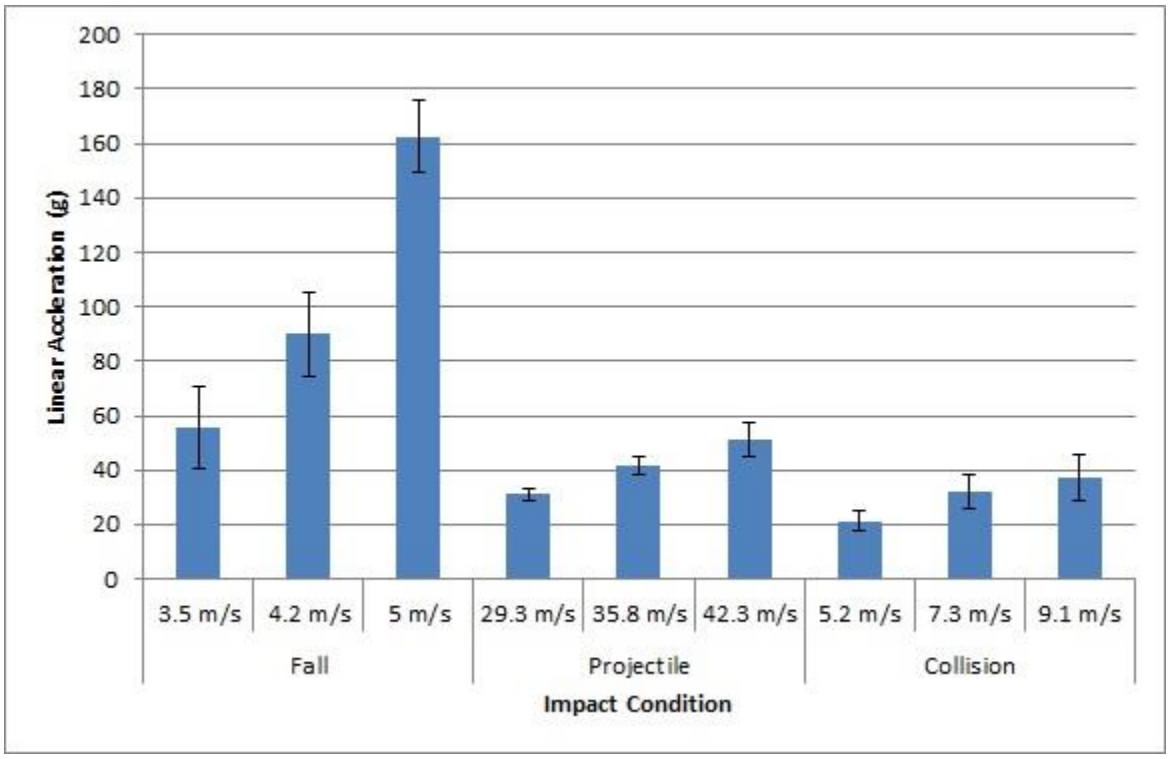

Figure 19: The influence of inbound velocity on mean peak linear acceleration for each accident event.

For falls, post hoc tests showed significant differences between Rear-D/L4-D and L4-D/R3-D for linear acceleration ($p < 0.01$). However no significant difference was found between impact locations Rear-D and R3-D ($p > 0.05$). Projectile impacts were found to have significant differences in linear accelerations for Front-D/R1-B and Front-D/R3-D ($p < 0.01$) but no

significant differences for R1-B/R3-D ($p > 0.05$). Peak linear accelerations produced by collisions were found to be significantly different for all impact locations ($p < 0.01$). Figure 20 demonstrates the influence of impact location for each accident event.

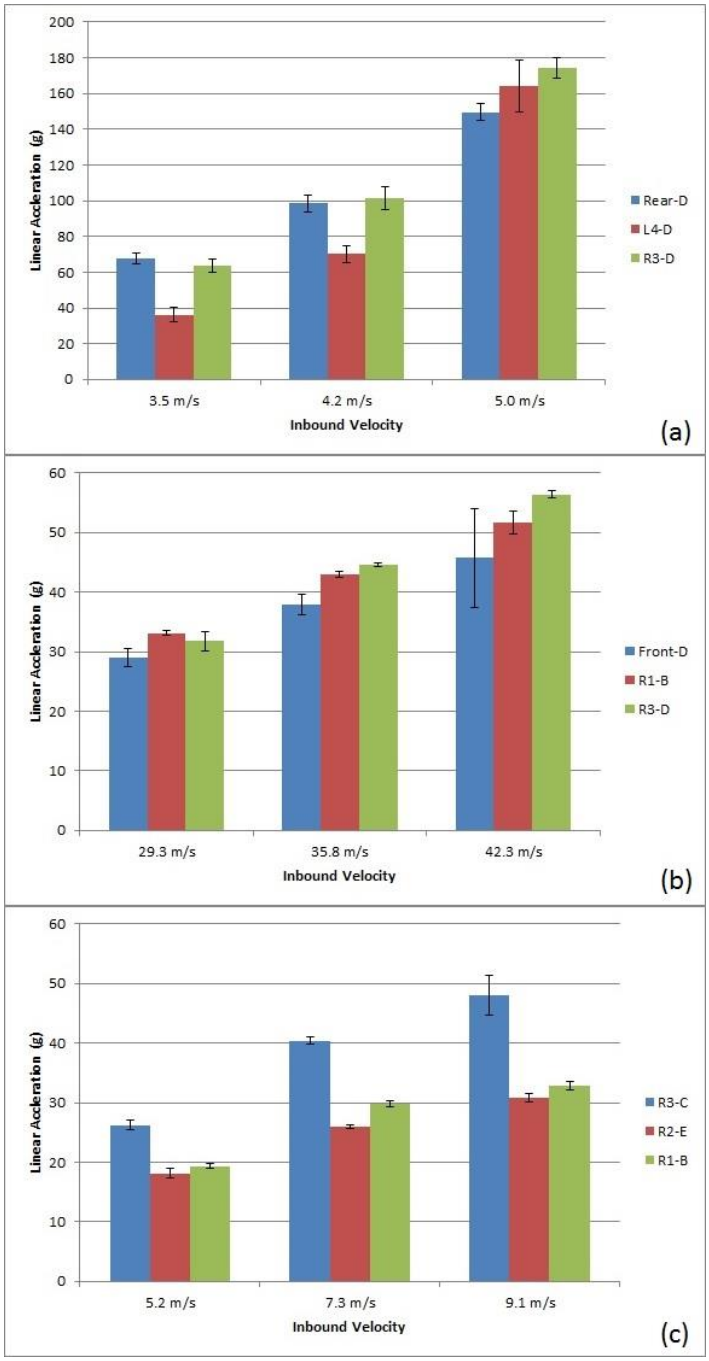

Figure 20: The influence of impact location on mean peak linear acceleration for each accident event: (a) Fall, (b) Projectile, (c) Collision.

4.1.3.2 Rotational Acceleration

For peak rotational acceleration, significant main effects of velocity and location were found for falls ($p < 0.01$). A significant interaction effect was found between location and velocity for peak rotational acceleration produced by falls ($p < 0.01$). Peak rotational accelerations produced by projectile impacts were found to have significant a main effect of velocity ($p < 0.01$) but no main effect of location was found ($p > 0.05$). A significant interaction effect was found between location and velocity for peak rotational acceleration produced of projectile conditions ($p < 0.05$). Collision conditions were found to produce significant main effects for peak rotational acceleration ($p < 0.01$). Peak rotational accelerations for collisions were found to have a significant interaction effect between velocity and location. As a result it was concluded that the null hypotheses regarding the influence of velocity and location on peak rotational acceleration were all rejected except for the effect of location on projectile impacts. Post hoc tests revealed significant differences between all three velocities for peak rotational acceleration of falls ($p < 0.01$). Peak rotational accelerations for projectile conditions were found to be significantly different for 29.3 m/s/35.8 m/s and 29.3 m/s/42.3 m/s ($p < 0.05$) but not for 35.8 m/s/42.3 m/s ($p > 0.05$). All three impact velocities were found to produce significantly different peak rotational accelerations for collisions ($p < 0.01$). The influence of velocity of mean peak rotational acceleration for all accident events is shown in Figure 21.

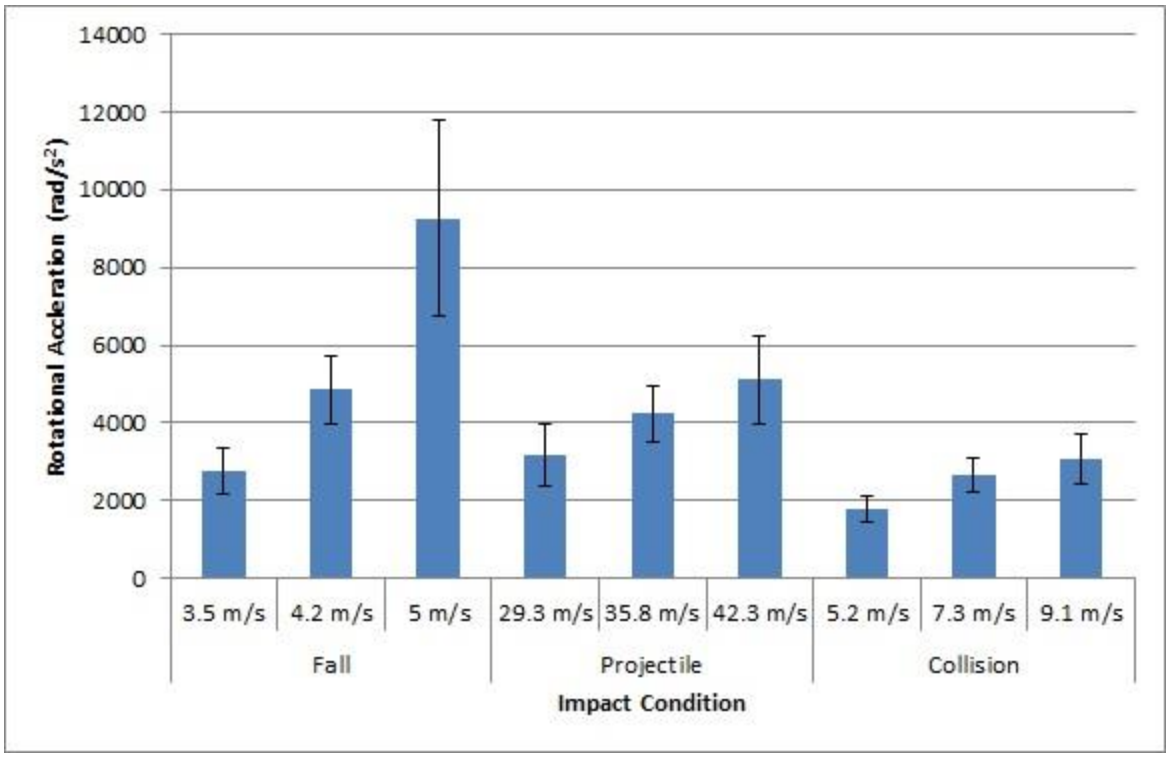

Figure 21: The influence of inbound velocity on mean peak rotational acceleration for each accident event.

Significant differences were found for Rear-D/L4-D and Rear-D/R3-D for peak rotational acceleration produced by falls ($p < 0.01$) but not for L4-D/R3-D ($p > 0.05$). Collisions were shown to produce significantly different rotational acclerations for R3-C/R2-E amd R2-E/R1-B ($p < 0.01$). No significant difference was found between R3-C amd R1-B ($p > 0.05$). The effect of impact location of peak rotational acceleration for each accident event is presented in Figure 22.

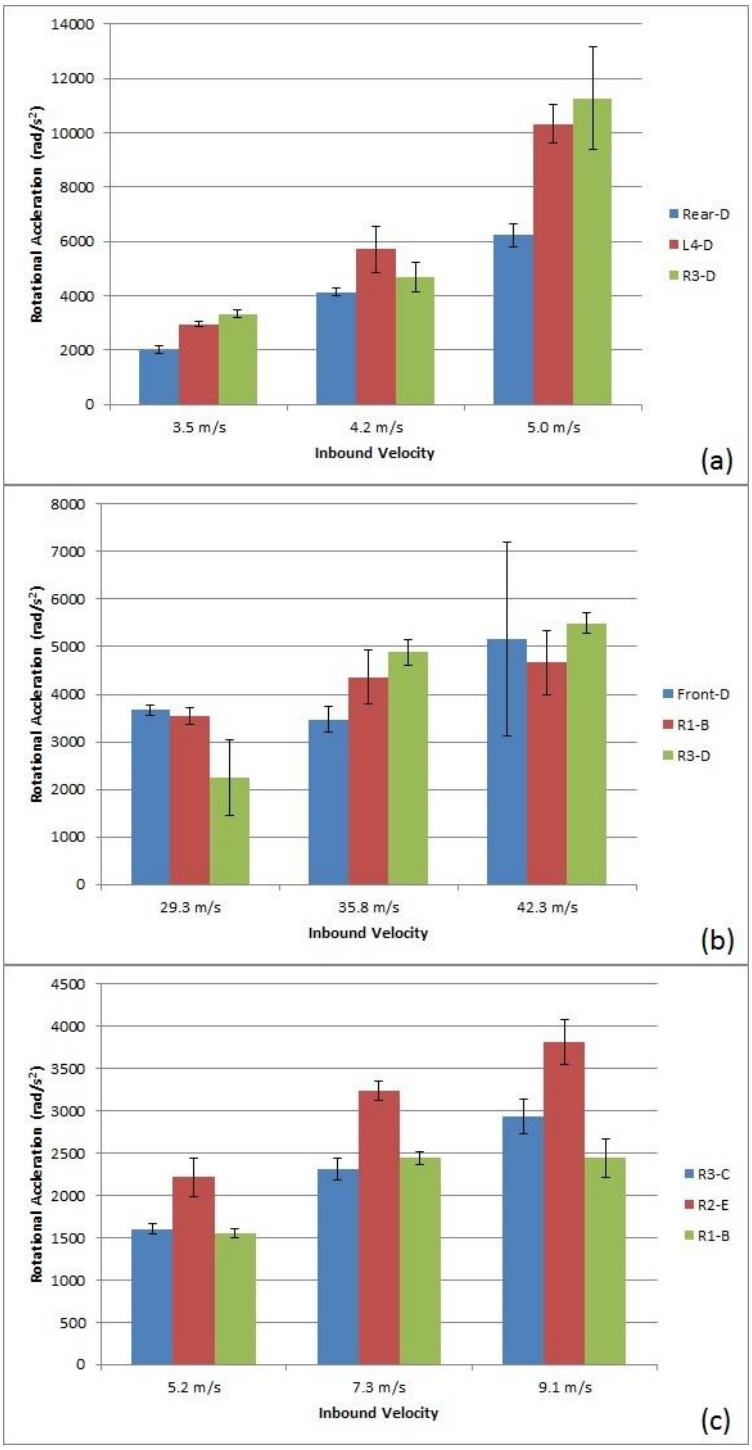

Figure 22: The influence of impact location on mean peak rotational acceleration for each accident event: (a) Fall, (b) Projectile, (c) Collision.

4.1.3.3 Rotational Velocity

Velocity and Location were found to produce significant main effects for peak rotational velocity of fall conditions ($p < 0.01$). A significant interaction effect between velocity and location was

found for peak rotational velocities produced by falls ($p < 0.01$). Peak rotational velocity showed significant main effects of velocity and location for projectile impacts ($p < 0.01$). However no interaction effect between velocity and location was found ($p > 0.05$). Significant main effects of velocity and location were found for rotational velocity of collisions ($p < 0.01$) but Rotational velocity for collisions did not produce a significant interaction between velocity and location ($p > 0.05$). As a result all null hypotheses regarding the effect of inbound velocity and impact location on peak rotational velocity were rejected for each accident event. Significant differences between all velocities for peak rotational velocities produced by falls were found ($p < 0.01$). Projectile impacts were found to produce significantly different peak rotational velocities for 29.3 m/s/35.8 m/s and 29.3 m/s/42.3 m/s ($p < 0.05$) but not for 35.8 m/s/42.3 m/s ($p > 0.05$). Peak rotational velocities produced by collisions were found to be significantly different for 5.2 m/s/7.3 m/s and 5.2 m/s/9.1 m/s ($p < 0.05$). No significant difference was found between 7.3 m/s and 9.1 m/s ($p > 0.05$). The effect of inbound velocity on mean peak rotational velocity for each accident events is illustrated in Figure 23.

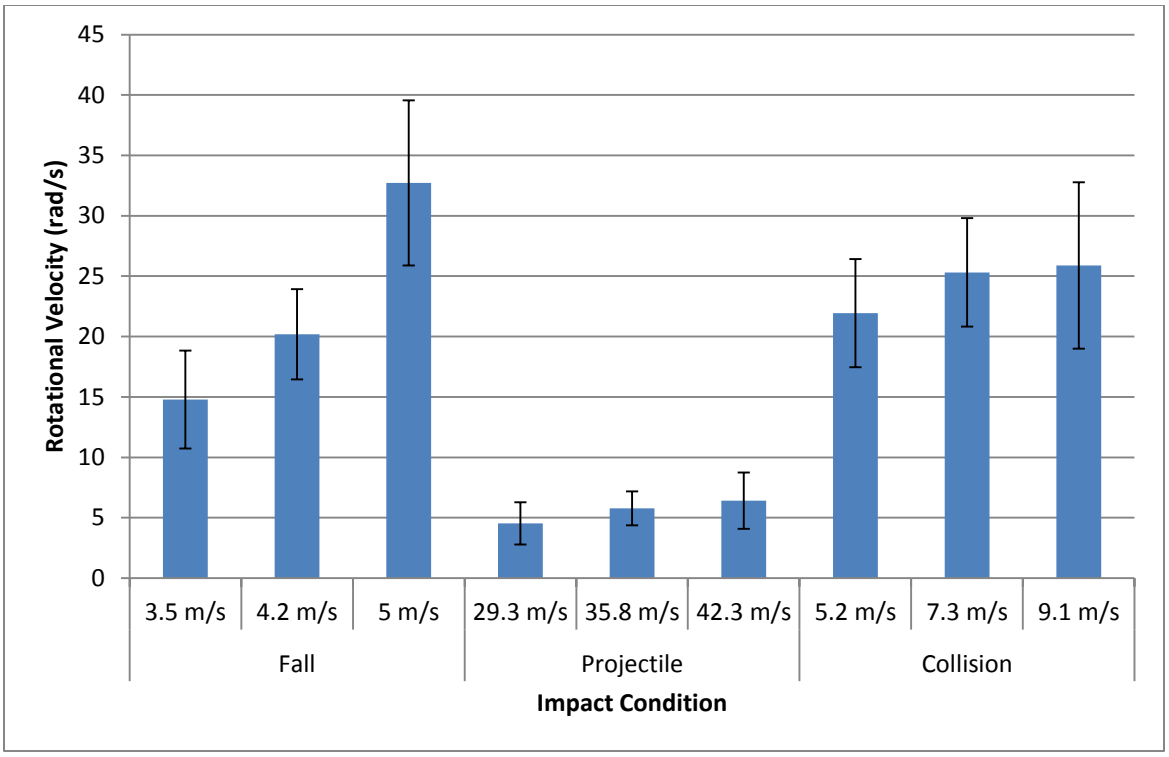

Figure 23: The influence of inbound velocity on mean peak rotational velocity for each accident event.

Tukey post hoc tests showed significant differences between Rear-D/L4-D and Rear-D-R3-D ($p < 0.01$) but no significant difference was found between L4-D and R3-D for peak rotational velocity ($p > 0.05$). No significant difference was found between Front-D/R1-B for peak rotational velocities produced by projectile impacts ($p > 0.05$). However projectile impacts were found to produce significantly different peak rotational velocities for Front-D/R3-D and R1-B/R3-D ($p < 0.01$). Figure 24 demonstrates the influence of impact location on mean peak rotational velocity for all accident events.

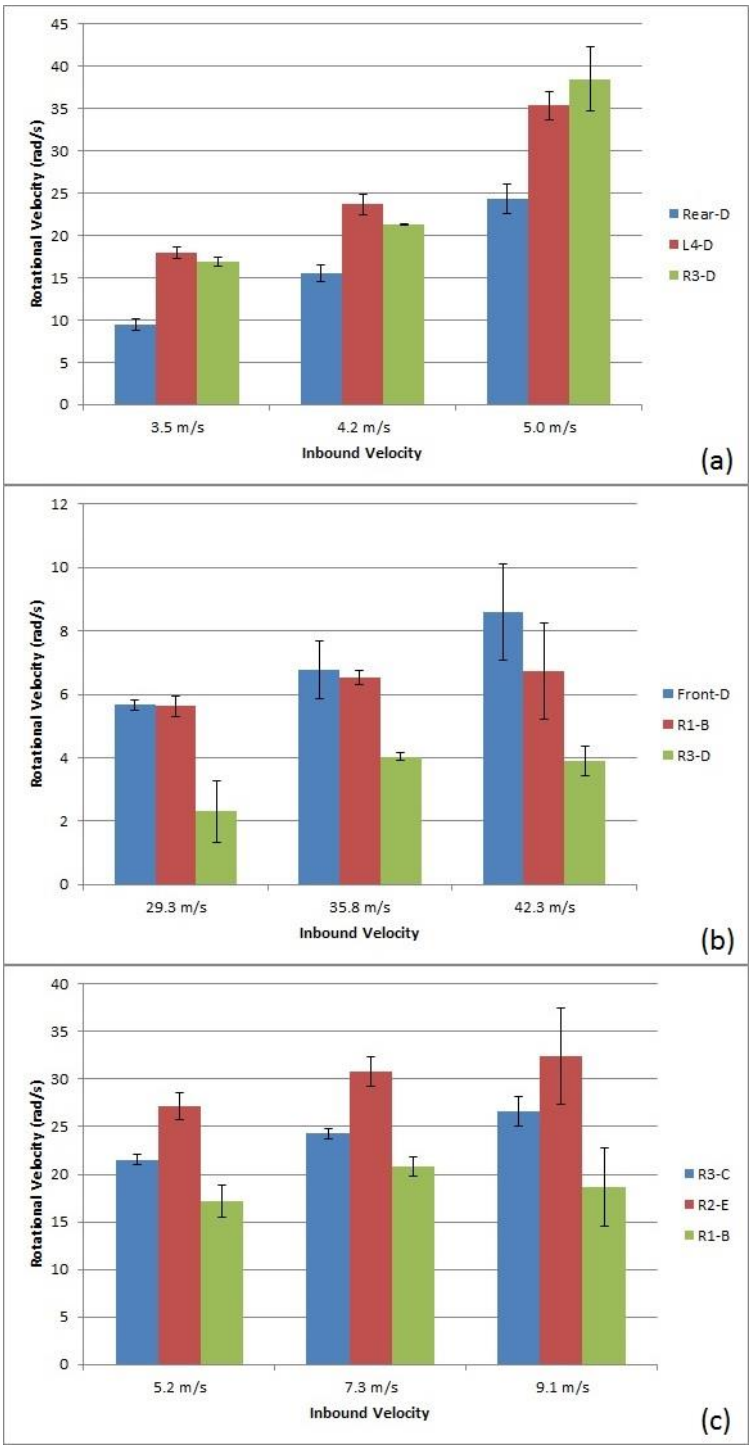

Figure 24: The influence of impact location on mean peak rotational velocity for each accident event: (a) Fall, (b) Projectile, (c) Collision.

4.2 Brain Deformation Results

Table 11 displays the mean and standard deviations for mean peak maximum principal strain and von Mises stress for all fall conditions.

Table 11: Mean peak brain tissue deformation metrics (±1 standard deviation) as determined from finite element analysis resulting from falls.

Location	Velocity (m/s)	No Helmet/Helmet	Maximum Principle Strain	von Mises Stress (kPa)
Rear-D	3.5	No Helmet	0.474 (0.014)	15.7 (0.8)
		Helmet	0.155 (0.018)	4.9 (0.4)
	4.2	Helmet	0.240 (0.006)	7.8 (0.3)
	5.0	Helmet	0.392 (0.033)	12.3 (0.8)
L4-D	3.5	No Helmet	0.558 (0.012)	16.2 (0.3)
		Helmet	0.205 (0.015)	6.8 (0.4)
	4.2	Helmet	0.324 (0.015)	9.9 (1.4)
	5.0	Helmet	0.557 (0.034)	18.0 (0.4)
R3-D	3.5	No Helmet	0.6155 (0.049)	20.2 (0.8)
		Helmet	0.250 (0.021)	8.2 (0.5)
	4.2	Helmet	0.318 (0.017)	10.6 (0.4)
	5.0	Helmet	0.570 (0.003)	18.8 (0.9)

Mean and standard deviations for peak maximum principal strain and von Mises stress produced by projectiles are presented in Table 12.

Table 12: Mean peak brain tissue deformation metrics (±1 standard deviation) as determined from finite element analysis resulting from projectiles.

Location	Velocity (m/s)	No Helmet/Helmet	Maximum Principle Strain	von Mises Stress (kPa)
Front-D	29.3	No Helmet	0.272 (0.019)	9.9 (1.1)
		Helmet	0.190 (0.002)	5.4 (0.1)
	35.8	Helmet	0.126 (0.11)	4.03 (0.5)
	42.3	Helmet	0.176 (0.023)	5.6 (0.5)
R1-B	29.3	No Helmet	0.240 (0.017)	8.0 (0.6)
		Helmet	0.168 (0.040)	5.1 (1.1)
	35.8	Helmet	0.125 (0.004)	3.9 (0.2)
	42.3	Helmet	0.113 (0.018)	3.6 (0.6)
R3-D	29.3	No Helmet	0.146 (0.007)	5.1 (0.2)
		Helmet	0.091 (0.013)	3.3 (0.5)
	35.8	Helmet	0.124 (0.015)	3.9 (0.1)
	42.3	Helmet	0.134 (0.016)	4.0 (0.1)

Table 13 presents the mean and standard deviations for peak maximum principal strain and von Mises stress produced by collisions.

Table 13: Mean peak brain tissue deformation metrics (±1 standard deviation) as determined from finite element analysis resulting from collisions.

Location	Velocity (m/s)	No Helmet/Helmet	Maximum Principle Strain	von Mises Stress (kPa)
R3-C	5.2	No Helmet	0.201 (0.021)	4.8 (0.02)
		Helmet	0.172 (0.020)	4.1 (0.3)
	7.3	Helmet	0.213 (0.008)	6.0 (0.2)
	9.1	Helmet	0.269 (0.025)	7.4 (0.3)
R2-E	5.2	No Helmet	0.323 (0.016)	10.9 (0.4)
		Helmet	0.254 (0.024)	8.3 (1.1)
	7.3	Helmet	0.328 (0.041)	10.9 (0.3)
	9.1	Helmet	0.418 (0.032)	14.0 (0.9)
R1-B	5.2	No Helmet	0.151 (0.007)	4.0 (0.1)
		Helmet	0.172 (0.007)	4.5 (0.1)
	7.3	Helmet	0.209 (0.011)	5.4 (0.5)
	9.1	Helmet	0.198 (0.007)	5.5 (0.2)

4.2.1 Independent Samples T-tests

Independent sample t-tests were conducted for each brain deformation variable to assess the protective capacity of ice hockey goaltender masks as measured by maximum principal strain and von Mises stress. The velocities and locations used for analysis are shown in Tables 3-6 (p. 55 - 56).

4.2.1.1 Maximum Principal Strain

Maximum principle strain was found to be significantly lower in helmeted fall conditions compared to unhelmeted fall conditions ($p < 0.01$). Projectile impacts to a helmeted headform produced significantly lower maximum principle strain values compared to projectile impacts to an unhelmeted headform ($p < 0.05$). Maximum principle strains for helmeted and unhelmeted collisions to R3-C were not significantly different for one another ($p > 0.05$), whereas impact locations R2-E and R1-B produced significantly lower maximum principle strains in helmeted conditions compared to unhelmeted conditions ($p < 0.05$). The null hypotheses regarding the effect of ice hockey goaltenders mask compared to a bare headform on peak maximum principle

strain were all rejected, except for collisions to the R3-C location. Mean maximum principle strains obtained for all accident events to an unhelmeted and helmeted conditions at low velocities are presented in Figure 25.

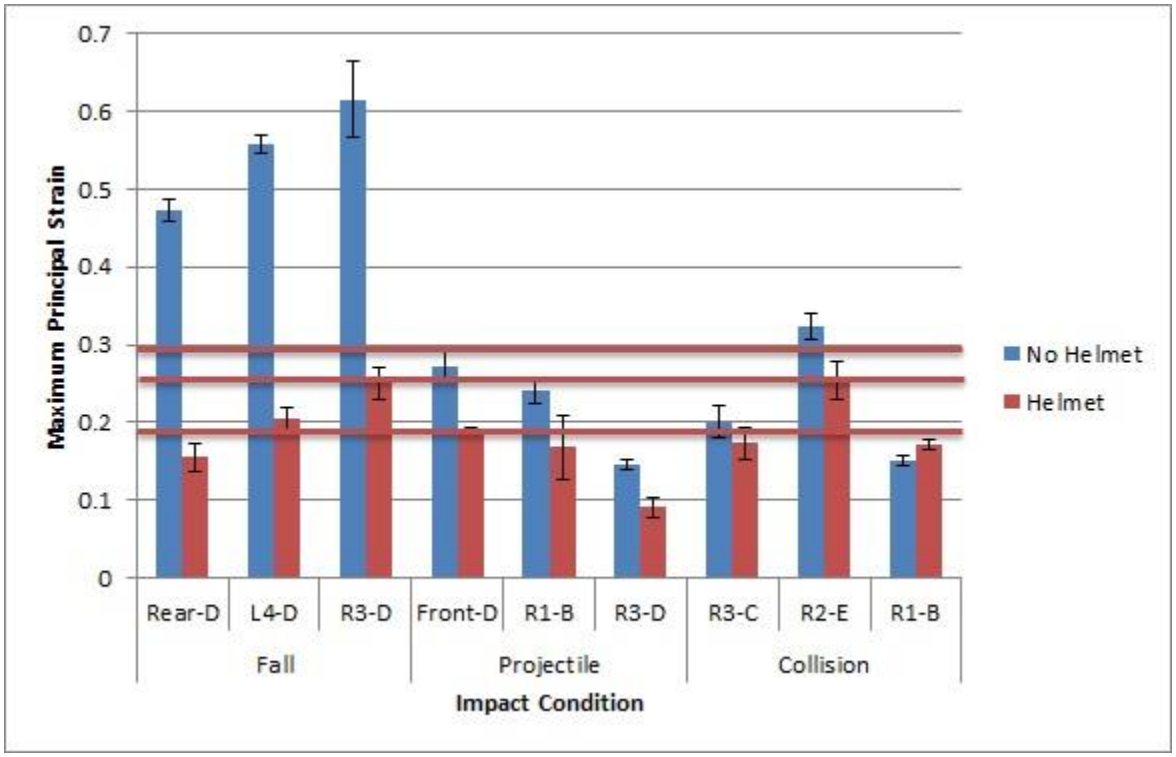

Figure 25: Mean peak maximum principle strain for helmeted and unhelmeted impacts at low velocities of each accident event. The three lines represent a 50 % probability of sustaining a concussion (Zhang et al., 2004; Kleiven, 2007, Rousseau, 2014).

4.2.1.2 Von Mises Stress

All helmeted falls were found to produce significantly lower von Mises stress than unhelmeted falls ($p < 0.05$). Von Misses stress for projectile impacts to a helmeted headform were found to be significantly lower compared to projectile impacts to an unhelmeted headform ($p < 0.05$). Helmeted conditions resulted in significantly lower von Mises stress than unhelmeted conditions for collisions ($p < 0.05$). As a result null hypotheses regarding the effect of ice hockey goaltenders mask compared to a bare headform on peak von Mises stress were all rejected.

Figure 26 shows the mean peak von Mises stress obtained for all accident events to an unhelmeted and helmeted conditions at low velocities.

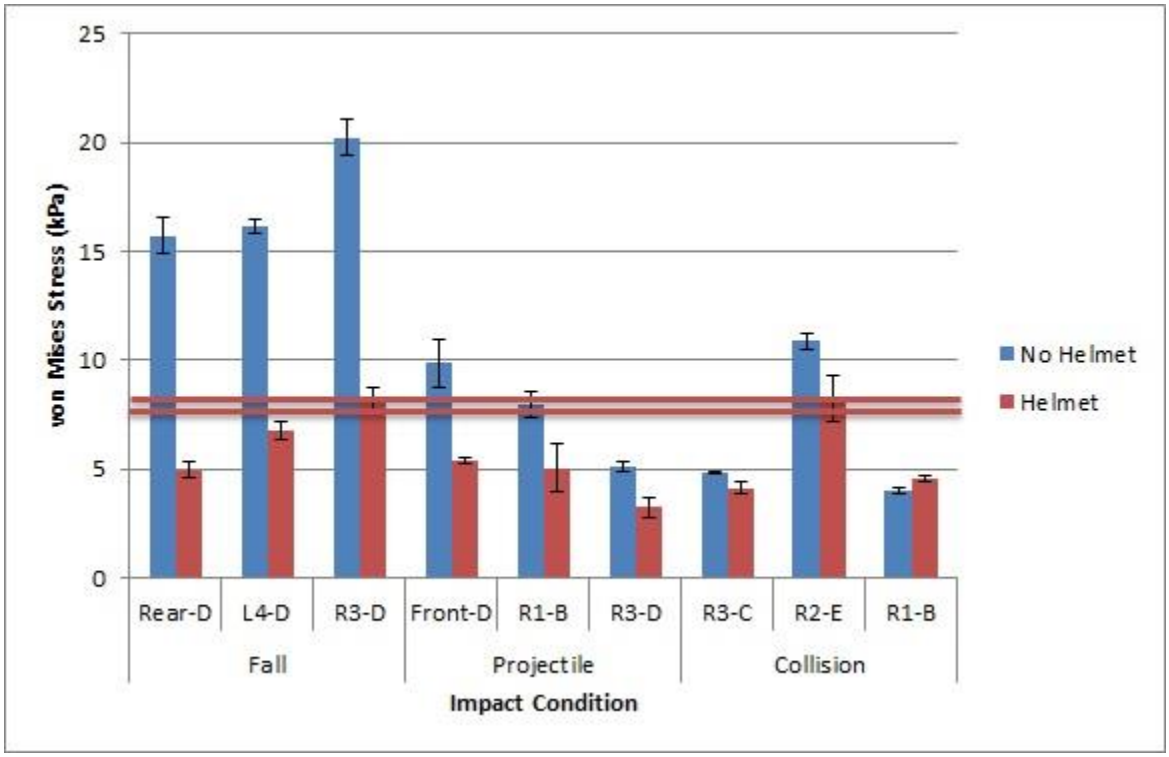

Figure 26: Mean peak von Mises stress for helmeted and unhelmeted impacts at low velocities of each accident event. The two lines represent 50 % probability of sustaining a concussion (Zhang et al., 2004; Kleiven, 2007).

4.2.2 One-Way Analysis of Variance (ANOVA)

To determine the effect of accident events on peak maximum principal strain and von Mises stress One-way ANOVAs were completed. Velocities and locations selected for analysis are presented in Tables 3-5 (p. 55).

4.2.2.1 Maximum Principal Strain

A significant main effect of accident events were found for peak maximum principal strain ($p < 0.01$). The null hypothesis regarding the effects of accident event on peak linear acceleration was rejected. Post hoc tested found peak maximum principal strain was significantly different for all

accidents events ($p < 0.01$). Mean peak maximum principal strain of helmeted impacts for each of the three accident events are shown in Figure 27.

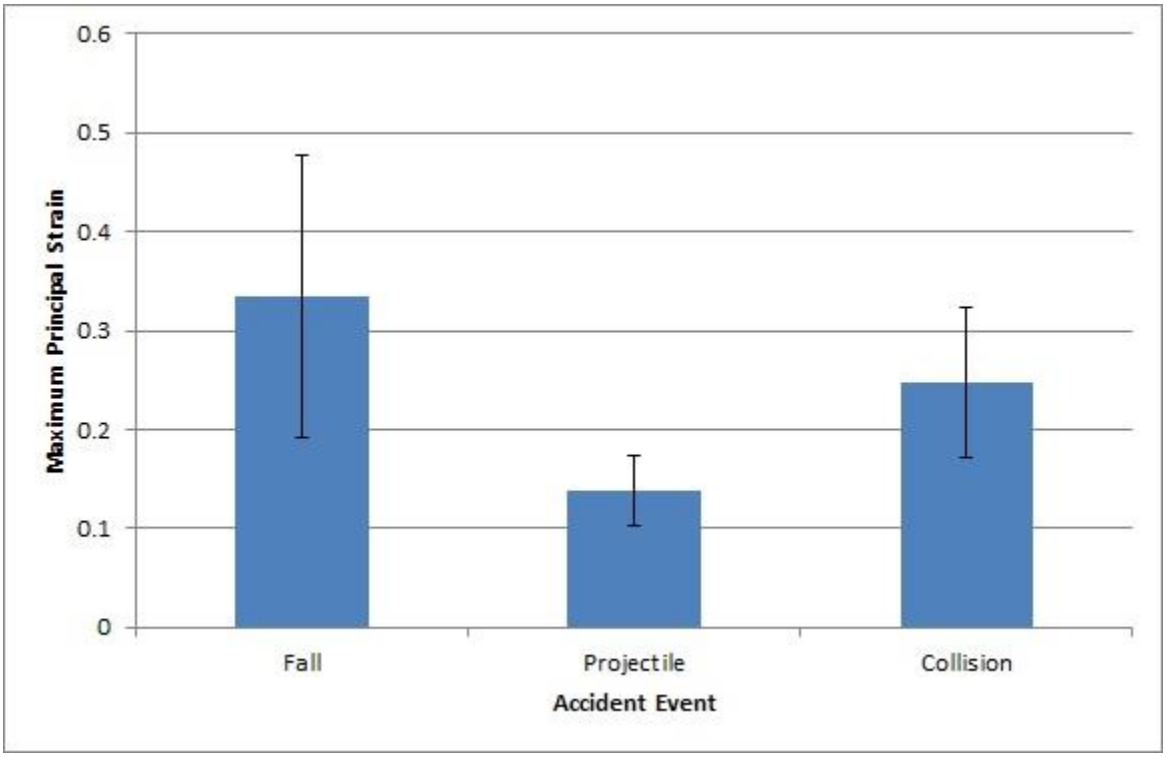

Figure 27: Mean peak maximum principal strain for helmeted impacts of each accident event.

4.2.2.2 Von Mises Stress

Peak Von Mises Stress was found to have a significant main effect of accident event ($p < 0.01$). The null hypothesis regarding the effects of accident event on peak von Mises stress was rejected. All accident events were found to produce significantly different peak rotational accelerations ($p < 0.01$). Figure 28 shows the mean peak von Mises stress obtained of helmeted impacts for each of the three accident events.

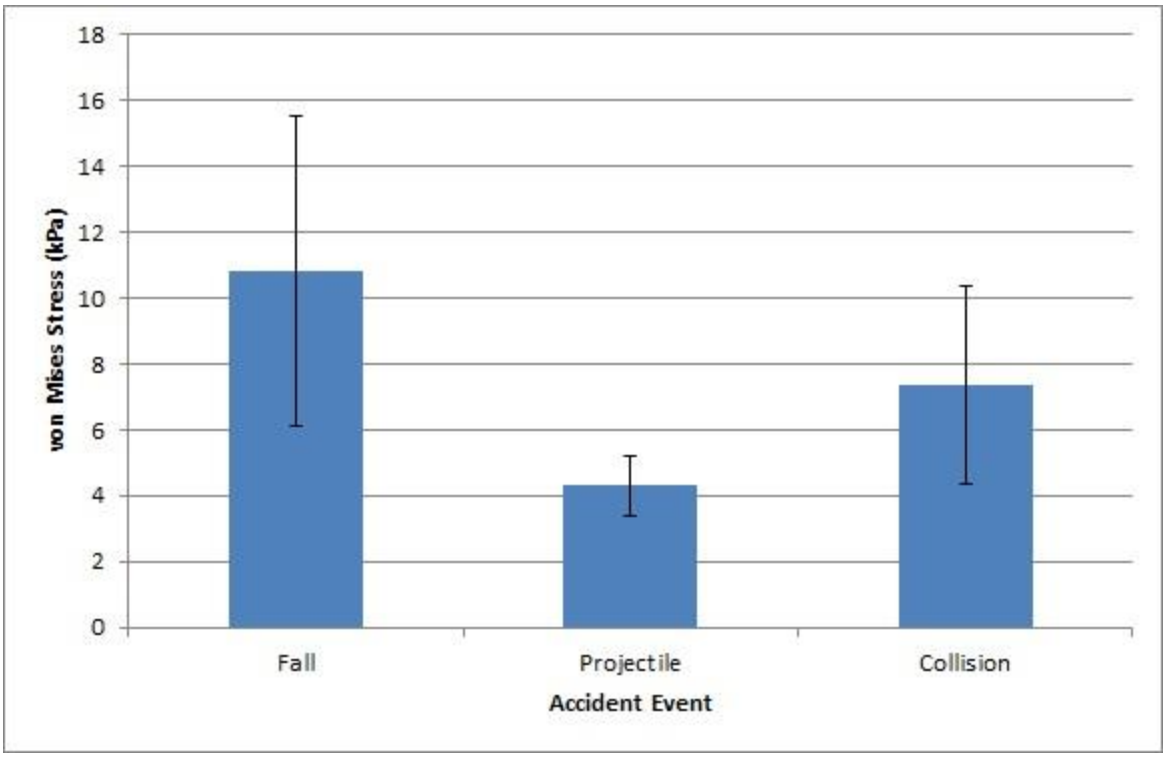

Figure 28: Mean peak von Mises stress for helmeted impacts of each accident event.

4.2.3 Two-Way Analysis of Variance (ANOVA)

Two-way ANOVAs were conducted to examine the influence of velocity and location of impact on peak maximum principle strain and von Mises stress. The velocities and locations used in the two-way ANOVA are shown in Tables 3-6 (p. 55).

4.2.3.1 Maximum Principal Strain

For peak maximum principal strain, significant main effects for velocity and location were found for falls ($p < 0.01$). A significant interaction effect was found between location and velocity for peak maximum principal strain produced by falls ($p < 0.01$). Significant main effects of velocity and location were found for peak maximum principle strain produced by projectile impacts ($p < 0.05$). Peak maximum principle strains produced by projectile impacts were found to have a significant interaction effect for velocity and location ($p < 0.01$). Collisions were found to have significant main effects of velocity and location for peak maximum principle strain ($p < 0.01$). A significant interaction effect was found between velocity and location for peak maximum

principle strain resulting from collisions ($p < 0.01$). The null hypotheses regarding the effect of inbound velocity and impact location on peak maximum principle strain were rejected for all accidents events. Tukey post hoc tests revealed significant differences between all three velocities for maximum principle strain of fall conditions ($p < 0.01$). Projectile impacts were found to produce significantly different maximum principle strains for 29.3 m/s/35.8 m/s ($p < 0.05$). Maximum principle strain was found to not significantly different for 29.3 m/s/42.3 m/s and 35.8 m/s/42.3 m/s ($p > 0.05$). Significantly different maximum principle strains were also found between all three velocities for collisions ($p < 0.01$). Figure 29 presents the effect of velocity on mean peak maximum principle strain for all accident events.

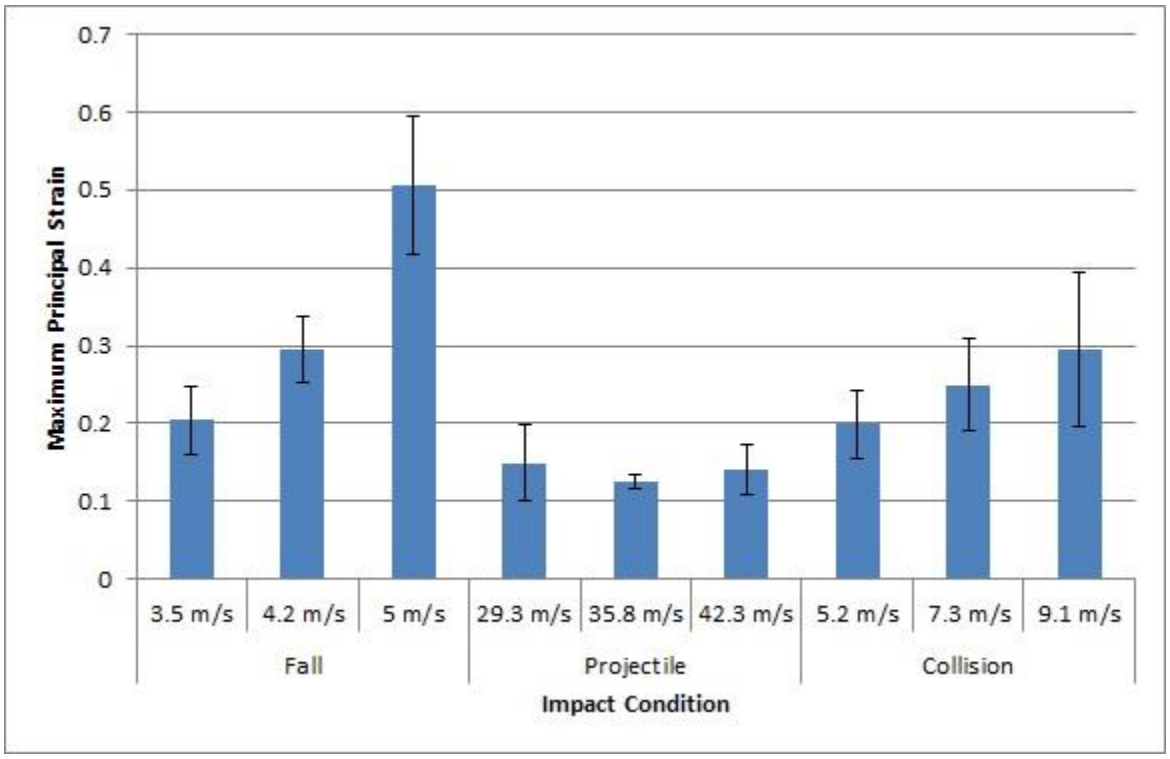

Figure 29: The influence of inbound velocity on mean peak maximum principle strain for each accident event.

Post hoc tests showed significantly different peak maximum principle strain for Rear-D/L4 and Rear-D/R3-D of fall conditions ($p < 0.01$). However no significant difference was found between

impact locations L4-D and R3-D ($p > 0.05$). Projectile impacts were found to produce significantly different peak maximum principle strains for Front-D/R1-B and Front-D/R3-D ($p < 0.05$). All impact locations were found to produce significantly different peak maximum principle strains for collisions ($p < 0.05$). The effect of impact location of peak maximum principle strains for each accident events is presented in Figure 22.

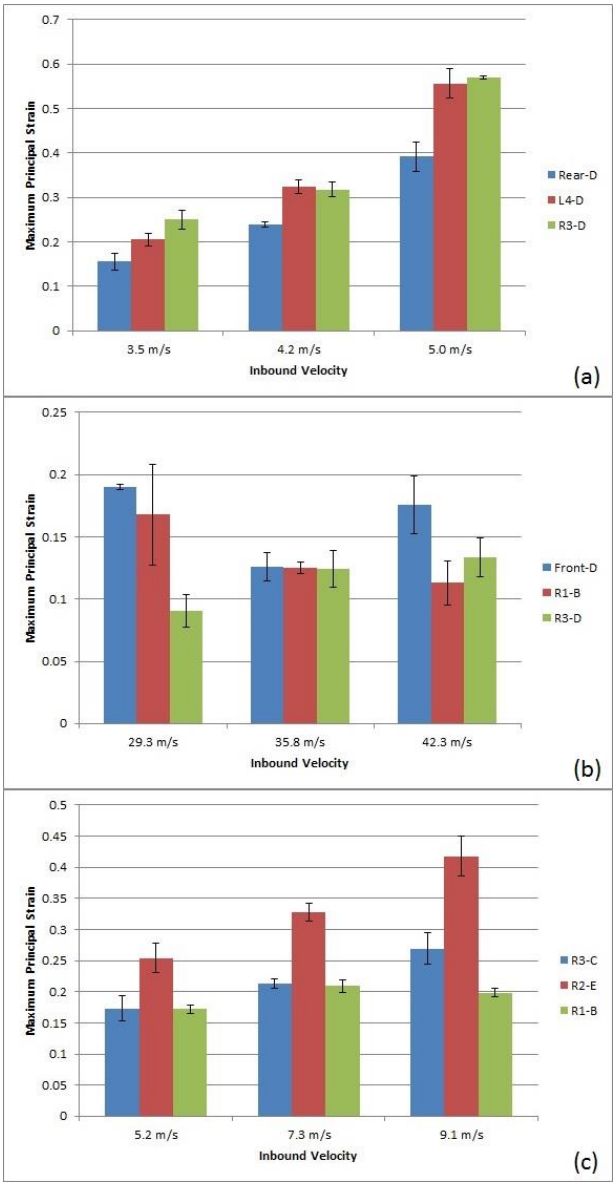

Figure 30: The influence of impact location on mean peak maximum principle strain for each accident event: (a) (a) Fall, (b) Projectile, (c) Collision.

4.2.3.2 Von Mises Stress

Peak von Mises stress for falls was found to have, significant main effects of velocity and location ($p < 0.01$). Falls were found to have a significant interaction effect between location and velocity for von Mises stress ($p < 0.01$). No significant main effect of velocity was found for peak von Mises stress produced by projectile impacts ($p > 0.05$). However a main effect of location was found ($p < 0.05$). Collisions were found to have significant main effects of velocity and location for peak von Mises stress ($p < 0.01$). Peak von Mises stress for collisions were found to have a significant interaction effect between velocity and location ($p < 0.01$). As a result the null hypotheses regarding the effect of inbound velocity and impact location on peak von Mises stress were rejected for all accidents events except for the effect of velocity on projectile impacts. Post hoc tests revealed all three velocities produced significant different peak von Mises stress for falls ($p < 0.01$). Collisions were found to produce significantly different peak von Mises stress for all three velocities ($p < 0.05$). The influence of velocity of mean peak rotational acceleration for all accident events is presented in Figure 31.

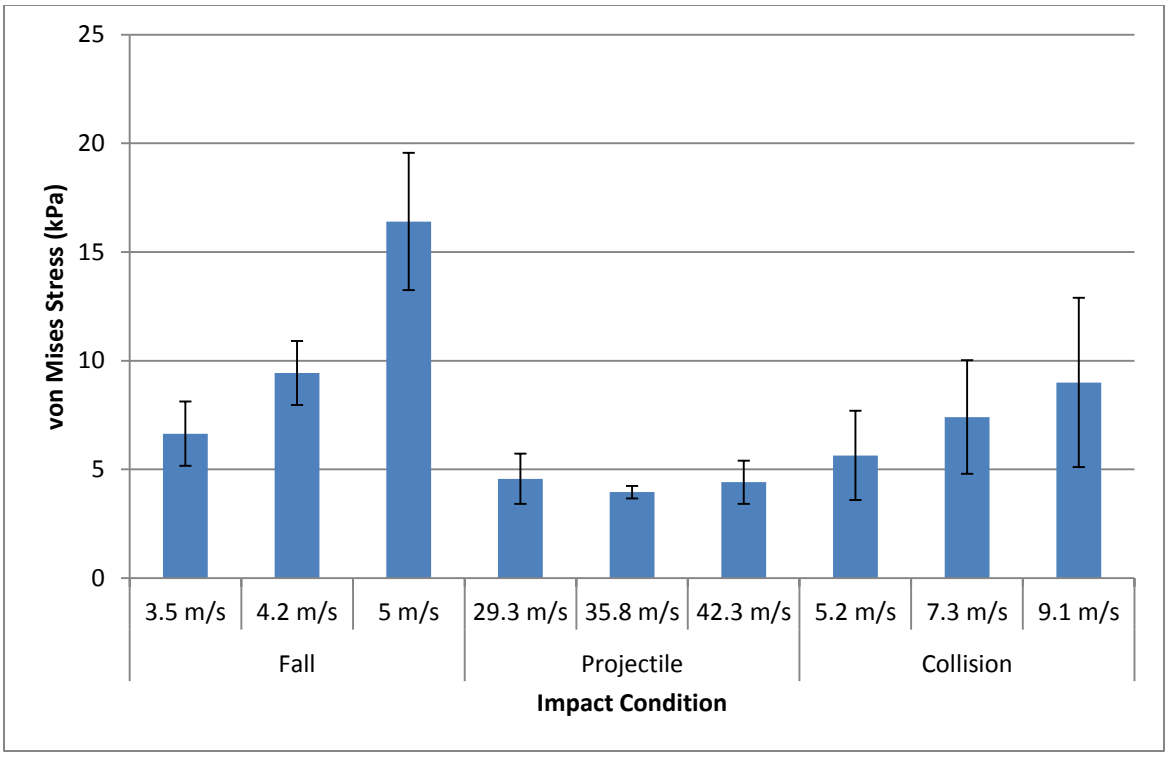

Figure 31: The influence of inbound velocity on mean peak von Mises stress for each accident event.

Falls produced significantly different peak von Mises stress for Rear-D/L4-D and Rear-D/R3-D ($p < 0.01$). No significant difference was found between impact locations L4-D and R3-D ($p > 0.05$). Projectile impacts were found to have significantly different peak von Mises stress for Front-D/R1-B and Front-D/R3-D ($p < 0.01$). However, no significant difference was found between impact locations R1-B and R3-D ($p > 0.05$). For collisions, all impact locations were found to produce significantly different peak von Mises stress ($p < 0.05$). Figure 32 shows the effect of impact location of peak von Mises stress for each accident event.

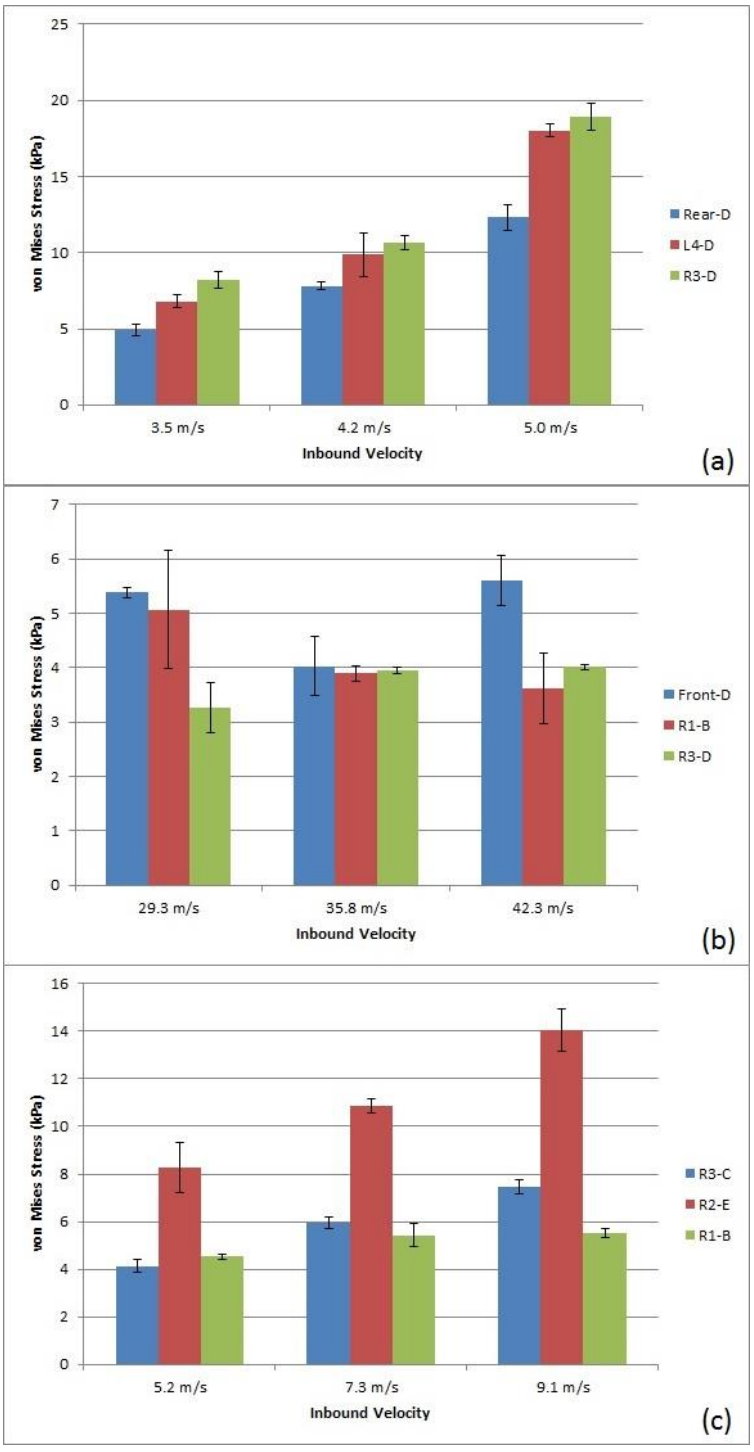

Figure 32: The influence of impact location on mean peak von Mises stress for each accident event: (a) (a) Fall, (b) Projectile, (c) Collision.

4.2.4 Distribution of Brain Deformation in the Cerebrum

The cerebrum was divided into ten regions. Dividing the brain in such a method allows for the identification of changes in stress and strain levels in these regions according to different impact conditions.

4.2.4.1 Maximum Principal Strain

The regions of the brain where the largest maximum principal strain magnitudes occurred for falls are presented in Table 14. All fall conditions produced the highest maximum principal strain in the auditory association area expect for helmeted falls at 3.5 m/s to impact location L4-D. For falls at 3.5 m/s to impact location L4-D the highest maximum principal strain was found in the primary somatosensory cortex.

Table 14: Average Maximal Principal Strain values (±1 standard deviation) for 10 regions of the brain for falls (*brain locations denoted below)

Location	Velocity (m/s)	No Helmet/Helmet	1	2	3	4	5	6	7	8	9	10
L4-D	3.5	No Helmet	0.558 (0.012)	0.315 (0.003)	0.335 (0.003)	0.241 (0.012)	0.188 (0.004)	0.313 (0.007)	0.505 (0.003)	0.384 (0.005)	0.242 (0.004)	0.109 (0.013)
		Helmet	0.204 (0.017)	0.154 (0.007)	0.154 (0.005)	0.105 (0.006)	0.133 (0.011)	0.136 (0.0140	0.204 (0.014)	0.180 (0.009)	0.129 (0.011)	0.084 (0.005)
	4.2	Helmet	0.324 (0.015)	0.202 (0.016)	0.229 (0.034)	0.148 (0.009)	0.161 (0.016)	0.195 (0.015)	0.291 (0.027)	0.252 (0.028)	0.182 (0.019)	0.097 (0.006)
	5.0	Helmet	0.557 (0.034)	0.313 (0.038)	0.330 (0.042)	0.230 (0.021)	0.194 (0.029)	0.299 (0.012)	0.443 (0.109)	0.352 (0.089)	0.225 (0.038)	0.153 (0.029)
R3-D	3.5	No Helmet	0.615 (0.049)	0.310 (0.021)	0.331 (0.006)	0.247 (0.005)	0.198 (0.008)	0.332 (0.004)	0.420 (0.094)	0.330 (0.020)	0.264 (0.025)	0.164 (0.029)
		Helmet	0.250 (0.021)	0.125 (0.010)	0.130 (0.004)	0.104 (0.007)	0.082 (0.006)	0.130 (0.004)	0.115 (0.003)	0.113 (0.003)	0.100 (0.004)	0.041 (0.001)
	4.2	Helmet	0.318 (0.017)	0.162 (0.013)	0.164 (0.006)	0.140 (0.015)	0.112 (0.008)	0.164 (0.006)	0.163 (0.014)	0.159 (0.015)	0.129 (0.015)	0.059 (0.012)
	5.0	Helmet	0.570 (0.003)	0.257 (0.029)	0.309 (0.007)	0.283 (0.045)	0.224 (0.029)	0.308 (0.008)	0.310 (0.022)	0.274 (0.028)	0.248 (0.012)	0.115 (0.007)
Rear-D	3.5	No Helmet	0.474 (0.014)	0.200 (0.004)	0.403 (0.008)	0.377 (0.005)	0.357 (0.010)	0.419 (0.005)	0.319 (0.006)	0.239 (0.002)	0.353 (0.004)	0.228 (0.011)
		Helmet	0.155 (0.018)	0.069 (0.003)	0.100 (0.001)	0.127 (0.005)	0.119 (0.002)	0.127 (0.005)	0.083 (0.001)	0.097 (0.010)	0.102 (0.006)	0.065 (0.014)
	4.2	Helmet	0.240 (0.006)	0.106 (0.002)	0.153 (0.009)	0.167 (0.004)	0.174 (0.0219)	0.165 (0.006)	0.123 (0.002)	0.146 (0.005)	0.171 (0.016)	0.093 (0.022)
	5.0	Helmet	0.392 (0.033)	0.172 (0.012)	0.260 (0.017)	0.269 (0.012)	0.262 (0.011)	0.255 (0.008)	0.219 (0.009)	0.213 (0.017)	0.260 (0.014)	0.163 (0.011)

*1 - Auditory Association Area, 2 – Auditory Cortex, 3 – Dorsolateral Prefrontal Area, 4 – Motor Association Cortex, 5 – Prefrontal Cortex, 6 – Primary Motor Cortex, 7 – Primary Somatosensory Cortex, 8 – Sensory Association Area, 9 – Visual Association Area, 10 – Visual Cortex

Table 15 shows the regions of the brain where the largest maximum principal strain magnitudes occurred for projectile impacts. The highest maximum principal strains were found to occur in the auditory association area for all projectile impacts.

Table 15: Average Maximal Principal Strain values (±1 standard deviation) for 10 regions of the brain for projectiles (*brain locations denoted below)

Location	Velocity (m/s)	No Helmet/Helmet	1	2	3	4	5	6	7	8	9	10
Front-D	29.3	No Helmet	0.272 (0.019)	0.078 (0.004)	0.147 (0.007)	0.141 (0.014)	0.114 (0.005)	0.146 (0.010)	0.228 (0.007)	0.186 (0.010)	0.254 (0.019)	0.088 (0.011)
		Helmet	0.190 (0.002)	0.020 (0.001)	0.049 (0.001)	0.048 (0.001)	0.047 (0.001)	0.034 (0.001)	0.056 (0.001)	0.044 (0.001)	0.071 (0.001)	0.050 (0.001)
	35.8	Helmet	0.126 (0.011)	0.029 (0.002)	0.058 (0.003)	0.057 (0.003)	0.062 (0.005)	0.042 (0.004)	0.059 (0.001)	0.059 (0.001)	0.102 (0.009)	0.063 (0.003)
	42.3	Helmet	0.176 (0.023)	0.032 (0.001)	0.072 (0.008)	0.067 (0.010)	0.074 (0.011)	0.053 (0.007)	0.064 (0.002)	0.067 (0.007)	0.126 (0.006)	0.075 (0.020)
R1-B	29.3	No Helmet	0.240 (0.017)	0.045 (0.001)	0.148 (0.002)	0.107 (0.002)	0.113 (0.003)	0.075 (0.003)	0.082 (0.005)	0.107 (0.019)	0.194 (0.010)	0.085 (0.002)
		Helmet	0.168 (0.004)	0.031 (0.010)	0.053 (0.005)	0.053 (0.002)	0.057 (0.002)	0.042 (0.009)	0.065 (0.003)	0.047 (0.001)	0.072 (0.008)	0.040 (0.004)
	35.8	Helmet	0.125 (0.004)	0.034 (0.010)	0.067 (0.005)	0.063 (0.002)	0.066 (0.002)	0.051 (0.009)	0.067 (0.003)	0.049 (0.008)	0.090 (0.008)	0.045 (0.004)
	42.3	Helmet										
R3-D	29.3	No Helmet	0.146 (0.007)	0.078 (0.001)	0.083 (0.006)	0.085 (0.002)	0.077 (0.002)	0.082 (0.006)	0.097 (0.004)	0.082 (0.005)	0.076 (0.003)	0.038 (0.001)
		Helmet	0.091 (0.013)	0.033 (0.004)	0.041 (0.003)	0.059 (0.008)	0.035 (0.003)	0.037 (0.003)	0.050 (0.002)	0.041 (0.009)	0.042 (0.003)	0.025 (0.004)
	35.8	Helmet	0.124 (0.015)	0.057 (0.003)	0.058 (0.003)	0.058 (0.001)	0.050 (0.002)	0.054 (0.002)	0.064 (0.006)	0.061 (0.004)	0.056 (0.006)	0.035 (0.004)
	42.3	Helmet	0.134 (0.016)	0.059 (0.005)	0.063 (0.008)	0.059 (0.002)	0.056 (0.003)	0.058 (0.003)	0.068 (0.006)	0.068 (0.007)	0.063 (0.008)	0.034 (0.002)

*1 - Auditory Association Area, 2 – Auditory Cortex, 3 – Dorsolateral Prefrontal Area, 4 – Motor Association Cortex, 5 – Prefrontal Cortex, 6 – Primary Motor Cortex, 7 – Primary Somatosensory Cortex, 8 – Sensory Association Area, 9 – Visual Association Area, 10 – Visual Cortex

The regions of the brain where the highest maximum principal strain magnitudes occurred for collisions are illustrated in Table 16. All collisions were found to produce the highest maximum principal strain in the auditory association area except for helmeted impacts to location R1-B. For helmeted collisions to impact location R1-B the highest maximum principal strain occurred in the visual association area.

Table 16: Average Maximal Principal Strain values (±1 standard deviation) for 10 regions of the brain for collisions (*brain locations denoted below)

Location	Velocity (m/s)	No Helmet/Helmet	1	2	3	4	5	6	7	8	9	10
R1-B	5.2	No Helmet	0.151 (0.006)	0.116 (0.005)	0.138 (0.007)	0.119 (0.004)	0.107 (0.006)	0.136 (0.007)	0.117 (0.005)	0.005 (0.007)	0.140 (0.001)	0.065 (0.003)
		Helmet	0.136 (0.008)	0.085 (0.012)	0.107 (0.012)	0.103 (0.010)	0.080 (0.009)	0.108 (0.011)	0.108 (0.002)	0.081 (0.001)	0.172 (0.007)	0.069 (0.006)
	7.3	Helmet	0.195 (0.003)	0.119 (0.001)	0.139 (0.003)	0.135 (0.005)	0.106 (0.005)	0.146 (0.005)	0.140 (0.010)	0.108 (0.004)	0.205 (0.018)	0.088 (0.002)
	9.1	Helmet	0.190 (0.011)	0.099 (0.011)	0.118 (0.006)	0.116 (0.005)	0.092 (0.012)	0.129 (0.010)	0.123 (0.013)	0.122 (0.025)	0.198 (0.007)	0.088 (0.003)
R2-E	5.2	No Helmet	0.323 (0.016)	0.171 (0.001)	0.179 (0.004)	0.173 (0.002)	0.129 (0.006)	0.182 (0.001)	0.176 (0.005)	0.181 (0.007)	0.175 (0.007)	0.083 (0.002)
		Helmet	0.254 (0.024)	0.133 (0.019)	0.142 (0.018)	0.135 (0.010)	0.099 (0.012)	0.142 (0.018)	0.132 (0.017)	0.154 (0.020)	0.139 (0.025)	0.062 (0.008)
	7.3	Helmet	0.328 (0.014)	0.163 (0.001)	0.167 (0.003)	0.166 (0.002)	0.134 (0.007)	0.173 (0.002)	0.182 (0.016)	0.169 (0.013)	0.164 (0.019)	0.081 (0.004)
	9.1	Helmet	0.418 (	0.269	0.232	0.222	0.159	0.237	0.219	0.218	0.174	0.086
R3-C	5.2	No Helmet	0.201 (0.021)	0.084 (0.003)	0.104 (0.006)	0.084 (0.005)	0.066 (0.004)	0.104 (0.006)	0.093 (0.005)	0.079 (0.002)	0.078 (0.009)	0.037 (0.006)
		Helmet	0.173 (0.020)	0.074 (0.002)	0.087 (0.005)	0.073 (0.003)	0.060 (0.003)	0.087 (0.005)	0.087 (0.005)	0.082 (0.010)	0.078 (0.010)	0.042 (0.008)
	7.3	Helmet	0.213 (0.008)	0.108 (0.005)	0.110 (0.003)	0.105 (0.002)	0.077 (0.004)	0.113 (0.002)	0.114 (0.007)	0.109 (0.004)	0.088 (0.014)	0.040 (0.007)
	9.1	Helmet	0.269 (0.025)	0.131 (0.011)	0.134 (0.008)	0.127 (0.015)	0.092 (0.007)	0.135 (0.010)	0.130 (0.004)	0.132 (0.006)	0.093 (0.009)	0.044 (0.001)

*1 - Auditory Association Area, 2 – Auditory Cortex, 3 – Dorsolateral Prefrontal Area, 4 – Motor Association Cortex, 5 – Prefrontal Cortex, 6 – Primary Motor Cortex, 7 – Primary Somatosensory Cortex, 8 – Sensory Association Area, 9 – Visual Association Area, 10 – Visual Cortex

4.2.4.2 Von Mises Stress

The regions of the brain where the largest von Mises stress magnitudes occurred for falls are shown in Table 17. The highest von Mises stress occurred in the auditory association area for all fall conditions with the exception of helmeted falls at 3.5 m/s to impact location L4-D. Falls at 3.5 m/s to impact location L4-D were found to produce the highest von Mises stress in the sensory association area.

Table 17: Average von Mises stress values (±1 standard deviation) for 10 regions of the brain for falls (*brain locations denoted below)

Location	Velocity (m/s)	No Helmet/Helmet	1	2	3	4	5	6	7	8	9	10
L4-D	3.5	No Helmet	16.2 (0.3)	11.4 (0.2)	13.0 (0.2)	7.9 (0.3)	7.3 (0.1)	10.3 (0.2)	15.2 (0.2)	13.7 (0.2)	7.6 (0.2)	3.5 (0.3)
		Helmet	6.5 (0.4)	5.9 (0.3)	5.7 (0.5)	3.2 (0.1)	4.9 (0.4)	4.6 (0.2)	6.2 (0.5)	6.8 (0.4)	4.4 (0.3)	2.6 (0.2)
	4.2	Helmet	9.9 (1.4)	8.2 (0.8)	8.1 (1.5)	4.3 (0.3)	5.9 (0.7)	5.9 (0.6)	8.9 (1.0)	9.6 (1.2)	5.8 (0.7)	3.1 (0.4)
	5.0	Helmet	18.0 (0.4)	11.6 (2.3)	11.0 (2.4)	7.9 (1.2)	6.7 (1.6)	9.3 (0.5)	13.1 (3.5)	12.5 (3.6)	7.4 (1.8)	4.8 (1.2)
R3-D	3.5	No Helmet	20.2 (0.8)	11.1 (1.2)	11.2 (0.4)	8.6 (0.2)	6.8 (0.6)	10.7 (0.4)	12.9 (2.6)	11.4 (1.5)	8.4 (0.6)	5.0 (0.8)
		Helmet	8.2 (0.5)	3.7 (0.3)	4.2 (0.2)	3.3 (0.2)	2.6 (0.1)	4.2 (0.2)	3.7 (0.2)	3.6 (0.2)	2.8 (0.1)	1.2 (0.1)
	4.2	Helmet	10.6 (0.5)	5.5 (0.6)	5.4 (0.1)	4.3 (0.3)	3.7 (0.5)	5.4 (0.1)	4.8 (0.2)	5.0 (0.7)	3.9 (0.5)	1.8 (0.2)
	5.0	Helmet	18.9 (0.9)	7.7 (0.9)	10.6 (0.8)	10.0 (2.3)	7.4 (1.6)	9.7 (0.2)	9.4 (0.6)	8.3 (0.8)	7.6 (0.5)	3.5 (0.8)
Rear-D	3.5	No Helmet	15.7 (0.8)	6.8 (0.2)	11.9 (0.4)	11.3 (0.2)	11.8 (0.3)	12.0 (0.2)	10.0 (0.2)	8.4 (0.3)	11.2 (0.1)	6.6 (0.3)
		Helmet	4.9 (0.4)	2.3 (0.1)	3.2 (0.1)	3.4 (0.1)	3.9 (0.1)	3.4 (0.1)	2.5 (0.1)	3.0 (0.5)	3.4 (0.3)	1.9 (0.4)
	4.2	Helmet	7.8 (0.3)	3.6 (0.1)	4.9 (0.4)	5.0 (0.2)	5.8 (0.7)	4.6 (0.2)	3.8 (0.1)	4.7 (0.6)	5.7 (0.3)	2.7 (0.6)
	5.0	Helmet	12.3 (0.8)	5.7 (0.4)	8.4 (0.4)	8.6 (0.4)	8.5 (0.4)	7.8 (0.1)	7.2 (0.4)	7.0 (1.0)	8.3 (0.3)	5.1 (0.3)

*1 - Auditory Association Area, 2 – Auditory Cortex, 3 – Dorsolateral Prefrontal Area, 4 – Motor Association Cortex, 5 – Prefrontal Cortex, 6 – Primary Motor Cortex, 7 – Primary Somatosensory Cortex, 8 – Sensory Association Area, 9 – Visual Association Area, 10 – Visual Cortex

Table 18 illustrates the regions of the brain where the largest von Mises stress magnitudes occurred for projectile impacts. Projectile impacts were found to produce the highest von Mises stress in the auditory association area.

Table 18: Average von Mises stress values (±1 standard deviation) for 10 regions of the brain for projectiles (*brain locations denoted below)

Location	Velocity (m/s)	No Helmet/Helmet	1	2	3	4	5	6	7	8	9	10
Front-D	29.3	No Helmet	9.9 (1.1)	3.6 (0.1)	6.3 (0.2)	4.9 (0.4)	3.7 (0.3)	4.9 (0.4)	7.3 (0.1)	6.2 (0.3)	9.1 (0.4)	2.9 (0.2)
		Helmet	5.4 (0.1)	0.8 (0.1)	1.6 (0.1)	1.5 (0.1)	1.4 (0.1)	1.1 (0.1)	1.7 (0.1)	1.4 (0.1)	2.3 (0.1)	1.6 (0.1)
	35.8	Helmet	4.0 (0.5)	0.9 (0.1)	2.0 (0.2)	1.8 (0.1)	1.9 (0.2)	1.5 (0.1)	1.8 (0.1)	2.0 (0.1)	3.3 (0.3)	2.1 (0.1)
	42.3	Helmet	5.6 (0.5	1.1 (0.2)	2.6 (0.6)	2.1 (0.3)	2.2 (0.3)	1.7 (0.2)	2.0 (0.1)	2.3 (0.2)	4.1 (0.2)	2.5 (0.6)
R1-B	29.3	No Helmet	8.0 (0.6)	1.9 (0.2)	6.3 (0.1)	3.6 (0.2)	3.5 (0.2)	3.2 (0.1)	3.0 (0.1)	3.8 (0.7)	6.4 (0.3)	2.8 (0.1)
		Helmet	5.1 (1.1)	0.9 (0.1)	1.7 (0.1)	1.6 (0.1)	1.7 (0.1)	1.4 (0.1)	2.0 (0.1)	1.5 (0.1)	2.4 (0.1)	1.3 (0.1)
	35.8	Helmet	3.9 (0.2)	1.0 (0.3)	2.3 (0.2)	2.0 (0.1)	2.0 (0.1)	1.7 (0.1)	2.1 (0.1)	1.6 (0.1)	3.0 (0.1)	1.5 (0.1)
	42.3	Helmet	3.6 (0.6)	1.5 (0.4)	2.8 (0.7)	2.3 (0.1)	2.3 (0.1)	2.0 (0.3)	2.1 (0.1)	1.8 (0.4)	3.5 (0.6)	1.9 (0.5)
R3-D	29.3	No Helmet	5.1 (0.2)	2.8 (0.2)	3.3 (0.3)	2.8 (0.2)	2.3 (0.6)	2.5 (0.1)	3.6 (0.1)	2.6 (0.1)	2.7 (0.1)	1.3 (0.1)
		Helmet	3.3 (0.5)	1.2 (0.1)	1.4 (0.2)	1.6 (0.1)	1.1 (0.1)	1.3 (0.2)	1.6 (0.1)	1.3 (0.1)	1.3 (0.1)	0.8 (0.1)
	35.8	Helmet	3.9 (0.1)	1.9 (0.1)	2.3 (0.2)	1.9 (0.1)	1.5 (0.1)	2.1 (0.1)	2.3 (0.1)	1.8 (0.2)	1.8 (0.2)	1.0 (0.1)
	42.3	Helmet	4.0 (0.1)	2.0 (0.2)	2.8 (0.2)	2.0 (0.1)	1.7 (0.1)	2.1 (0.1)	2.3 (0.3)	2.0 (0.3)	1.9 (0.3)	1.1 (0.1)

*1 - Auditory Association Area, 2 – Auditory Cortex, 3 – Dorsolateral Prefrontal Area, 4 – Motor Association Cortex, 5 – Prefrontal Cortex, 6 – Primary Motor Cortex, 7 – Primary Somatosensory Cortex, 8 – Sensory Association Area, 9 – Visual Association Area, 10 – Visual Cortex

The regions of the brain where the largest von Mises stress magnitudes occurred for collisions are shown in Table 19. The highest maximum principal strains for all collisions were found to in the auditory association area except for helmeted impacts to location R1-B. For collisions to a helmeted headform at impact location R1-B the highest von Mises stress occurred in the visual association area.

Table 19: Average von Mises stress values (±1 standard deviation) for 10 regions of the brain for collisions (*brain locations denoted below)

Location	Velocity (m/s)	No Helmet/Helmet	1	2	3	4	5	6	7	8	9	10
R1-B	5.2	No Helmet	4.0 (0.1)	2.8 (0.2)	3.5 (0.2)	2.8 (0.2)	2.6 (0.2)	3.2 (0.2)	2.8 (0.1)	2.9 (0.2)	3.6 (0.1)	1.7 (0.2)
		Helmet	3.4 (0.2)	2.4 (0.17)	2.8 (0.2)	2.6 (0.3)	2.1 (0.2)	2.6 (0.3)	2.9 (0.1)	2.5 (0.3)	4.5 (0.1)	1.9 (0.1)
	7.3	Helmet	5.0 (0.1)	3.6 (0.1)	3.9 (0.3)	3.4 (0.2)	2.9 (0.2)	3.7 (0.1)	4.0 (0.1)	3.9 (0.1)	5.4 (0.5)	2.3 (0.2)
	9.1	Helmet	5.2 (0.1)	3.5 (0.1)	3.5 (0.2)	3.1 (0.2)	2.9 (0.1)	3.3 (0.1)	3.6 (0.3)	4.2 (0.9)	5.5 (0.2)	2.4 (0.4)
R2-E	5.2	No Helmet	10.9 (0.4)	5.3 (0.1)	5.7 (0.1)	5.3 (0.2)	4.4 (0.1)	5.8 (0.1)	5.6 (0.1)	5.1 (0.1)	4.7 (0.2)	2.8 (0.1)
		Helmet	8.3 (1.0)	4.7 (0.6)	4.7 (0.7)	3.9 (0.3)	3.4 (0.3)	4.7 (0.7)	4.1 (0.4)	4.4 (0.5)	3.7 (0.7)	2.0 (0.5)
	7.3	Helmet	10.9 (0.3)	6.3 (0.3)	5.7 (0.1)	5.2 (0.2)	4.5 (0.1)	5.7 (0.1)	5.3 (0.2)	5.4 (0.1)	4.2 (0.5)	2.1 (0.1)
	9.1	Helmet	14.0 (0.9)	9.5 (0.7)	8.3 (0.5)	6.5 (0.5)	5.3 (0.6)	8.3 (0.5)	6.7 (0.6)	7.3 (0.7)	4.8 (0.9)	2.6 (0.3)
R3-C	5.2	No Helmet	4.8 (0.1)	2.1 (0.1)	2.5 (0.2)	1.1 (0.1)	1.7 (0.1)	2.5 (0.2)	2.2 (0.1)	2.1 (0.1)	1.9 (0.3)	1.0 (0.1)
		Helmet	4.1 (0.3)	2.3 (0.1)	2.3 (0.1)	2.0 (0.1)	1.6 (0.1)	2.1 (0.1)	2.1 (0.2)	2.0 (0.3)	2.1 (0.2)	1.2 (0.1)
	7.3	Helmet	6.0 (0.2)	3.2 (0.1)	3.1 (0.1)	2.6 (0.1)	2.4 (0.1)	3.1 (0.1)	2.9 (0.1)	3.0 (0.2)	2.5 (0.4)	1.2 (0.3)
	9.1	Helmet	7.4 (0.3)	3.9 (0.2)	3.6 (0.1)	3.5 (0.4)	2.8 (0.4)	3.6 (0.1)	3.5 (0.2)	3.6 (0.2)	2.7 (0.1)	1.3 (0.1)

*1 - Auditory Association Area, 2 – Auditory Cortex, 3 – Dorsolateral Prefrontal Area, 4 – Motor Association Cortex, 5 – Prefrontal Cortex, 6 – Primary Motor Cortex, 7 – Primary Somatosensory Cortex, 8 – Sensory Association Area, 9 – Visual Association Area, 10 – Visual Cortex

Chapter 5. Discussion

Understanding the protective capacity of ice hockey goaltenders will provide ice hockey equipment manufacturers with information to develop equipment to protect ice hockey goaltenders from the risk of concussion. Research has shown different accident events create unique impact conditions that influence the direction and magnitude of the dynamic response and subsequent brain tissue deformation stresses and strains (Post et al., 2013; Karton et al., 2013). These accident events have been shown to characterize different levels of risk for concussion (Zhang et al., 2004; Kleiven, 2007; Kendall et al., 2012a; Zanetti et al., 2013). As such, it is important to consider the protective capacity of helmets across all expected accident events. Considerable research has been conducted to assess the protective capacity of ice hockey helmets for common accident events (Wall, 1996; Rousseau et al., 2009a; Rousseau et al., 2009b; Post et al., 2011; Walsh et al., 2012; Hoshizaki et al., 2013; Post et al., 2014b; Rousseau et al., 2014; Ouckama and Pearsall, 2014). However, little research has been conducted to assess the protective capacity of ice hockey goaltenders (Nur et al., submitted). The objective of this thesis is to describe the protective capacity of ice hockey goaltender masks for three distinct accident events (fall, collision, projectile) of varying locations and velocities, as measured by peak resultant linear and rotational acceleration, rotational velocity peak von Mises and peak maximum principal strain.

5.1 Comparison of Accident Events

To examine the effect of accident events on the performance of ice hockey goaltender's masks, falls, collisions and projectiles were assessed. To reconstruct the three impact events inbound velocity and impact locations for each event were determined using video analysis of real world concussions experienced by ice hockey goaltenders (p. 55). The results demonstrated each

accident event was significantly different from the other with the exception of linear acceleration between collisions and projectile impacts and rotational velocity between fall and collisions. These differences are consistent with previous literature and reflect the unique impact parameters such as impact site, mass, velocity, angle of impact, and compliance of impactor, resulting in unique dynamic response curves creating different head and brain injuries (Gennarelli et al., 1982; 1987; Zhang et al., 2001a; Kleiven, 2003, Pellman et al., 2003; Post et al., 2012a).

Falls were found to create the highest peak dynamics response values associated with the highest risk of injury compared to the other accident events. Falls were characterized by the mass of the protected or unprotected head onto an immovable and rigid impact surface (Hoshizaki et al., 2014). This causes a large amount of energy to be transferred to the head due to the rigid surfaces offering little compliance (Hoshizaki et al., 2014), resulting in high magnitude and short duration linear and rotational acceleration (Post et al., 2012a; Post, 2013; Post et al., 2014a). Falls were found to create the highest linear and rotational accelerations which resulted in high rotational velocities, MPS and von Mises stress. These results are in agreement with Kendall et al. (2012a), who compared three accident events associated with a risk of concussion in ice hockey. Kendall et al. (2012a) found falls to the ice to produce the highest linear accelerations and MPS values. Although Kendall et al. (2012a) did not report falls producing the highest rotational accelerations, the highest rotational accelerations were achieved by punches. Falls produced the second highest rotational acceleration, greater than those of shoulder impacts (Kendall et al., 2012a). This demonstrates that falls create high dynamic and brain tissue deformation responses associated with a high risk of injury.

In addition falls were also found to have a large variance compared to projectile and collisions. This is a result of energy transfer and the range in which concussions can occur. In a fall a large

amount of energy is transferred to the head due to impacting a rigid surface (Hoshizaki et al., 2014). As such, this causes a large range in which concussions can occur as seen in Tables 8 and 11. This large range has also been seen in persistent concussive syndrome (PCS) (Post et al., 2015b). Therefore, it causes a large variance when all falls are considered together. Whereas, with projectiles and collisions, less energy is transferred to the head and the range where concussions occur is much smaller. For projectile impacts to an ice hockey goaltender mask, the puck is deflected and as a result not all the impact energy is absorbed by the head and some of the energy remains in the puck. Similarly not all the impact energy in a collision is transferred to the head as the shoulder pushes the head out of the way and continues along its original path. As such the range of response in which concussions can occur to in ice hockey goaltenders is much smaller than that of falls (Pellman et al., 2003; Rousseau, 2014; Post et al., 2015b).

Projectile impacts were found to produce the lowest dynamics response and brain tissue values however rotational acceleration was found to produce higher values than collisions. These results are likely due to the design of the ice hockey goaltenders mask causing most of the energy of the puck impact to be absorbed or deflected. The thick and stiff shell design of the ice hockey goaltender mask has been shown to result in low linear and rotational accelerations associated with a low risk of concussion (Nur et al. submitted). In contrast, puck impacts to ice hockey helmets which are made of a softer plastic shell such as polyethylene have been found to produce high dynamic response and brain tissue deformation values resulting in a risk for concussion and TBI (Ouckama & Pearsall, 2014; Rousseau et al., 2014). This suggested that projectile impacts were found to produce lower dynamics response and brain tissue values compared to other accident events due to the design of the ice hockey goaltender mask.

Shoulder impact produced the lowest dynamic response with the exception of rotational velocity and the second highest brain tissue deformation response. Shoulder impacts produced the lowest linear and rotational acceleration due to this accident event being characterized by high compliance. Soft structures act to absorb impact energy and decrease linear and rotational accelerations (Gilchrist, 2003). Such results have been observed when using strikers of different compliance to simulate shoulder impacts. Kendall et al. (2012a; 2014) used a stiff striker which consisting of a hemispherical nylon pad covering a MEP 60 Shore Type A (0.05m thick) disc covered with a shoulder pad to reconstruct concussive impacts for shoulder impacts and found linear and rotational accelerations above the 50 % risk for concussions, (Newman et al., 2000; Zhang et al., 2004). whereas Rousseau (2014) used a used a more compliant (softer) shoulder pad striker (Rousseau and Hoshizaki, 2015) to reconstruct shoulder impacts resulting in concussions in elite ice hockey and found mean peak linear acceleration of 24.7 ± 12 g and a mean peak rotational acceleration of 3.0 ± 1.1 krad/s^2. They reported a more compliant striker produced lower peak linear and rotational accelerations. However, more compliance causes long duration impacts (Gilchrist, 2003) which results in high rotational velocities. Rotational velocity is a measure of duration and magnitude. Falls create short duration, but high magnitude rotational accelerations (Post et al., 2012a; Post, 2013; Post et al., 2014a), whereas shoulder impacts result in low magnitude and long duration rotational accelerations (Rousseau, 2014). The result is both falls and collisions create high and similar rotational velocities associated with a risk of concussion (Ommaya 1985; Rowson et al., 2012; McIntosh et al., 2014). In addition, high compliant collisions to ice hockey goaltender mask were found to create high MPS and Von Mises stress. Gurdjian et al. (1966) created the Wayne State Tolerance Curve (WSTC) which demonstrated at short durations high accelerations can be managed by the brain but at long

durations low magnitude durations will cause injury. This research has been supported as long duration impacts have been shown to cause high brain stress and strain (Willinger et al., 1992; Gilchrist, 2003; Rousseau, 2014). Such impacts have been found to cause diffuse axonal injury and concussions (Willinger et al., 1992; Rousseau, 2014). As a result shoulder impacts were found produce the low linear and rotational accelerations but high rotational velocities, MPS and von Mises stress associated with a risk of concussion (Zhang et al., 2004; Kleivin, 2007; Rowson et al., 2012; Rousseau, 2014). These results demonstrate it is unlikely evaluating a single accident event can adequately evaluate head protection for all accident events (Hoshizaki et al., 2014). Therefore it is important to assess protective capacity of ice hockey goaltenders masks for the accident events associated with concussion.

5.2 Protective Capacity of Ice Hockey Goaltender Masks

To assess the baseline protective capacity of ice hockey goaltender masks a helmeted and unhelmeted headform was impacted for three distinct accident events associated with concussion (p. 55 - 56). In comparison of the no-helmet to helmet, significant differences were found for most conditions; however the degree to which it reflected a decrease in the risk of concussion varies. When examining the accident events in reference to the literature (Newman et al., 2000; Zhang et al., 2004; Doorly, 2007; Kleiven, 2007; Rowson et al., 2012; Rousseau, 2014 Post et al., 2015a; Post et al., 2015b), ice hockey goaltender masks were effective at reducing the risk for both concussion and TBI as measured by dynamic response and brain tissue deformation for falls and projectiles but less so for collisions. These results demonstrate ice hockey goaltender masks are well designed to decrease the risk of injury from falls and puck impacts but limited in their protection from shoulder collisions.

5.2.1 Falls

Ice hockey goaltenders masks were successful at reducing the risk of concussion and TBI for falls at 3.5 m/s. Falls at 3.5 m/s to an unhelmeted headform were found to produce linear and rotational acceleration and rotational velocities above 50% risk of sustaining a concussion (Newman et al., 2000; Zhang et al., 2004; Rowson et al., 2012). Whereas MPS and von Mises stress produced by falls to an unhelmeted headform were associated with a risk of PCS and TBI (Post et al., 2015a; Post et al., 2015b). When the headform was fitted with an ice hockey goaltender mask, it lowered dynamic response and brain tissue deformation measures to be associated with a low risk of concussion except for MPS to locations L4-D and R3-D and von Mises stress to impact location R3-D which associated with a 50% risk of concussion (Newman et al., 2000; Zhang et al., 2004; Rowson et al., 2012). MPS and von Mises stress for helmeted falls were found to be associated with a 50% risk of concussion except for MPS to locations Rear-D and von Mises stress to locations Rear-D and L4-D which were below 50% (Zhang et al., 2004; Kleiven, 2007). The decrease in the risk of injury seen in this study reflect the low incidence of TBI and concussions in ice hockey due to falls (Wennberg and Tator 2003; Hutchinson et al., 2013a). These results would suggest safety certification standards and equipment manufacturers should develop standards and ice hockey goaltenders mask which are more effective at reducing the risk of injury due to falls.

Ice hockey goaltenders masks are seen to be effective in reducing the risk of concussion and TBI for falls due to the method in which they are tested and designed. The research which led to the development of current ice hockey helmet certification standards was primarily concerned with the prevention of TBI. In the examination of the mechanism of TBI in monkeys and cadavers, researchers found that peak resultant linear acceleration correlated with injurious pressure waves

within the skull (Haddad et al., 1955; Gurdjian et al., 1966; Thomas et al., 1966). This led Gurdjian et al. (1966) to create a linear acceleration–time curve (Wayne State Tolerance Curve [WSTC]) based on cadaver head drops to a rigid surface. This formed the foundation for current sports helmet certification standards, and as a result current sports helmet certification standards aimed to replicate the mechanism of injury examined by Gurdjian et al. (1966). As a result, the current safety certification standard for ice hockey goaltender masks consists of a drop test to a hard surface to simulate falls to the ice (Canadian Standards Association, 2009) in which a peak resultant linear acceleration of 275 g associated with an indicator of TBIs is commonly used as the pass/fail limit for the safety certification of ice hockey helmets (Hoshizaki and Brien, 2004). Ice hockey goaltender masks are designed to reduce the risk of injury from falls to hard surfaces such as ice; supporting the findings that ice hockey goaltender masks can decrease the risk of injury for falls.

5.2.2 Projectiles

When examining the projectile impacts assessed in this study with reference to the literature (Newman et al., 2000; Zhang et al., 2004; Doorly, 2007; Kleiven, 2007) ice hockey goaltender masks were effective at reducing the risk of injury as determined by dynamic response and brain tissue deformation. Projectile impacts to an unhelmeted headform were found to produce linear and rotational accelerations associated with a 50% risk of sustaining a concussion (Newman et al., 2000; Zhang et al., 2004) except for impacts to the Front-D location which produced rotational accelerations within the risk of TBI (Doorly, 2007). When the headform was fitted with an ice hockey goaltenders mask, the risk of concussion was considered to be low, as measured by linear and rotational acceleration (Newman et al., 2000; Zhang et al., 2004). Despite larger differences in rotational velocity both helmeted and unhelmeted impacts remained

below 10% risk of concussion (Rowson et al., 2012). The result that there was no decrease in the risk of concussion as measured by rotational velocity, is likely due to concussion thresholds proposed by Rowson et al. (2012) are specific to football collisions recorded by the HIT System and do not reflect the risk of injury due to puck impacts in ice hockey. Maximum principle strain and von Mises stress have been found to be better predictors of brain injury (Schreiber et al. 1997; Willinger and Baumgartner 2003; Zhang et al. 2004; Kleiven 2007). When MPS and von Mises stress were used, unhelmeted conditions were found to above a 50% risk of concussion expect for impacts to R3-D and helmeted conditions were found decrease the risk below 50% (Zhang et al., 2004; Kleiven 2007). The low incidence of TBI and concussions seen in ice hockey would reflect the decreased risk of injury seen in this study when wearing an ice hockey goaltenders mask (Wennberg and Tator 2003; Hutchinson et al., 2013b), suggesting ice hockey goaltender masks are well designed to decrease the risk of injury from puck impacts.

Ice hockey goaltender's masks are seen to be effective in reducing the risk of concussion and TBI for puck impact likely due to the high and short duration and high magnitude dynamic response created by puck impacts and the stiff shell design. Projectile impacts produce very short duration of linear and rotational acceleration pulses (Rousseau et al., 2014). These pulses are similar to falls which typically result in high magnitude and short duration linear and rotational acceleration (Post et al., 2012a; Post, 2013; Post et al., 2014a). As ice helmets are designed to decrease the risk of injury for falls it would seem helmets are also effective at decreasing the risk of injury due to other accident events which cause high magnitude and short duration linear events. However ice hockey helmets are designed to protect against falls but only produce effective protection for puck impacts at low velocities (Ouckama and Pearsall, 2014; Rousseau et al., 2014), whereas ice hockey goaltenders masks were found to perform well over a large range

in velocity. The difference between the performance of the ice hockey goaltenders masks and ice hockey helmets may be attributed to differences in shell and liner design (Rousseau, et al., 2009a; 2009b; Ouckama & Pearsall, 2014; Post et al., 2014). Ice hockey helmets are typically made with a plastic shell such as high density polyethylene vinyl nitrile (VN) or expanded polypropylene (EPP) foam liners. Whereas ice hockey goaltender's masks are made with a thicker and stiffer shell material such as carbon and Kevlar composite, fiberglass or polycarbonate and contain a VN foam liner. Thick-shelled HDPE ice hockey helmets with EPP foams have been shown to perform differently than ice hockey helmets with a thin polycarbonate shell and lightweight foam when impacted by a puck (Ouckama & Pearsall, 2014). The difference in shell thickness between ice hockey helmeted and goaltenders masks could account for differences in the performance. Further, the stiffer shell of ice hockey goaltenders masks may have also attributed to an increase in protection from puck impacts (Nur et al., submitted). This suggests that for projectile impacts such as puck impact, having a stiff shell is a desirable design as it can help to distribute the impact energy (Post et al., 2015c). As a result all ice hockey goaltender masks and other helmets which mange energy from projectile impacts should be designed with a stiff shell.

5.2.3 Collisions

Ice hockey goaltender's masks were found to be less effective at reducing the risk of concussion for collisions. Despite significant differences being found for most conditions in the dynamic response between helmeted and unhelmeted conditions, the differences were very small and did not represent a decrease in the risk of concussion (Newman et al., 2000; Zhang et al., 2004; Rowson et al., 2012; Rousseau, 2014). Similar results were found for MPS and von Mises stress as small changes in response did not result in a decrease in the risk of concussion when

examining the literature (Zhang et al., 2004; Kleiven 2007; Rousseau, 2014). This limited protection from collisions could explain why ice hockey goaltenders have a high rate of concussion due to collisions (LaPrade et al., 2009).

Ice hockey goaltender's masks are in part less effective at reducing the risk of concussion from collisions due to the method in which they are tested. Current ice hockey goaltender mask standards only consider a drop test representing falls to the ice and do not consider collisions. Falls and collisions create unique responses as falls are typically characterized by the mass of the head impacting an immovable and rigid impact surface (Hoshizaki et al., 2014), which cause high magnitude and short duration linear and rotational acceleration (Post et al., 2012b; Post, 2013; Post et al., 2014a). Collisions are dependent on the characteristics of the body part impacting the head (Hoshizaki et al., 2014). In the case of collisions such as shoulder impacts Rousseau and Hoshizaki, (2015) identified the striking mass to be 12.9 kg with a highly compliant impacting surface resulting in low magnitude and long duration linear and rotational acceleration (Rousseau, 2014). Falls and shoulder collisions are defined by different impact characteristics, resulting in different impact responses, it is unlikely that falls alone can provide an adequately description of the risk for all concussions occurring in sport (Hoshizaki et al., 2014). As a result, the limited ability of ice hockey goaltender masks to effectively reduce the risk of concussion for shoulder impacts found in this study is a result of the high compliance shoulder impacts compared to falls. For high compliant impacts such as shoulder impacts, most of the energy is absorbed by the shoulder and not the helmet. The ice hockey goaltender mask helmet is not effective in reducing the risk of injury due to shoulder impacts, as the mask does not effectively engage in absorbing energy for the impact. As a result ice hockey goaltender's masks appear to be limited in their ability to reduce the risk of concussions from collisions. As

such an emphasis to establish new rules to protect ice hockey goaltenders from collisions may prove to be more effective in reducing the rate of concussions.

5.3 Influence of Impact Conditions

To assess the performance of ice hockey goaltender's masks across the continuum of concussion, three velocities and three impact locations were chosen. The velocities and impact locations represent a range in which these impact parameters vary for real world concussions experienced by ice hockey goaltenders (p. 55). The results demonstrate the dynamic response and brain tissue response were influenced by changes in velocity and location for all three accident events. Three impacts for each condition to an ice hockey goaltender mask had little effect on the dynamic response and brain tissue deformation response and the small differences in impact measures are likely a reflection of the variance in the test method used and small degradation of helmet materials. As such an ice hockey goaltender mask can withstand a minimum of three impacts with minor differences in response, however impacts to the cage of an ice hockey goaltender mask (Front-D) caused the cage to bend and as performed in this study the cage should be replaced after such an impact. In addition, significant interactions effects were found between velocity and impact location, demonstrating, the relationship between velocity and location changes for different velocities and locations. That is at a particular velocity one location may produce the highest response but at a different velocity another location may produce the highest response. As the impact conditions change it will affect the performance of the ice hockey goaltender's mask to reduce the risk of injury.

5.3.1 Velocity

The velocity of this study was chosen based on velocity ranges determined from video analysis of real world concussions experienced by ice hockey goaltenders (p.55). Increases in velocity

were found to cause an increase in the dynamic response and brain tissue deformation response. This is consistent with previous literature in which increases in inbound velocity have been shown to cause increases in dynamic response and brain tissue deformation response for falls, projectiles and collisions (Rousseau et al., 2009a; Rousseau et al., 2009b; Rousseau et al., 2014; Kendall et al., 2012b Post et al., 2012a; Post et al., 2013a ; Post et al., 2014c). In addition an increase in dynamic response and brain tissue deformation response due to increases in velocity result in an increase in the risk of injury for falls and collisions but not projectile impacts.

With increases in velocity for falls the ice hockey goaltender mask demonstrated a decrease in performance to manage dynamic response and brain tissue deformation below injury thresholds. For 3.5 m/s falls all injury metrics were below 50% risk of sustaining a concussion except for MPS which was associated with 50% risk of injury (Newman et al., 2000; Zhang et al., 2004; Kleivin, 2007; Rowson et al., 2012), while an increase in velocity to 4.2 m/s resulted in an increase in all injury metrics and an increase in the risk of concussion to be above 50% except for rotational acceleration and velocity which remained below 50% (Newman et al., 2000; Zhang et al., 2004; Kleivin, 2007; Rowson et al., 2012). An increase to a drop velocity of 5.0 m/s resulted in the greatest risk of injury in which dynamic response measures were above 75% risk of concussion (Newman et al., 2000; Zhang et al., 2004; Rowson et al., 2012) and brain deformation metrics within the risk of PCS and TBI (Post et al., 2015a; Post et al., 2015b). This suggests ice hockey goaltender's masks can manage the risk of injury below injury thresholds for low velocities, but as velocity increases so does the risk of concussion.

Projectile impacts demonstrated a different relationship between increases in velocity and increases in injury metrics than falls. An increase in velocity across a range of 29.3 m/s to 42.3 m/s was found to result in an increase in dynamic response. These were consistent with previous

research findings examining puck impacts to ice hockey helmets for dynamic response demonstrating increase in velocity produced an increase in response (Ouckama and Pearsall, 2014; Rousseau et al., 2014). However, when MPS and von Mises stress were measured an increase in velocity did not result in an increase in response. These findings are in contrast to previous research which demonstrated an increase in velocity resulted in an increase in brain tissue deformation response for puck impacts (Ouckama and Pearsall, 2014; Rousseau et al., 2014). The differences between this study and previous research could be a result of this study using a NOCSAE headform compared to previous research using a Hybrid III headform. Hybrid III and NOCSAE headforms have shown the two headforms produce different linear and rotational loading curve shapes (Kendall et al., 2012b). Different linear and rotational loading curves shapes have been shown to influence the response of peak MPS and von Mises stress (Post et al., 2012b). As a result MPS and von Mises stress not increasing with increases in velocity for projectile impacts could be a result of the unique linear and rotational load curves created by impacting a NOCSAE headform. Despite the differences, all injury metrics across a range of velocity of 29.3 m/s and 42.3 m/s were found to be associated with a low risk of concussion (Newman et al., 2000; Zhang et al., 2004; Kleivin, 2007; Rowson et al., 2012), demonstrating ice hockey goaltenders masks are well designed to reduce the risk of concussion for puck impacts across a wide range of shot velocities seen in ice hockey.

Increases in collisions velocity were found to produce increases in dynamics response and brain tissue deformation response. For collisions across a velocity range of 5.2 to 9.1 m/s dynamics response measured were below 50% risk of sustaining a concussion (Newman et al., 2000; Zhang et al., 2004; Kleivin, 2007; Rowson et al., 2012). When assessing rotational accelerations using thresholds specific to ice hockey shoulder impacts, it was found impacts at 7.3 and 9.1 m/s

were above 50% risk of concussion (Rousseau, 2014). As velocities of collisions increase the risk of concussion for ice hockey goaltenders also increased as measured by dynamic response. Further, von Mises stress was found to associate with a low risk of concussion for collisions at 5.2 and 7.3 m/s, but at 9.1 m/s the risk of injury was above 50% (Zhang et al., 2004; Kleivin, 2007). However, von Mises stress has been reported to be a poor predictor of concussion following a shoulder check to the head in ice hockey (Rousseau, 2014). When assessing MPS which has been found to be a better predictor of concussion following shoulder impacts in ice hockey all velocities were with a 50% risk of concussion (Zhang et al., 2004; Kleivin, 2007; Rousseau, 2014). This demonstrates that ice hockey goaltenders maybe at risk of sustaining a concussion across velocity range of 5.2 to 9.1 m/s. In addition it can also be noted that linear and rotational accelerations were higher in helmeted impacts at 7.3 m/s and 9.1 m/s than unhelmeted impacts at 5.2 m/s. This result could be a result of the total mass and in addition to an increase in velocity influencing the momentum and energy transfer in collisions with an ice hockey goaltender mask compared to an unhelmeted condition. These results highlight the importance of protecting ice hockey goaltenders from high velocity collisions such as players who lose control while on a breakaway (Liberman & Mulder, 2007). As a result it is important to minimize the number of collisions goaltenders are faced with and improve the equipment to protect goaltenders from the risk of concussion due to collisions.

5.3.2 Location

The impact locations chosen in this study were based on common impact locations of real world concussions experienced by ice hockey goaltenders (p. 55). When comparing impact sites to each other, significant differences were present, but not between all sites. This could be due to high standard deviations from collapsing all velocities into one analysis.

These results highlight the importance of assessing both centric and non-centric impact locations when evaluating the protective capacity of ice hockey goaltender's masks to reduce the risk of injury for falls.

When assessing the performance of an ice hockey goaltender mask by impact location for falls the differences between centric and non-centric impact locations are highlighted. Impact location R3-D was found to produce dynamic response and brain tissue deformation response, which were among the highest in comparison to other locations. This demonstrated the importance of protecting the side of the head form impacts as researches have shown impacts to the side of the head result in an increase injury risk (Kleiven, 2003; Zhang et al., 2001a; Zhang et al. 2004; Delaney et al., 2006). Impacts to the side of the head result in higher magnitudes of dynamic response and brain tissue deformation (Post et al., 2011; Hoshizaki et al., 2012; Walsh et al., 2012; Post et al., 2014c). Impact location L4-D produced the highest rotational kinematics alongside impact location R3-D but the lowest linear accelerations. Impact location L4-D was found to produce high rotational kinematics and lower linear accelerations due to the non-centric nature of the impact site causing greater rotation of the head (Walsh et al., 2011; Post et al., 2014d). High rotational kinematics from the non-centric site caused high levels of brain stress and strain (Post et al., 2012c; Post et al., 2012d) resulting in the highest MPS values along with impact location R3-D and the second highest von Mises stress. Impact location Rear-D was found to produce the highest linear acceleration along with impact location R3-D and the lowest rotational accelerations due to the centric nature of the impact location causing greater translation (Walsh et al., 2011; Post et al., 2014d). These results highlight the importance of assessing both centric and non-centric impact locations when evaluating the protective capacity of ice hockey goaltender's masks to reduce the risk of injury for falls.

In assessing the performance of an ice hockey goaltenders mask for projectile impacts to the front and side of the head interesting relationships were found. No main effect of location was found for rotational acceleration. These findings were consistent with previous research examining the capacity of ice hockey goaltender masks for protection from puck impacts (Nur et al., submitted). Further, impact locations R1-B and R3-D were found to produce higher linear accelerations but lower rotational velocity, MPS and von Mises stress than impact location Front-D. These results suggest when assessing the performance of helmets for puck impacts, rotational velocity may be a better predictor of brain tissue deformation metrics than linear and rotational acceleration (Ouckama and Pearsall, 2014). Interestingly, both R1-B and R3-D represent impacts to the shell of the ice hockey goaltender's mask were found to produce similar responses for all injury metrics measured with the exception of rotational velocity. These responses were found to be different than impact location Front-D which represents an impact to the cage. This suggests that impacts to the shell of the ice hockey goaltenders mask, mange energy differently than impacts to the cage. When assessing the protective capacity of an ice hockey goaltender mask it is important to consider both puck impacts to the shell and cage.

The influence of impact location of the protective capacity of an ice hockey goaltender's mask demonstrates the importance of impacting both centric and non-centric locations. Impact location R3-C produced the highest linear acceleration followed by impact location R1-B. The higher linear accelerations observed in impact locations R3-C and R1-B, are likely due to the centric nature of the impact creating high linear accelerations (Walsh et al., 2011). Location R3-C was also found to produce higher rotational velocities, MPS and von Mises stress compared to impact location R1-B. This is likely due to R3-D representing an impact to the side of the head which researchers have found to be more prone to cause injures than impacts to the forehead as

represented by impact location R1-B (Kleiven, 2003; Zhang et al., 2001a; Zhang et al. 2004; Delaney et al., 2006). However, these two impact locations were found to produce lower rotational kinematics, MPS and von Mises stress than location R2-E. Location R2-E produced the lowest linear acceleration, but higher rotational kinematics due to it representing a non-centric impact to the side of the face. In the reconstruction of punches in ice hockey Kendall et al. (2012a) found similar results in which a non-centric impact to the jaw caused high rotational accelerations and low linear accelerations, demonstrating impacting the side of the face can produce high linear accelerations but low linear acceleration. Further location R2-E was found to result the highest MPS and von Mises stress. These results indicate rotational kinematic as a result of non-centric impacts to the head to result in high levels of MPS and von Mises stress (Post et al., 2012c; Post et al., 2012d; Post et al., 2014d). As a result, it was demonstrated that the location of impact will affect the performance of ice hockey goaltender's mask. This highlights the importance of impacting multiple impact locations (centric and non-centric) when assessing the protective capacity of ice hockey goaltenders masks.

5.4 Distribution of Brain Deformation in the Cerebrum

To examine the effect of how different accident events and impact conditions influence the different regions of the cerebrum, the UCDBTM was divided into ten regions (Figure 12). For all accident events the majority of largest MPS and von Mises stress was found in the auditory association area. This could suggest the auditory association area is a region of high risk for injury. Further it could also suggest that similar symptoms of concussion are reported despite differences in the accident events which caused the concussion, as the same location of the brain is being damaged for each accident event. However, these findings are in contrast to Kendall et al. (2012a). Kendall et al. (2012a) who found the region with the highest MPS was shown to vary

depending on the accident event. Falls to the ice were found to have the highest MPS at the prefrontal cortex and shoulder collisions were found to produce the highest MPS in the dorsolateral prefrontal cortex (Kendall et al., 2012a). It is important to note Kendall et al. (2012) restricted data to regions of the cerebrum not in contact with the tentorium. As a result, the highest MPS and von Mises stress values occurring in the auditory association area for all accident events could be an influence of the tentorium resulting in larger brain stresses and strains in the auditory association area (Doorly, 2007).

Despite no influence of accident events on the different regions of the cerebrum, velocity and location were found to have an influence the different regions of the cerebrum. For falls at 3.5 m/s to impact location L4-D the highest MPS and von Mises stress were found in the primary somatosensory cortex and sensory association area. An increase in velocity caused a shift in the location of highest MPS and von Mises stress to the auditory association area. Such a phenomena as also been reported by Post et al. (2014d) for MPS but not for von Mises stress. The differences between (Post et al., 2014d) could be a result on impact location. Impact location has been shown to influence the regions of the cerebrum in which the largest MPS and von Mises stress occur (Post et al., 2014d). As L4-D is towards the back of the head and Post et al. (2014d) impacting the side of the head and towards the front of the head it could cause the relationships to change. The influence of impact location on the different regions of the cerebrum was also observed in collisions. For collisions to a helmeted headform at impact, location R1-B produced the largest MPS and von Mises stress in the visual association area. Whereas collisions to a helmeted headform at impact locations R3-D and R2-E were found to occur in the auditory association area. The influence of impact location and velocity on the distribution of brain deformation in the cerebrum may also explain why reported symptoms can vary from concussion

to concussion. As seen in Table 7 different regions of the brain are responsible for different functions. Therefore if a different part of the brain is damaged it could be expected that differences in symptoms would be expressed. For example in the case of collisions to impact location R1-B, the largest MPS and von Mises stress is in the visual association area and an ice hockey goaltender and there may be reports of symptoms of blurred vision (Price, 2000). However when collisions to R3-D and R2-E occur blurred vision may no longer be a symptom as the as the largest MPS and von Mises stress is in the auditory association area. In such cases an ice hockey goaltender may report hearing loss (Purves et al., 2001). Whereas in the case of falls to impact location L4-D, an ice hockey goaltender that falls at 3.5 m/s may report symptoms such as loss of balance or vertigo (Price, 2000) but as impact velocity increases these symptoms may no longer be reported. As a result, this thesis demonstrated that location and velocity can influence in which region the largest MPS and von Mises stress occur and may influence the symptoms which a concussed ice hockey goaltender reported.

Chapter 6. Conclusion

6.1 Summary

Concussions in ice hockey can occur as a result of many different accident events. This study investigated the protective capacity of ice hockey goaltender masks for three accident events (fall, collision, projectile) of varying locations and velocities as measured by dynamic response of a NOCSAE headform and brain tissue deformation. The results demonstrated that each accident event created a unique dynamic head response and brain tissue response. This demonstrated the importance to assess the protective capacity of ice hockey goaltenders masks for each type of accident. When comparing helmeted and unhelmeted impacts it was found ice hockey goaltender mask are effective at reducing dynamic response and brain tissue deformation for falls and projectiles but less so for collisions. Further, when velocity increases so does the dynamic response and brain tissue deformation. The results also demonstrate that impact location affects the performance of ice hockey goaltenders mask. This highlights the importance of impacting multiple locations (centric and non-centric) when assessing the protective capacity of ice hockey goaltenders masks. In addition, the location of the region where the largest brain tissue deformation occurs could be influenced by location and velocity but not accident event. Overall this study demonstrates ice hockey goaltender masks are limited in reducing the dynamic response and brain tissue deformation across all accident events and impact conditions; supporting the notion that in order to decrease the incidence of concussion in ice hockey, goaltender mask designs and current safety standards need to better reflect the nature of risk within the sport.

References

Adams, J.H., Graham, D.I. & Gennarelli, T.A. (1981). Acceleration induced head injury in the monkey: II. *Neuropathology*, *7*, 26-28.

Adams, J.H., Graham, D.I., Murray, L.S. & Scott, G. (1982). Diffuse axonal injury due to nonmissile head injury in humans: an analysis of 45 cases. *Annals of Neurology*, *12*(6), 557-563.

Agel, J., Dompier, T.P., Dick, R., Marshall, S.W. (2007). Descriptive epidemiology of collegiate men's ice hockey injuries: National Collegiate Athletic Association Injury Surveillance System, 1988-1989 through 2003-2004. *J Athl Train*, *42*(2):241-248.

Association, C. S. (2009). Ice Hockey Helmets. *Z262.1-09*. Mississauga, Ontario, Canada.

Association, C. S. (2009). Face Protectors for Use in Ice Hockey. *Z262.2-09*. Mississauga, Ontario, Canada.

ASTM Standard F1587-12a, "Standard Specification for Head and Face Protective Equipment for Ice Hockey Goaltenders," ASTM International, West Conshohocken, PA, 2014, DOI: 10.1520/F1587-12A, www.astm.org.

Astrup, J., Rehncrona, S. & Siesjo, B.K. (1980). The increase in extracellular potassium concentration in the ischemic brain in relation to the preischemic functional activity and cerebral metabolic rate. *Brain Research*, *199*, 161–174.

Bain, A.C. & Meaney, D.F. (2000). Tissue-Level Thresholds for Axonal Damage in an Experimental Model of Central Nervous System White Matter Injury, J. Biomech. Eng, *122*, 615–622.

Ballanyi, K., Grafe, P. & ten Bruggencate, G. (1987). Ion activities and potassium uptake mechanisms of glial cells in guinea-pig olfactory cortex slices. *Journal of Physiology*, *382*, 159–174.

Bancroft, R.W. (1989). Type, Location, and Severity of Hockey Injuries Occurring during Competition and Practice. Safety in Ice Hockey 2nd Volume, ASTM STP 1212, C. R. Castaldi, P. J. Bishop, and E. F. Hoerner, eds., ASTM International, Philadelphia, PA.

Barth, J.T., Freeman, J.R., Broshek, D.K. & Varney, R.N. (2001). Acceleration-deceleration sport-related concussion: The gravity of it all. *Journal of Athletic Training. 36*, 253-256

Biasca, N., Battaglia, H &, Tegner, Y. (1999). Diagnose und Behandlungsvorschläge der Commotio cerebri bei Kontakt- und Kampf-sportarten: Beispiel im Eishockey. Schweizerische Ärtzezeitung, *80*, 595–8.

Bailes, J.E. & Cantu, R.C. (2001). Head injury in athletes. *Neurosurgery*, *48*(1), 26-45.

Biasca, N. (2000). Review and consequences of the typical ice hockey related injuries in the Swiss Ice Hockey Association (SIHA) 1996–1998. In: Biasca N, Montag WD, Gerber C, eds. Safety in ice hockey: Eighth International Symposium of the International Ice Hockey Federation IIHF. Zurich: IIHF, 36–52.

Biasca, N., Wirth, S. & Tegner, Y. (2002). The avoidability of head and neck injuries in ice hockey: an historical review. *Br J Sports Med*, *36*, 410-427.

Bishop, P.J., Arnold, J. (1993). The effectiveness of hockey helmets in limiting localized loading on the head. In: Castaldi CR, Bishop PJ, Hoerner EF, eds. Safety in ice hockey: volume 2, ASTM STP 1212. Philadelphia: American Society for Testing and Materials, 175–82.

Bishop, P.J. (1997). Impact performance characteristics of hockey helmets with liners of differing thickness, In: Ashare A, ed. Third international symposium on safety in ice hockey. Philadelphia: American Society for Testing and Materials, 112–17.

Bishop, P.J. (2000). Biomechanics of sports protective equipment in ice hockey to prevent injuries. In: Biasca N, Montag WD, Gerber C, eds. Safety in ice hockey: Eighth International Symposium of the International Ice Hockey Federation IIHF. Zurich: IIHF, 36–52.

Benson, B.W., Meeuwusse, W.H., Rizos, J., Kang, J. & Burke, C.J. (2011). A prospective study of concussions among National Hockey League players during season games. *Canadian Medical Association Journal*, *183*(8), 905-911.

Braddick, O.J., O'Brien, J.M., Wattam-Bell, J., Atkinson, J., Hartley, T. & Turner, R. (2001). Brain areas sensitive to coherent visual motion. *Perception*, *30*, 61–72.

Bull, R.J. & Cummins, J.T. (1973). Influence of potassium on the steady-state redox potential of the electron transport chain in slices of rat cerebral cortex and the effect of ouabain. *Journal of Neurochemistry*, *21*, 923–937.

Bush, M. A., Cooper, H. I. & Dorion, R. B. (2010). Inquiry into the scientific basis for bitemark profiling and arbitrary distortion compensation. *Journal of forensic sciences*, *55*(4), 976-983.

Cantu, R.C. (1996). Head injuries in sport. *Br J Sports Med*. *30*(4):289-296.

Cantu, R.C, & Mueller, F.O. (2003). Catastrophic spine injuries in American football, 1977-2001. *Neurosurgery, 53*(2), 358-362.

Casson, I.R., Viano, D.C., Powell, J.W. & Pellman, E.J. (2010). Twelve years of national football league concussion data. Sports Health: A Multidisciplinary Approach, *2*(6), 471-484.

Cater, H.L., Sundstrom, L.E., and Morrison, B., III. (2006). Temporal Development of Hippocampal Cell Death Is Dependent on Tissue Strain but Not Strain Rate. *J. Biomech*, *39*, 2810–2818.

Crisco, J.J., Fiore, R., Beckwith, J.G., Chu, J.J., Brolinson, P.G., Duma, S., McAllister, T.W., Duhaime, A.C. & Greenwald, R.M. (2010). Frequency and location of head impact exposures in individual collegiate football players, *Journal of Athletic Training, 45*, 549-559

Coulson, N.R., Foreman, S.G., Hoshizaki, T.B. (2009). Translational and rotational accelerations generated during reconstructed ice hockey impacts on a hybrid III head form, *Journal of ASTM International*, *6*(2), 1-8.

Creutzfeldt, O., Ojemann, G. & Lettich, E. (1989a). Neuronal activity in human lateral temporal lobe. I. Responses to speech. *Exp. Brain Res, 77*, 451-475.

Creutzfeldt, O., Ojemann, G. & Lettich, E. (1989b). Neuronal activity in human lateral temporal lobe. II. Responses to subjects own voice. *Exp. Brain Res, 77*,476-489.

D'Ambrosio, R., Maris, D.O., Grady, M.S., Winn, H.R. & Janigro, D. (1999). Impaired K(+) homeostasis and altered electrophysiological properties of posttraumatic hippocampal glia. *Journal of Neuroscience, 19*, 8152–8162.

Deck, C. & Willinger, R. (2009). The current state of the human head finite element modelling. *International journal of vehicle safety*, *4*(2), 85-112.

Delaney, J.S., Lacroix, V.J., Leclerc, S. & Johnston, K.M. (2002). Concussions among university football and soccer players. *Clinical Journal of Sports Medicine, 12*, 331-338.

Delaney, J.S. (2004). Head injuries presenting to emergency departments in the United States from 1990-1999 for ice hockey, soccer, and football. *Clinical Journal of Sport Medicine*, *14*, 80-87.

Delaney, J.S., Puni, V.& Rouah, F. (2006). Mechanisms of injury for concussions in university football, ice hockey, and soccer. *Clin J Sports Med, 16*(2), 162–165.

Doorly, M.C. & Gilchrist, M.D. (2006). The use of accident reconstruction for the analysis of traumatic brain injury due to head impacts arising from falls. *Computer Methods in Biomechanics and Biomedical Engineering*, *9*(6), 371-377.

Doorly, M.C. (2007). Investigations into head injury criteria using numerical reconstruction of real life accident cases. *PhD thesis*, University College Dublin.

Donaldson, L., Asbridge, M. & Cusimano M.D. (2013). Bodychecking Rules and Concussion in Elite Hockey. *PLOS One*. *8*(7), 1-6.

Echemendia, R.J., Putukian, M., Mackin, R,S,, et al,. (2001). Neuropsychological test performance prior to and following sports-related mild traumatic brain injury. *Clin J Sport Med, 11*, 22–31.

Elkin, B.S. and Morrison, B., III. (2007). Region-Specific Tolerance Criteria for the Living Brain. *Stapp Car Crash J, 51*, 127–138.

Emery, C.A. & Meeuwisse, W.H. (2006). Injury Rates, Risk Factors, and Mechanisms of Injury in Minor Hockey. *Am. J. Sports Med*., *34*,1960–1969.

Faul, M., Xu, L. & Wald, M.M. (2010). Coronado, VG. Traumatic Brain Injury in the United States: Emergency Department Visits, Hospitalizations and Deaths 2002-2006. US Department of Health and Human Services

Finkelstein, E., Corso, P. & Miller, T. (2006). The Incidence and Economic Burden of Injuries in the United States. New York, NY: Oxford University Press

Flik, K., Lyman, S. & Marx, R.G. (2005). American collegiate men's ice hockey: an analysis of injuries. *American Journal of Sports Medicine*. *33*(2):183-187.

Forero Rueda, M.A., Cui, L. & Gilchrist, M.D. (2010). Finite element modeling of equestrian helmet impacts exposes the need to address rotational kinematics in future helmet designs. *Computer Methods in Biomechanics and Biomedical Engineering, 1,* 1-11.

Fréchède, B. & McIntosh, A. (2007). Use of MADYMO's human facet model to evaluate the risk of head injury in impact. *Proceedings of the 20th Enhanced Safety of Vehicles Conference*, Lyon, France, June 18-21.

Galbraith, J.A., Thibault, L.E. & Matteson, D.R. (1993). Mechanical and Electrical Responses of the Squid Giant Axon to Simple Elongation. *J. Biomech. Eng*, *115*, 13–22.

Gasquoine, P.G. (1997). Postconcussion symptoms. *Neuropsych Rev*, *7*(2):77–85.

Gennarelli, T., A. Ommaya and L. Thibault (1971). Comparison of translational and rotational head motions in experimental cerebral concussion. *Proc. 15th Stapp Car Crash Conference*.

Gennarelli, T.A, Thibault, L.E. & Ommaya, A.K. (1972). Pathophysiological Responses to Rotational and Translational Accelerations of the Head, SAE Paper No. 720970, in: *16thh Stapp Car Crash Conference*, Society of Automotive Engineers, p. 296-308.

Gennarelli, T.A., Abel, J.M., Adams, H. & Graham, D. (1979). Differential Tolerance of Frontal and Temporal Lobes to Contusion Induced by Angular Acceleration.

Gennarelli, T.A., Thibault, L.E., Adams, H., Graham, D.I., Thompson, C.J. & Marcincin, R.P. (1982). Diffuse Axonal Injury and Traumatic Coma in the Primate. *Annals of Neurology, 12*(6), 564-574.

Gennarelli, T.A., Thibault, L., Tomei, G., Wiser, R., Graham, D. & Adams, J. (1987). Directional dependence of axonal brain injury due to centroidal and non-centroidal acceleration. Proceedings in the 31st *Stapp Car Crash Conference*, p. 49-53. Society of Automotive Engineers, Warrendale, Philadelphia.

Gerberich, S.G., Finke, R., Madden, M., Priest, J.D., Aamoth, G. & Murray, K. (1987). An 263 Epidemiological Study of High School Ice Hockey Injuries. *Child. Nerv. Syst, 3*(264), 59–64.

Gilenstam, K., Henriksson-Larse´n, K. & Thorsen, K. (2009). Influence of Stick Stiffness and Puck Weight on Puck Velocity during Slap Shots in Women's Ice Hockey. *Sports Eng*, *11*, 103–107.

Gilchrist, M.D. (2003). Modelling and Accident Reconstruction of Head Impact Injuries. *Key Engineering Materials, 245-246*, 417-429.

Giza, C.C. & Hovda, D.A. (2001). The neurometabolic cascade of concussion, *Journal of Athletic Training, 36*, 228-235.

Goodman, D., Gaetz, M.& Meichenbaum, D. (2001). Concussions in hockey: there is cause for concern. *Med Sci Sports Exerc*. *33*(12), 2004-2009.

Gurdjian, E.S., Lissner, H.R., Latimer, F.R., Haddad, B.F. & Webster, J. E. (1953). Quantitative Determination of Acceleration and Intracranial Pressure in Experimental Head Injury. *Neurology, 3*(6), 417-423

Gurdjian, E.S., Lissner, H.R., & Patrick, L.M. (1963). Concussion-mechanism and pathology. *Proc. 71' Stapp Car Crash Conf*, 470-482.

Gurdjian, E.S., Roberts, V.L. & Thomas, L.M. (1966). Tolerance curves of acceleration and intracranial pressure and protective index in experimental head injury. *Journal of trauma, 6*(5), 600-604.

Gurdjian, E.S. (1975). Re-evaluation of the biomechanics of blunt impact injury of the head. *Surgery, Gynecology & Obstetrics, 140*(6), 845-850.

Guskiewicz, K.M., Marshall, S.W., Bailes, J., McCrea, M., Cantu, RC., Randolph, C. & Jordan, B.D. (2005). Association between recurrent concussion and late-life cognitive impairment in retired professional football players. *Neurosurgery, 57*(7), 719–726.

Guskiewicz, K.M. & Mihalik, J.P. (2006). The biomechanics and pathomechanics of sport related concussion: Looking at history to build the future. In: Slobounov SM and Sebastianelli W (eds), Foundations of sport related brain injuries, Springer, New York, 65-83.

Haddad, B.F., Lissner, H.R., Webster, J.E. & Gurdjian, E.S. (1955). Experimental concussion; relation to acceleration to physiologic effect. *Neurology, 5*(11), 798-800.

Hansen, A.J. (1997). Extracellular potassium concentration in juvenile and adult rat brain cortex during anoxia. *Acta Physiol Scand, 99*, 412–420.

Hansen, A.J. (1978). The extracellular potassium concentration in brain cortex following ischemia in hypo- and hyperglycemic rats. *Acta Physiol Scand, 102*, 324–329.

Hardy, W.N., Foster, C.D., Mason, M.J., Yang, K.H., King, A.I. & Tashman S. (2001). Investigation of head injury mechanisms using neutral density technology and high-speed biplanar X-ray. *Stapp Car Crash J* [The Stapp Association, Ann Arbor, Michigan].

Hardy, W.N., Mason, M.J., Foster, C.D., Shah, C.S., Kopacz, J.M., Yang, K.H., King, A.L., Bishop, J., Bey, M., Anderst, W., Tashman, S. (2007) A Study of the Response of the Human Cadaver Head to Impact. *Stapp Car Crash Journal, 51*, 17-80.

Hodgson, V.R. (1967). Tolerance of the facial bones to impact. *American Journal of Anatomy, 120*, 113-122.

Hodgson, V.R. & Thomas, L.M. (1971). Breaking strength of the human skull vs impact surface curvature. *National Technical Information Service Report*, DOT HS 800 583. Springfield, VA, USA.

Hodgson, V.R., Thomas, L.M. & Khalil, T.B. (1983). The role of impact location in reversible cerebral concussion, SAE Paper No. 831618, in: 27th Stapp Car Crash Conference, *Society of Automotive Engineers*, 225-240.

Holbourn, A.H. (1943). Mechanics of head injuries. *Lancet, 2*, 438-441.

Horgan, T.J. & Gilchrist, M.D. (2003). The creation of three-dimensional finite element models for simulating head impact biomechanics. *International Journal of Crashworthiness, 8*(4), 353-366.

Horgan, T.J. & Gilchrist M.D. (2004). Influence of FE model variability in predicting brain motion and intracranial pressure changes in head impact simulations, *International Journal of Crashworthiness, 9*(4), 401-418.

Horgan, T. (2005). A Finite Element Model of the Human Head for use in the Study of Pedestrian Accidents. PhD Thesis. University College Dublin.

Hoshizaki, T.B. & Brien, S.E. (2004). The science and design of head protection in sport. *Neurosurgery, 55*(4), 956-967.

Hoshizaki, T.B., Walsh, E., Post, A., Rousseau, P., Kendall, M., Karton, C., Oeur, A., Foreman, S. & Gilchrist, M.D. (2012). The application of brain tissue deformation values in assessing the safety performance of ice hockey helmets. *Journal of Sports Engineering and Technology, 0*(0), 1-11.

Hoshizaki, T.B., Post, A., Kendall, M., Karton, C. & Brien, S. (2013). The Relationship between Head Impact Characteristics and Brain Trauma. *J Neurol Neurophysiol, 5*(1), 1-8.

Hoshizaki, T.B., Post, A., Oeur, A. & Brien, S. (2014). Current and Future Concepts in Helmet and Sports Injury Prevention. *Neurosurgery, 75*(4), S136-S138.

Hovda, D.A., Prins, M., Becker, D.P. Lee, S., Bergsneider, M. & Martin, N.A. (1999), Neurobiology of concussion, Sports Related Concussion. *Quality Medical Publishing Inc*, St. Louis, MO.

Hubschmann, O.R. & Kornhauser, D. (1983). Effects of intraparenchymal hemorrhage on extracellular cortical potassium in experimental head trauma. *Journal of Neurosurgery*, 59, 289-293.

Hutchison, M,H. (2011). Concussion in the National Hockey League (NHL): The video analysis project. *PhD Thesis*. University of Toronto, Toronto, Canada

Hutchison, M.G., Comper, P., Meeuwisse, W.H. & Echemendia R.J. (2013a). A systematic video analysis of National Hockey League (NHL) concussions, part I: who, when, where and what*? Br J Sports Med, 00,* 1-5.

Hutchison, M.G., Comper, P., Meeuwisse, W.H. & Echemendia R.J. (2013b). A systematic video analysis of National Hockey League (NHL) concussions, part II: how concussions occur in the NHL. *Br J Sports Med, 00,* 1-5.

Hutchison, M.G., Comper, P., Meeuwisse, W.H. & Echemendia R.J. (2014). An observational method to code concussions in the National Hockey League (NHL): the heads-up checklist. *Br J Sports Med, 48,* 125–129.

ICD-10, WHO 1989

ISO 10256:2003, Head and Face Protection for Use in Ice Hockey.

Iverson, G.L., Lange, R.T., Brooks, B.L. & Rennison, V.L.A. (2010). ―Good Old Days‖ Bias Following Mild Traumatic Brain Injury. *The Clinical Neuropsychologist, 24*, 177-37.

Julian, F. & Goldman, D. (1962). The effects of mechanical stimulation on some electrical properties of axons. *Journal of General Physiology*, *46*, 297–313.

Karton C., Hoshizaki T.B., Gilchrist M. (2013). The influence of impactor mass on the dynamic response of the Hybrid III headform and brain tissue deformation, *ASTM International*, in press.

Katayama, Y., Becker, D.P., Tamura, T. & Hovda, D.A. (1990), Massive increases in extracellular potassium and the indiscriminate release of glutamate following concussive brain injury, *Journal of Neurosurgery*, *73*, 889-900.

Kelly, J.P., Nichols, J.S., Filley, C.M., Lillehei, K.O., Rubinstein D & Kleinschmidt-DeMasters B.K. (1999) Concussion in sports. Guidelines for the prevention of catastrophic outcome. JAMA., *266*(20), 2867-2869.

Kelly, J.P. (2001). Return to play following a concussion: International Symposium on Concussion in Sport [abstract]. *Br J Sports Med*, 35:372.

Kendall, M., Post, A., Rousseau, P., Oeur, A., Gilchrist, M. D. & Hoshizaki, B. (2012a). A comparison of dynamic impact response and brain deformation metrics within the cerebrum of head impact reconstructions representing three mechanisms of head injury in ice hockey, *IRCOBI Conference*, 430-440

Kendall, M., Walsh, E.S. & Hoshizaki, T.B. (2012b). Comparison between Hybrid III and Hodgson-WSU headforms by linear and angular dynamic impact response. *J Sports Engineering and Technology*, *0*(0), 1–6.

Kendall, M., Post, A., Rousseau, P. & Hoshizaki, T.B., (2014). The effect of shoulder pad design on reducing peak resultant linear and rotational acceleration in shoulder-to-head impacts. *Mechanism of Concussion in Sports, STP 1552, ASTM International, West Conshohocken, PA*, 142–152.

King, A.I., Yang, K.H., Zhang, L. & Hardy, W. (2003). Is head injury caused by linear or angular acceleration? *IRCOBI Conference*, Lisbon, Portugal, pp.1-12.

Kleiven, S. (2002). *Finite Element Modeling of the Human Head*. PhD Thesis.

Kleiven, S. & von Holst, H. (2002). Consequences of brain size following impact in prediction of subdural hematoma evaluated with numerical techniques. In: *Proceedings of the IRCOBI*, 161–72.

Kleiven, S. (2003). Influence of impact direction to the human head in prediction of subdural haematoma. *Journal of Neurotrauma*, *20*(4), 365-379.

Kleiven S. (2007). Predictors for traumatic brain injuries evaluated through accident reconstruction, *Stapp Car Crash Journal, 51,* 81- 114

Kuffler, S.W. (1967). Neuroglial cells: physiological properties and a potassium mediated effect of neuronal activity on the glial membrane potential. *Proceedings of the Royal Society of London - Series B: Biological Sciences*, *168*, 1–21.

LaPrade, R.F., Wijdicks, C.A. & Spiridonov, S.I. (2009). A Prospective Study of Injuries in NCAA Intercollegiate Ice-Hockey Goaltenders. *Journal of ASTM International, 6*(3), 1-8.

Leclerc, S., Lassonde, M., Delaney, J.S., Lacroix, V.J. & Johnston, K.M. (2001). Recommendations for Grading of Concussion in Athletes. *Journal of Sports Medicine*, *31*(8), 629-636.

Liberman, M. & Mulder, D.S. (2007). Airway Injuries in the Professional Ice Hockey Player. *Clin. J.Sport Med*, *17*, 61–67.

Lincoln A.E., Caswell S.V., Almquist J.L., Dunn R.E., & Hinton, R.Y. (2013). Video incident analysis of concussions in boys' high school lacrosse, The American Journal of Sports Medicine, *41*(4), 756-761.

Luppino, G. & Rizzolatti, G. (200). The organization of the frontal motor cortex. *News Physiol. Sci*., *15*, 219-224.

Marchie, A. & Cusimano, M.D. (2003). Bodychecking and concussions in ice hockey: Should our youth pay the price? *CMAJ*, *169*(2), 124-128.

Marieb, E.N. (1998). Human anatomy and physiology, 4th ed. *Benjamin/Cummings Science Publishing*, California.

Martini, F., Timmons, M.J. & Tallitsch, R.B. (2009). Human Anatomy Sixth Edition. *Pearson Education, Inc.*, San Franscisco, CA. 387-394.

Mayevsky, A. & Chance, B. (1974). Repetitive patterns of metabolic changes during cortical spreading depression of the awake rat. *Brain Research*, *65*, 529–533.

McCrory P, Meeuwisse W, Johnston K, et al. (2009) Consensus statement on concussion in sport--the 3rd International Conference on concussion in sport, held in Zurich, November 2008. *J Clin Neurosci*. *16*(6), 755–763

McIntosh, T.K., Smith, D.H., Meaney, D.F., Kotapka, M.J., Gennarelli, T.A. & Graham, D.I. (1996). Neuropathological sequelae of traumatic brain injury: relationship to neurochemical and biochemical mechanisms. *Laboratory Investigation*, *74*, 315-342.

McIntosh, A. S., & McCrory, P. (2005). Preventing head and neck injury. *British Journal of Sports Medicine, 39*(6), 314-318.

McIntosh, A.S., Patton, D.A., Fréchède, B., Pierré, P., Ferry, E. & Barthels, T. (2014). The biomechanics of concussion in unhelmeted football players in Australia: a case–control study. *BMJ Open*, *4:e005078*, 1-9.

McKee, A.C., Gavett, B.E., Stern, R.A., Nowinski, C.J., Cantu, R.C., Kowall, N.W., Perl, D.P., Hedley-White, T., Price, B., Sullivan, C., Morin, P., Lee, H., Kubilus, C.A., Daneshvar, D.H., Wulff, M., and Budson, A.E. (2010). TDPE-43 proteinopathy and motor neuron disease in chronic traumatic encephalopathy. *Journal of Neuropathology and Experimental Neurology*, *69*(9), 918-929.

Meaney, D. F. & D. H. Smith. (2011). Biomechanics of Concussion. *Clinics in sports medicine 30*(1), 19-31.

Mendis, K., Stalnaker, R. & Advani, S. (1995). A constitutive relationship for large deformation finite element modeling of brain tissue. *Journal of Biomechanical Engineering*, *117*(4), 279-285.

Mihalik, J.P., Guskiewicz, K.M., Jeffries, J.A., Greenwald, R.M. & Marshall, S.W. (2008). Characteristics of head impacts sustained by youth ice hockey players. *Journal of Sports Engineering and Technology*, *222*, 45-52.

Miller, K. & Chinzei, K. (1997). Constitutive modelling of brain tissue: Experiment and theory. *Journal of Biomechanics*, *30*(11), 1115-1121.

Miller, R., Margulies, S., Leoni, M., Nonaka, M., Chen, Z., Smith, D. & Meaney, D. (1998). Finite element modeling approaches for predicting injury in an experimental model of severe diffuse axonal injury. In Proceedings of the 42nd Stapp Car Crash Conference, SAE paper No. 983154.

Molsa, J., Airaksinen, O. & Nasman, O. (1997) Ice Hockey Injuries in Finland. A Prospective Epidemiologic Study, *Am. J. Sports Med*., *25*, 495–499.

Nahum A.M., Smith R., Ward C.C. (1977). Intracranial pressure dynamics during head impact. In: Proceedings 21st stapp car crash conference. SAE paper No. 770922.

Newman, J.A. (1993). Biomechanics of Human Trauma: Head Protection,‖ in Accidental Injury Biomechanics and Prevention. Springer Verlag: New York, p 292-310.

Newman, J., Barr, C., Beusenberg, M. C., Fournier, E., Shewchenko, N., Welbourne, E., & Withnall, C. (2000). A new biomechanical assessment of mild traumatic brain injury. Part 2: results and conclusions. *In Proceedings of the International Research Council on the Biomechanics of Injury conference*.

Nicholson, C. & Kraig, R.P. (1981). The behavior of extracellular ions during spreading depression. *In: Zeuthen T, ed. The Application of Ion-Selective Electrodes.* New York, NY: Elsevier, North-Holland, 217–238.

Nur, S., Kendall, M., Rousseau, P. & Hoshizaki, T.B. (submiited). A Comparison of the Capacity of Ice Hockey Goaltender Masks for Protection from Puck Impacts. *Sport Biomechanics*.

Nusholtz, G.S., Lux, P., Kaiker, P.S. & Janicki, M.A. (1984). Head impact response - Skull deformation and angular accelerations. *Proceedings of the 28th Stapp car crash conference*, Chicago, IL, p.41–74.

Ommaya, A.K., Hirsch, A.E. & Martinez, J.L. (1966). The role of whiplash in cerebral concussion. Paper presented at the 10th Stapp Car Crash Conference.

Ommaya, A.K., Yarnell, P., Hirsch, A.E. & Harris, E.H. (1967). Scaling of experimental data on cerebral concussion in sub-human primates to concussion threshold for man. Proceedings of the 11th Stapp Car Crash Conference, SAE paper No. 970906.

Ommaya, A.K. & Hirsch, A.E. (1971). Tolerances for cerebral concussion from head impact and whiplash in primates. Journal of Biomechanics, *4*, 13-21.

Ommaya, A.K. (1985). Biomechanics of head injuries: Experimental aspects. In: Biomechanics of Trauma, edited by A. Nahum and J. W. Melvin. Norwalk: *Appleton-Century-Crofts*.

Ono, K., Kikuchi, A., Nakamura, M., Kobayashi, H. & Nakamura, N. (1980). Human head tolerance to sagittal impact reliable estimation deduced from experimental head injury subhuman primates and human cadaver skull. *Proceedings in the 24th Stapp Car Crash Conference*, SAE Paper No. 801303.

Ouckama, R. & Pearsall, D. (2014). Projectile Impact Testing of Ice Hockey Helmets: Headform Kinematics and Dynamic Measurement of Localized Pressure Distribution. *IRCOBI Conference*, 62-71.

Padgaonkar, A.J., Krieger, K.W. & King, A.I. (1975). Measurement of angular acceleration of a rigid body using linear accelerometers. *Journal of Applied Mechanics, 42*(3), 552-556.

Pashby, T., Carson, J.D., Ordogh, D., Johnston, K.M., Tator, C.H. & Mueller F.O. (2001). Eliminate head-checking in ice hockey. *Clin J Sport Med, 11*(4), 211-213.

Paulson, O.B. & Newman, E.A. (1987). Does the release of potassium from astrocyte end feet regulate cerebral blood flow? *Science*, *237*, 896–898.

Pearsall, D.J., Montgomery, N., Rothsching, N. & Turcotte, R. A. (1999). The Influence of Stick Stiffness on the Performance of Ice Hockey Slap Shots. *Sports Eng*, *2*, 3–11.

Pellman E.J., Viano D.C., Tucker A.M., Casson I.R., Waeckerle J.F. (2003). Concussion in professional football: reconstruction of game impacts and injuries, *Journal of Neurosurgery*, *53*, 799- 814.

Pellman, E.J., Powell, J.W., Viano, D.C., Casson, I.R., Tucker, A.M., Feuer, H., Lovell, M., Waeckerle, J. & Robertson, D.W. (2004). Concussion in professional football: epidemiological features of game injuries and review of literature – Part 3. *Neurosurgery*. *54*(1), 81–96

Post, A. & Hoshizaki, T.B. (2012). Mechanisms of brain impact injuries and their prediction: A review. *Trauma, 14*(4) 327–349

Post, A., Hoshizaki, T. B., Gilchrist, M., & Brien, S. (2012a). Analysis of the influence of independent variables used for reconstruction of a traumatic brain injury incident. Journal of *Sports Engineering and Technology*, *0*(0), 1-9.

Post, A., Hoshizaki, T.B. & Gilchrist, M.D. (2012b). Finite element analysis of the effect of loading curve shape on brain injury predictors. *Journal of Biomechanics*, *45*(4), 679-683.

Post A, Oeur A, Hoshizaki TB, Gilchrist MD (2012c) The Influence of Centric and Non-Centric Impacts to American Football Helmets on the Correlation Between Commonly Used Metrics in Brain Injury *Research. International Research Council on Biomechanics of Injury Conference (IRCOBI)*, Dublin, Ireland.

Post A, Oeur A, Hoshizaki TB, Gilchrist MD (2012d) On the importance of using a centric/non-centric protocol for the evaluation of ice hockey helmet performance. *Proceedings of ASTM Symposium on the mechanism of concussion in sports*. Atlanta, GA, USA.

Post, A. (2013). The influence of dynamic response characteristics on traumatic brain injury. *PhD Thesis*. University of Ottawa, Canada.

Post A., Oeur A., Hoshizaki T.B. &Gilchrist M.D. (2013a) The influence of velocity on injury risk in American football. Proceedings of Helmet Performance and Design Conference.

Post, A., Hoshizaki, T.B., Gilchrist, M.D., Brien, S., Cusimano, M.D. & Marshall, S. (2013b). The influence of dynamic response and brain deformation metrics on the occurrence of subdural hematoma in different regions of the brain. J Neurosurg, 1-9.

Post, A., Hoshizaki, T.B., Gilchrist, M.D., Brien, S., Cusimano, M.D. & Marshall, S. (2014a). The influence of acceleration loading curve characteristics on traumatic brain injury. *Journal of Biomechanics*, *57*, 1074-1081.

Post, A., Karton, C., Hoshizaki, T.B., Gilchrist, M.D. (2014b). Analysis of the protective capacity of ice hockey helmets in a concussion injury reconstruction. *IRCOBI Conference*, 72-80.

Post, A., Oeur, A., Hoshizaki, T.B. & Gilchrist, M.D. (2014c). Differences in region-specific brain tissue stress and strain due to impact velocity for simulated American football impacts. *Journal of Sport Engineering and Technology*, *Special Issue*, 1-11.

Post, A., Oeur, A., Walsh, E., Hoshizaki B. & Gilchrist, M.D. (2014d). A centric/non-centric impact protocol and finite element model methodology for the evaluation of American football helmets to evaluate risk of concussion. *Computer Methods in Biomechanics and Biomedical Engineering*, *17*(16), 1785-1800.

Post, A., Hoshizaki, T.B., Gilchrist, M.D., Brien, S., Cusimano, M. & Marshall, S. (2015a). Traumatic brain injuries: the influence of the direction of impact. *Neurosurgery*, *51*, 325-335.

Post, A., Kendall, M., (2015b). Characterization of Persistent Concussive Syndrome Through Injury Reconstruction and Finite Element Modelling. *Journal of the Mechanical Behavior of Biomedical Materials*, *51*, 325-335.

Post, A., Karton, C., Hoshizaki, T.B., Gilchrist, M.D. & Bailes, J. (2015c). Evaluation of the protective capacity of baseball helmets for concussive impacts. *Computer Methods in Biomechanics and Biomedical Engineering*, 1-10.

Powell, J.W. (2001). Cerebral Concussion: Causes, Effects, and Risks in Sports. *J Athl Train*., *3*6(3), 307-311.

Price, C.J. (2000). The anatomy of language: contributions from functional neuroimaging. *Journal of anatomy*, *197*(3), 335-359.

Prince, D.A., Lux, H.D. & Neher, E. (1973). Measurement of extracellular potassium activity in cat cortex. *Brain Research*, *50*, 489–495.

Rabadi, M.H. & Jordan, B.D. (2001). The cumulative effect of repetitive concussion in sports. *Clin J Sport* Med, *11*, 194–8.

Roe, C., Sveen, U., Alvsaker, K. & Bautz-Holter, E. (2009). Post-concussion symptoms after mild traumatic brain injury: Influence of demographic factors and injury severity in a 1-year cohort study. *Disability and Rehabilitation*, *31*(15), 1235-1243.

Rosenthal, M., LaManna, J., Yamada, S., Younts, W. & Somjen, G. (1979). Oxidative metabolism, extracellular potassium and sustained potential shifts in cat spinal cord in situ. *Brain Research*, *162*, 113–127.

Rousseau P. & Hoshizaki, T.B. (2009). The influence of deflection and neck compliance on the impact dynamics of a hybrid III headform, *Sports Engineering and Technology*, *223*, 89-97.

Rousseau, P., Post, A., Hoshizaki, T.B. (2009a). A comparison of peak linear and angular headform accelerations using ice hockey helmets. *Journal of ASTM International 6*, 1, 1-11.

Rousseau, P., Post, A., Hoshizaki, T.B. (2009b). The effects of impact management materials in ice hockey helmets on head injury criteria. *J Sport Eng Tech*. *223*, 159-165.

Rousseau, P. (2014). An Analysis of Concussion Metrics Associated with Elite Ice Hockey Elbow-to-Head and Shoulder-to-Head Collisions. *PhD Thesis*. University of Ottawa, Canada.

Rousseau, P., Hoshizaki, T. B., and Gilchrist, M. D. (2014). For ASTM F-08: Protective Capacity of Ice Hockey Player Helmets against Puck Impacts," Mechanism of Concussion in Sports, STP 1552, Alan Ashare and Marcus Ziejewski, Eds., pp. 1–12, in press

Rousseau, P., & Hoshizaki, T. B. (2015). Defining the effective impact mass of elbow and shoulder strikes in ice hockey. *Sports Biomechanics*, 1-11.

Rowson, S., Duma, S. M., Beckwith, J. G., Chu, J. J., Greenwald, R. M., Crisco, J. J., Brolinson, P. G., Duhaime, A-C., McAlister, T. W., Maerlender, A. C., (2012) Rotational Head Kinematics in Football Impacts: An Injury Risk Function for Concussion, *Annals of Biomedical Engineering*, *40*(1), 1-13.

Roy, B. & Dore´, R. (1975). Kinematics of the Slap Shot in Ice Hockey as Executed by Players of Different Age Classifications. 5th International Congress of Biomechanics, International Congress of Biomechanics, Jyv¨askyla¨, Finland.

Ruan, J. (1994). Impact Biomechanics of head injury by mathematical modelling. *PhD thesis*, Wayne State University.

Ryan, L.M. & Warden, D.L. (2003). Post concussion syndrome. *International Review of Psychiatry, 15*(4), 310-316.

Schreiber, D.I., Bain, A.C. & Meaney, D.F. (1997). In vivo thresholds for mechanical injury to the blood-brain barrier. *In: Proceedings of the Stapp Car Crash Conference*, 277-291, SAE paper 973335.

Shewchenko, N., Withnall, C., Keown, M., Gittens, R. & Dvorak, J. (2005). Heading in football. Part 3: Effect of ball properties on head response. *British Journal of Sports Medicine, 39*, 33-39.

Sigurdardottir, S., Andelic, N., Roe, C., Jerstad, T. & Schanke, A.K. (2009). Post-concussion symptoms after traumatic brain injury at 3 and 12 months post-injury: A prospective study. *Brain Injury, 23*(6), 489-497.

Silva, V.D. (2006). Mechanics and Strength of Materials. New York, NY, Springer Berlin Heidelberg.

Sim, F. H. & Chao, E. Y. (1978). Injury Potential in Modern Ice Hockey. *Am. J. Sports Med*, *6*, 378–384.

Shah, K.R. & West, M. (1983). The effect of concussion on cerebral uptake of 2-deoxy-D-glucose in rat. *Neuroscience Letters*, *40*, 287–291.

Somjen, G.G. & Giacchino, J.L. (1985). Potassium and calcium concentrations in interstitial fluid of hippocampal formation during paroxysmal responses. *Journal of Neurophysiology*, *53*, 1098–1108.

Strich, S. (1961). Shearing of nerve fibers as a cause of brain damage due to head injury. *Lancet, 2*, 443-448.

Stuart, M.J. & Smith, A. (1995). Injuries in junior A ice hockey. A three-year prospective study. *Am J Sports Med*, *23*, 458–61.

Stuart, M.J., Smith, A.M., Malo-Ortiguera SA, et al. (2002). A comparison of facial protection and the incidence of head, neck, and facial injuries in Junior A hockey players. A function of individual playing time. *Am J Sports*, *30*, 39–44.

Styrke, J., Stålnacke, B.M., Sojka, P. & Björnstig U. (2007). Traumatic brain injuries in a well-defined population: epidemiological aspects and severity. *J Neurotrauma*, *24*, 1425-1436.

Sugaya, E., Takato, M. & Noda, Y. (1975). Neuronal and glial activity during spreading depression in cerebral cortex of cat. *Journal of Neurophysiology*. *38*, 822–841.

Sunami, K., Nakamura, T., Ozawa, Y., Kubota, M., Namba, H. & Yamaura, A. (1989). Hypermetabolic state following experimental head injury. *Neurosurgical Review*, 12(suppl 1), 400–411.

Takahashi, H., Manaka, S. & Sano, K. (1981). Changes in extracellular potassium concentration in cortex and brain stem during the acute phase of experimental closed head injury. *Journal of Neurosurgery, 55*, 708–717.

Takhounts, E.G., Hasija, V., Ridella, S.A., Tannous, R.E., Campbell, J.Q., Malone, D., Danelson, K., Stitzel, J., Rowson, S., Duma, S, (2008) Investigation of Traumatic Brain Injuries Using the Next Generation of Simulated Injury Monitor (SIMon) Finite Element Head Model. *Stapp Car Crash Journal*, *52*, 1-32.

Takhounts, E.G., Craig, M.J., Moorhouse, K., McFadden, J. & Hasija, V. (2013). Development of Brain Injury Criteria (BrIC). *Stapp Car Crash Journal*, *57*, 243-266.

Tegner, Y. & Lorentzon, R. (1996) Concussion among Swedish elite ice hockey players. *Br J Sports Med*, *30*, 252–255.

Tegner, Y. (2001). Concussion experiences: Swedish elite ice hockey league: International Symposium on Concussion in Sport [abstract]. *Br J Sports Med*, 35:376.

Thomas LM, Roberts VL, Gurdjian ES. 1966. Experimental intracranial pressure gradients in the human skull. *Journal of Neurology, Neurosurgery & Psychiatry*, *29*, 404–411.

Unterharnscheidt, F.J. & Higgins, L.S. (1969). Traumatic lesions of brain and spinal cord due to nondeforming angular acceleration of the head. *Texas Reports on Biology & Medicine. 27*, 127-166.

Van Harreveld, A. (1978). Two mechanisms for spreading depression in the chicken retina. *Journal of Neurobiology*, *9*, 419–431.

Viano, D.C., King, A.I., Melvin, J.W. & Weber, K. (1989). Injury biomechanics research: an essential element in the prevention of trauma. *Journal of Biomechanics*, *22*(5), 403-417.

Viano DC, Casson IR, Pellman EJ, Bir CA, Zhang L, Sherman DC, and Boitano MA (2005), Concussion in professional football: Comparison with boxing head impacts: Part 10, *Neurosurgery*, *57*, 1154-1172.

Viano, D.C., Casson, I.R. & Pellman, E.J. (2007). Concussion in professional football: Biomechanics of the struck player – Part 14, *Neurosurgery*, *61*, 313-328.

Walilko, T.J., Viano, D.C. & Bir, C.A. (2005). Biomechanics of the head for Olympic boxer punches to the face, *British Journal of Sports Medicine*, *39*, 710-719.

Wall, R.E. (1996). Comparison of International Certification Standards for Ice Hockey Helmets. *Masters Thesis*. McGill University, Canada.

Rousseau, P. (2014). An Analysis of Concussion Metrics Associated with Elite Ice Hockey Elbow-to-Head and Shoulder-to-Head Collisions. *PhD Thesis*. University of Ottawa, Canada.

Walsh, E.S. & Hoshizaki, T.B. (2010). Sensitivity Analysis of a Hybrid III Head-and Neckform to Impact Angle Variation. *Proceedings in 8th Conference of the International Sports Engineering Association.*

Walsh, E.S., Rousseau, P. & Hoshizaki, T.B. (2011). The influence of impact location and angle on the dynamic impact response of a hybrid III headform. *Journal of Sports Engineering*, *13*(3), 135-143.

Walsh, E.S. & Hoshizaki, T.B. (2012). Comparative analysis of the Hybrid III neckform to unbiased neckforms using a centric and non-centric impact protocol. *ASTM Symposium on the mechanism of concussion in sports*, Atlanta, GA, November 13th

Walsh, E.S., Post, A., Rousseau, P., Kendall, M., Karton, C., Ouer, A., Foreman S. & Hoshizaki, T.B. (2012). Dynamic impact response characteristics of a helmeted Hybrid III headform using a centric and non-centric impact protocol. *Journal of Sports Engineering, 0*(0), 1-6.

Ward, C. & Thompson, R.B. (1975). The development of a detailed finite element brain model. *Proceedings of the 19th Stapp Car Crash Conference*, San Diego, California, USA, SAE 751163.

Ward, C.C. & Nagendra, G.K. (1985). Mathematical Models: Animal and Human Models. *The Biomechanics of Trauma*, A. M. Nahum and J. Melvin, Eds., Appleton-Century-Crofts, Norwalk, CT, 77–100.

Wennberg, R.A. & Tator, C.H. (2003). National hockey league reported concussions, 1986–87 to 2001–02. *Can J Neurol Sci*, *30*(3), 206–209.

Willinger, R., Ryan, G. A., McLean, A. J. & Kopp, C. M. (1992). Mechanisms of brain injury related to mathematical modeling and epidemiological data, *Proceedings of the International IRCOBI Conference on the Biomechanics of Impacts*, 179-192.

Willinger, R., Taleb, L. & Kopp, C. (1995). Modal and temporal analysis of head mathematical models. *J Neurotrauma*, *12*, 743–54.

Willinger, R.,D. Baumgartner, B. Chinn, E. & Schuller (2001). New dummy head prototype : development, validation and injury criteria. *International Journal of Crashworthiness, 6*(3), 281-294.

Willinger, R. & Baumgarthner, D. (2003). Human head tolerance limit to specific injury mechanisms. *International Journal of Crashworthiness*, *8*(6), 605-617.

Wood, R.L. (2004). Understanding the 'miserable minority': A diasthesis-stress paradigm for post-concussion syndrome. *Brain Injury, 18*(11), 1135-1153.

Wu, T.C., Pearsall, D., Hodges, A., Turcotte, R., Lefebvre, R., Montgomery, D. & Bateni, H. (2003). The Performance of the Ice Hockey Slap and Wrist Shots: The Effects of Stick 279 Construction and Player Skill. *Sports Eng*, *6*, 31–40.

Yang, Y., Raine, A., Colletti, P., Toga, A.W. & Narr, K.L. (2009). Abnormal temporal and prefrontal cortical gray matter thinning in psychopaths. *Molecular Psychiatry, 14*, 561–562.

Yoganandan, N. & Pintar, F. A. (2004). Biomechanics of Temporo-Parietal Skull Fracture. *Clin. Biomech*, *19*, 225–239.

Yoshino, A., Hovda, D.A., Kawamata, T., Katayama, Y., Becker, D.P. (1991). Dynamic changes in local cerebral glucose utilization following cerebral conclusion in rats: evidence of a hyper- and subsequent hypometabolic state. *Brain Research, 561*, 106–119.

Yu, Z., Elkin, B.S. & Morrison, B., III. (2009). Modeling Traumatic Brain Injury in vitro: Functional Changes in the Absence of Cell Death. Biomedical Science & Engineering Conference, Institute of Electrical and Electronics Engineers, Oak Ridge, TN, 1–4.

Zanetti, K., Post, A., Karton C.., Kendall M., Hoshizaki, T.B., Gilchrist M.D. (2013). Identifying Injury Characteristics for Three Player Positions in American Football Using Physical and Finite Element Modeling Reconstructions. *IRCOBI Conference*, 525-535.

Zhang, L.,Yang, K.H. & King, A.I. (2001a). Biomechanics of neurotrauma. *Neurological Research 23*(2-3), 144-156.

Zhang, L., Yang, K.H. & King, A.I. (2001b). Comparison of brain responses between frontal and lateral impacts by finite element modeling. *Journal of Neurotrauma, 18*(1), 21-31.

Zhang, L., Yang, K.H., King, A.I. & Viano, D.C. (2003) A new biomechanical predictor for mild traumatic brain injury – A preliminary report. Summer Bioengineering Conference, Key Biscayne, Florida.

Zhang, L., Yang, K.H. & King, A.I. (2004). A proposed injury threshold for mild traumatic brain injury. *Journal of Biomechanical Engineering, 126,* 226-236.

Zhou, C., Khalil, T.B. & King, A.I. (1995). A New Model Comparing Impact Responses of the Homogeneous and Inhomogeneous Human Brain. *39th Stapp Car Crash Conference,* Coronado CA, SAE International, Warrendale, PA.

Appendix A: Validation of Element Rotation for Head Impacts

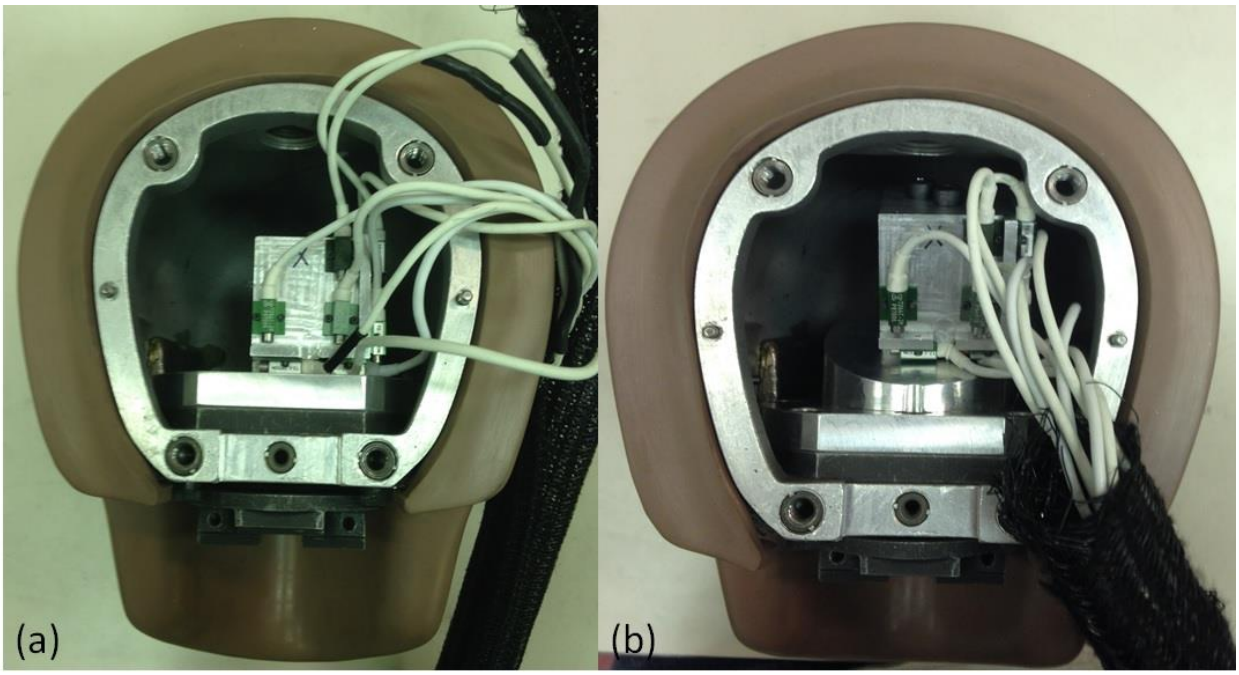

Figure 33: Accelerometers blocks mounted at the centre of gravity of the Hybrid III headform: (a) flat orientation (0°), (b) angled orientation (rotated 25° clockwise in the y-axis).

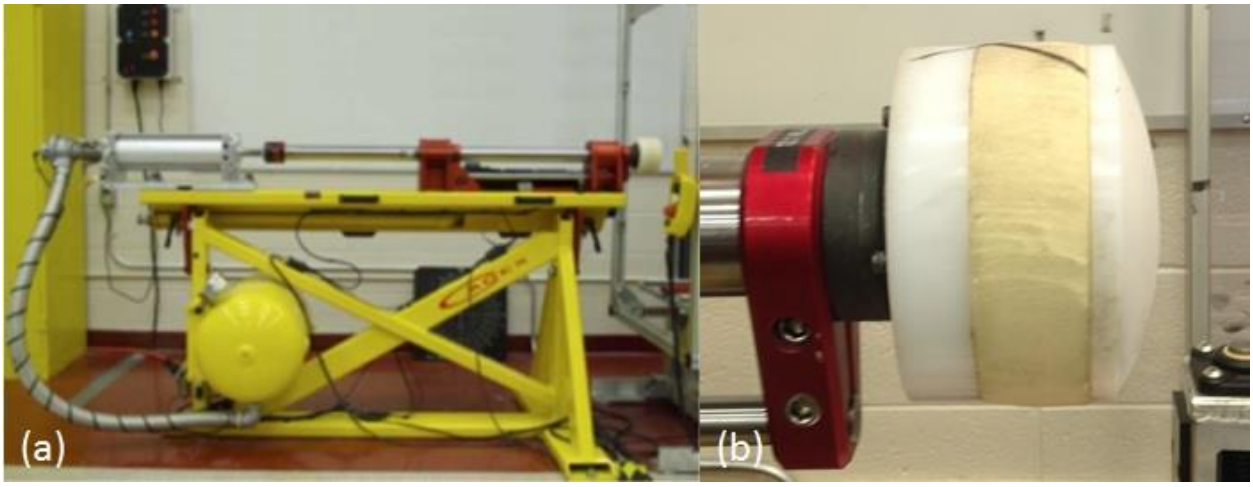

Figure 34: Pneumatic Linear Impactor: (a) frame supporting the impacting arm, (b) vinyl nitrile striker.

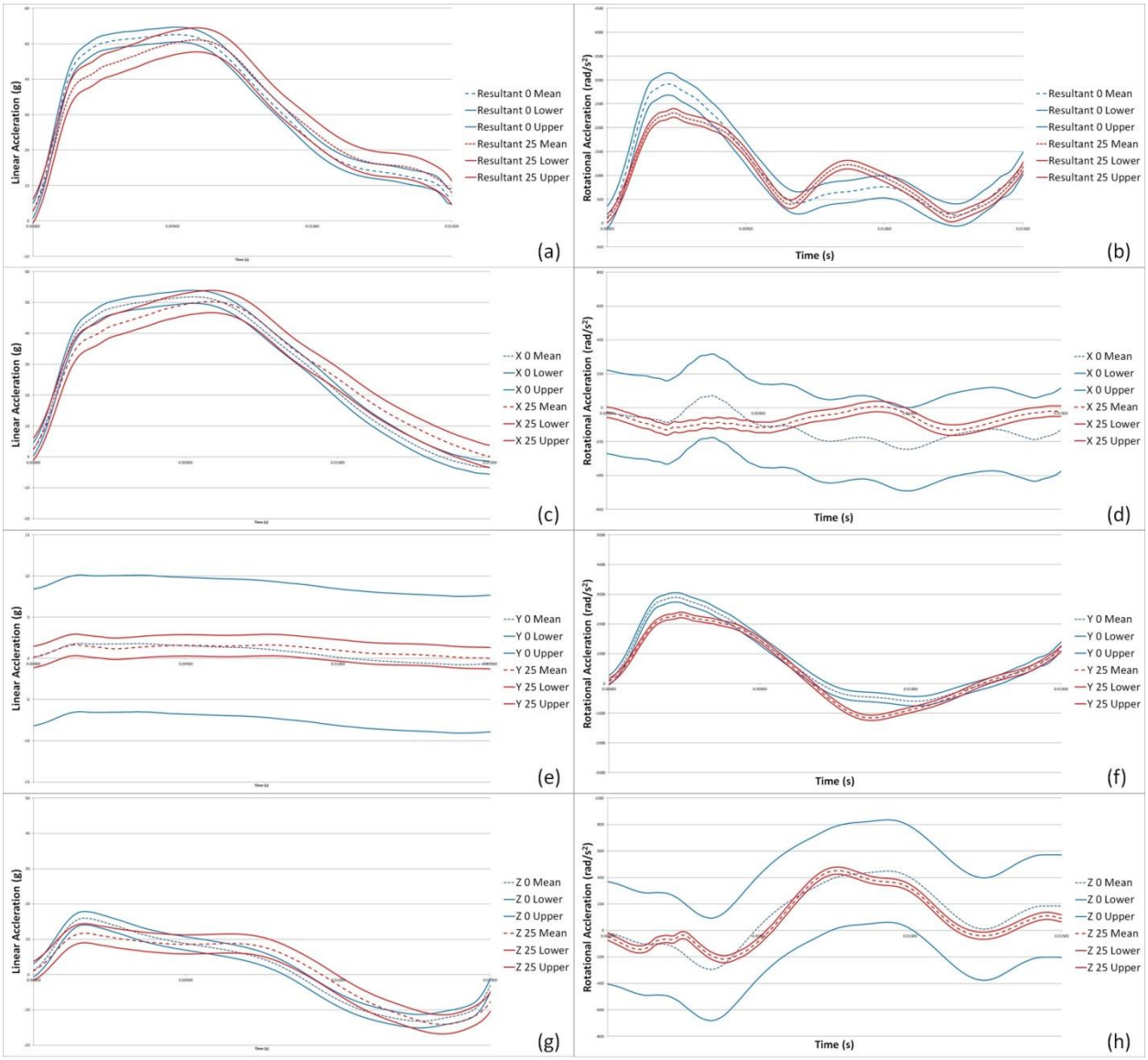

Figure 35: Mean acceleration-time histories for a Hybrid III headform of accelerometer block orientations of 0° and 25° at site 1: (a) Mean resultant linear acceleration-time histories, (b) Mean resultant rotational acceleration-time histories, (c) Mean x-axis linear acceleration-time histories, (d) Mean x-axis rotational acceleration-time histories, (e) Mean y-axis linear acceleration-time histories, (f) Mean y-axis rotational acceleration-time histories, (g) Mean z-axis linear acceleration-time histories, (h) Mean z-axis rotational acceleration-time histories.

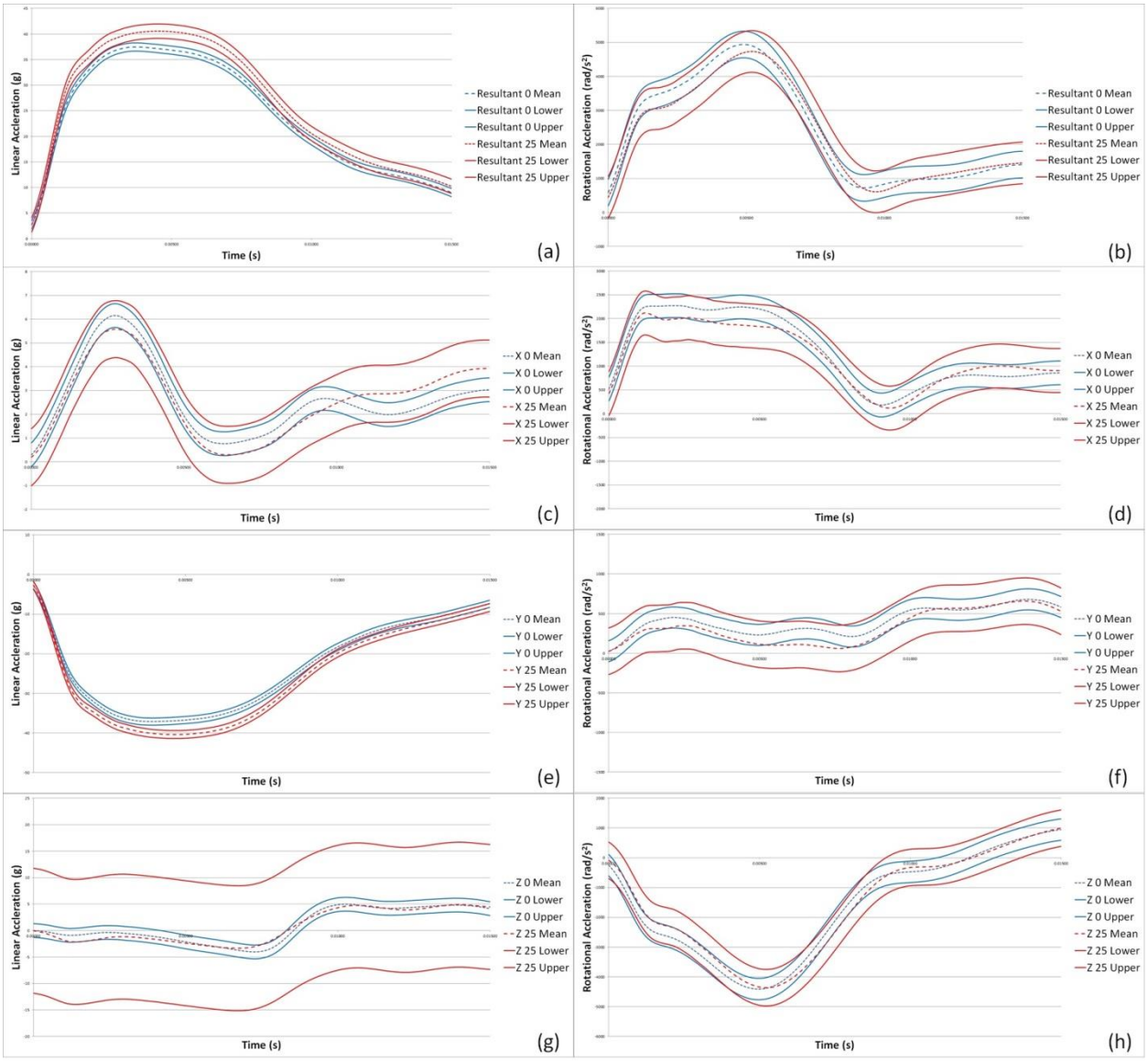

Figure 36: Mean acceleration-time histories for a Hybrid III headform of accelerometer block orientations of 0° and 25° at site 2: (a) Mean resultant linear acceleration-time histories, (b) Mean resultant rotational acceleration-time histories, (c) Mean x-axis linear acceleration-time histories, (d) Mean x-axis rotational acceleration-time histories, (e) Mean y-axis linear acceleration-time histories, (f) Mean y-axis rotational acceleration-time histories, (g) Mean z-axis linear acceleration-time histories, (h) Mean z-axis rotational acceleration-time histories.

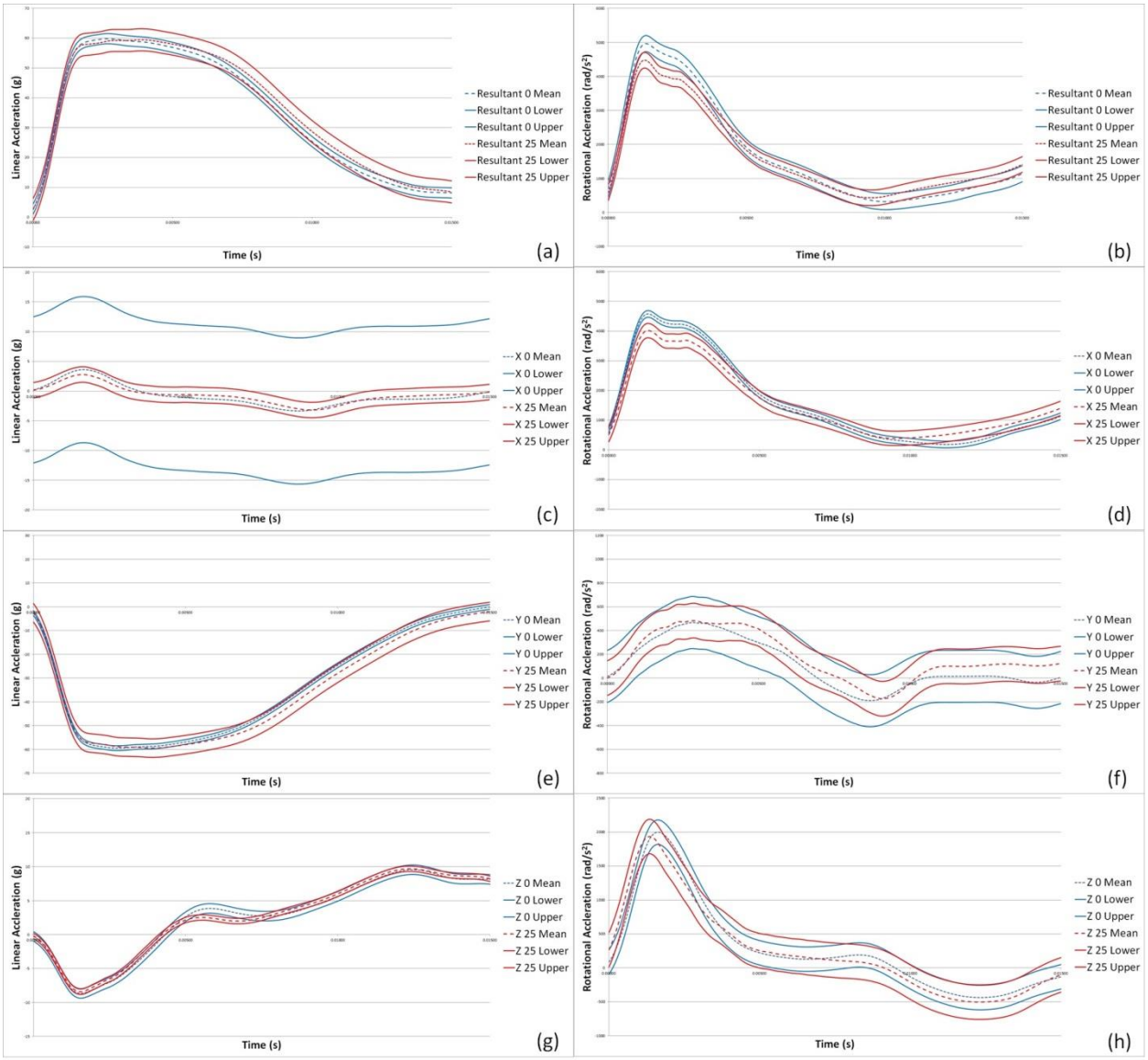

Figure 37: Mean acceleration-time histories for a Hybrid III headform of accelerometer block orientations of 0° and 25° at site 3: (a) Mean resultant linear acceleration-time histories, (b) Mean resultant rotational acceleration-time histories, (c) Mean x-axis linear acceleration-time histories, (d) Mean x-axis rotational acceleration-time histories, (e) Mean y-axis linear acceleration-time histories, (f) Mean y-axis rotational acceleration-time histories, (g) Mean z-axis linear acceleration-time histories, (h) Mean z-axis rotational acceleration-time histories.

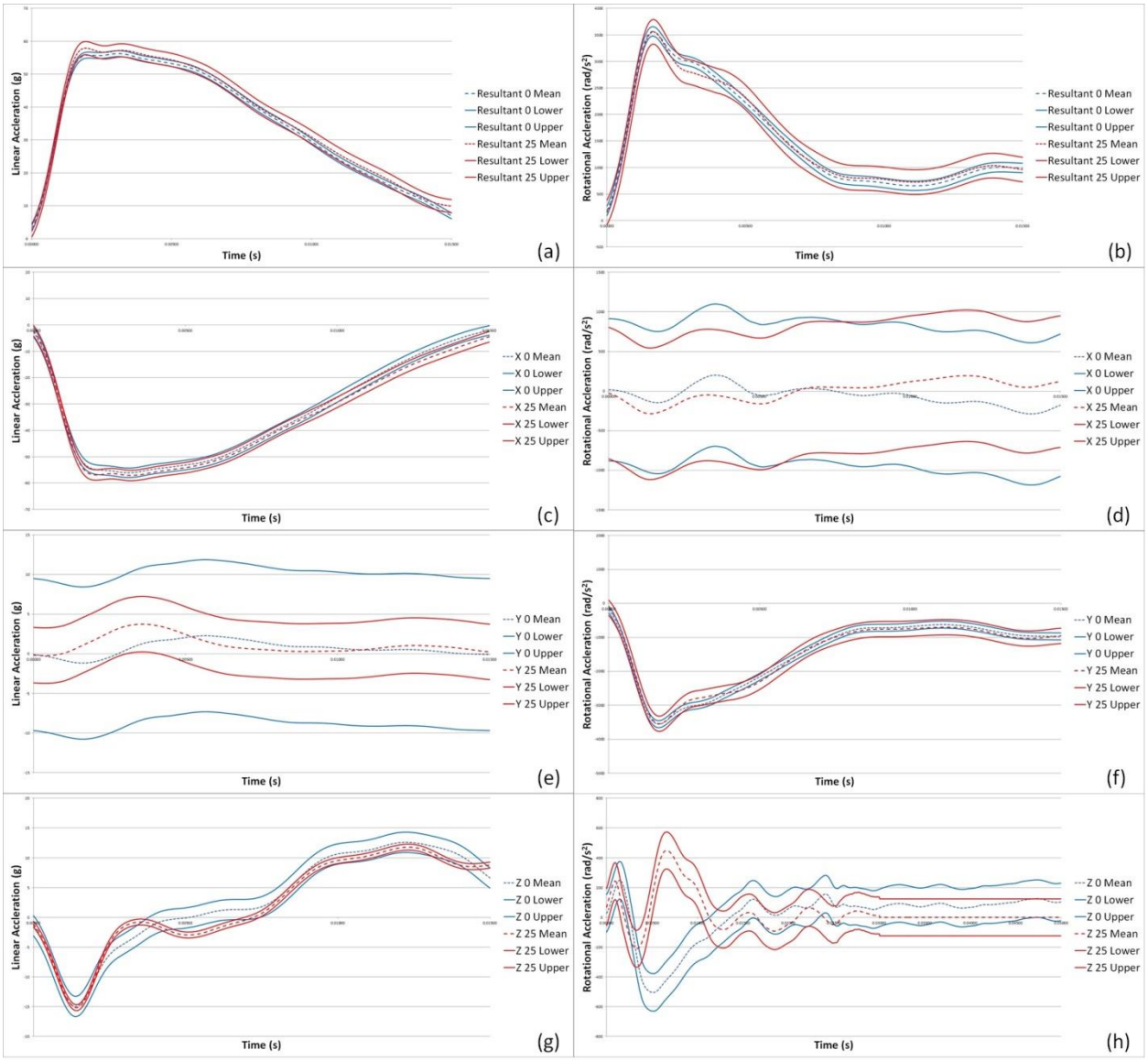

Figure 38: Mean acceleration-time histories for a Hybrid III headform of accelerometer block orientations of 0° and 25° at site 4: (a) Mean resultant linear acceleration-time histories, (b) Mean resultant rotational acceleration-time histories, (c) Mean x-axis linear acceleration-time histories, (d) Mean x-axis rotational acceleration-time histories, (e) Mean y-axis linear acceleration-time histories, (f) Mean y-axis rotational acceleration-time histories, (g) Mean z-axis linear acceleration-time histories, (h) Mean z-axis rotational acceleration-time histories.